Evaluation of Early In-Place Concrete Performance Based on Test Results of Cores and Cylinders

by

Adam Felinczak

A thesis

presented to the University of Waterloo

in fulfillment of the

thesis requirement for the degree of

Master of Applied Science

in

Civil Engineering

Waterloo, Ontario, Canada, 2018

Author's Declaration

I hereby declare that I am the sole author of this thesis. This is a true copy of this thesis including any required final revisions, as accepted by my examiners.

I understand that my thesis may be made electronically available to the public.

Abstract

The evaluation of in-place concrete performance, relating to its mechanical properties, continues to remain a challenge for engineers and researchers, but is essential for determining the safety of a structure and from the client's perspective, necessary for ensuring adherence to specified quality. The results of testing standard concrete cylinders provides a limited indication of the performance of a structure, due to both the different placement and compaction procedures, as well as the variable conditions caused by both temperature and moisture content during concrete hydration. Therefore, a correlation between the performance of a structure and the results of concrete cylinder testing is open to question. Cores, which are samples drilled from the concrete structure, can provide a more accurate estimate of the in-place concrete properties and indicate defects resulting from construction techniques and environmental conditions during curing. However, core testing is typically completed only following low results from standard compressive testing of cylinders on day 28 after casting.

Increasing social and economic pressures for constructing highway infrastructure more quickly poses a challenge for using concrete in rapid construction, since it is often specified by its 28 day properties. If the early in-place concrete performance can be evaluated through core testing as early as 3 or 7 days after casting for acceptance of the in-place concrete, construction and production sequencing can be improved in both cast-in-place concrete and precast concrete plants. Extracting cores at earlier ages is not common practice, as it is evident from the limited amount of research data available on early age concrete coring. However, many modern high-performance concretes undergo most of their hydration and strength growth more quickly than in the past allowing the possibility of extracting and testing cores earlier.

The experimental component of this research included testing and evaluating cores extracted on days 3, 7, and 28 from structures constructed in the University of Waterloo laboratory and structures constructed in prefabrication plants. The cores were evaluated for compressive strength, rapid chloride permeability, electrical bulk resistivity, density, and air void system to develop an understanding of the behaviour of the concrete in the structure during the early stages of concrete hydration until day 28. The laboratory structures included two sets of beams and one set of girder webs. The beam sets consisted of one low strength (design strength of 30 MPa) and one high strength (design strength of 50 MPa) concrete and were designed to replicate large beams or pier caps in bridge infrastructure. Cores were extracted vertically from the top and horizontally from the mid-height of the beams to evaluate the two alternatives of extracting cores in similar bridge elements. The girder webs were constructed to

replicate large girders used in bridges and cores were extracted near the top and bottom of the webs to determine the variation along the height. The prefabricated structures included one girder web, one complete girder, and one valve chamber, each from a different precast concrete plant. The concrete mixes used in each of the prefabricated structures resembled those used in bridge elements typical to Ontario and cores were extracted along the height of the structures to determine the variation in concrete performance along the height.

Based on the experimental results, it is concluded that it is acceptable to extract and test cores as early as day 7 for all concretes and, for the high strength concretes, as early as day 3. For day 7 coring and testing, the compressive strength of the cores were at least 90% of the day 28 cores and exceeded the specified 28 day design strength. The day 7 electrical resistivity was approximately 70% of its 28 day value. A comparison of the strengths of cores and cylinders from the prefabricated structures indicates that the cores have, on average, 90% of the cylinder strength on both day 3 and day 28.

The horizontal cores from the mid-height of the beams had compressive strengths 10% higher than those of the vertical cores, due to reduced compaction and hydration experienced in the top section of the beams. There was little difference in compressive strength and bulk resistivity along the height of the web of laboratory-cast girders on each testing day. However, due to large variation in the results of prefabricated structures, errors in the data, and missing information on days 3 and 7, no conclusions were drawn for the variation along the height at early age.

A linear correlation was observed between the results of rapid chloride permeability and the electrical resistivity. Thus, it is recommended to use the easier technique of measuring electrical resistivity in place of the rapid chloride permeability test. Using the established relationship, values for electrical resistivity relating to rapid chloride permeability limits in Ontario standards were recommended.

Acknowledgements

I would like to express my sincere gratitude to my supervisors Dr. Carolyn Hansson and Dr. Jeffrey West, as well as Dr. Rania Al-Hammoud, for their guidance and support throughout this project and my pursuit of graduate studies. I would like to thank the University of Waterloo Laboratory technicians, Douglas Hirst, Richard Morrison, Peter Volcic, and Mark Griffet for their tremendous efforts in assisting the experimental component of this project. Their experiences and advice was crucial for the planning and completion of the experimental testing.

I would like to extend my gratitude to Marc Johnson, the second graduate student associated with this project, as well as my lab group consisting of Peter Loudfoot, Colin Van Niejenhuis, Leah Kristufek, Ibrahim Ogunsanya, and Michael Benoit, for their friendship and support throughout the course of this project. I would like to thank the many graduate and undergraduate students who provided their own physical *core strength* during with the experimental component of the project: Shelley H. Yang, Dylan Dowling, James St. Onge, Nicholas Charron, Kyle Balkos, and Graeme Milligan.

I would like to thank the Ministry of Transportation of Ontario and its representatives who provided research feedback, sample testing, and funding, without which this project would not be possible. I would like to thank the local ready-mix concrete producers and the precast concrete plants who supplied materials and support for the construction of the structures used in this research. I would like to thank the Centre for Pavement and Transportation Technology (CPATT) and Dr. Maurice B. Dusseault for supplying testing equipment. Lastly, I would like to thank the Natural Sciences and Engineering Research Council of Canada and the Ontario Graduate Scholarship Program who graciously provided the funding for this research.

Dedication

I wish to dedicate my thesis to my family, Izabella, Andrzej, Michael, and Joy

for their love, care, and encouragement throughout my studies.

Table of Contents

List of Figures

List of Tables

1 Introduction

1.1 Background

The evaluation of in-place concrete performance, relating to its mechanical properties, has been studied for many years and continues to remain a challenge for engineers and researchers (F Michael Bartlett and MacGregor 1994; Bloem 1965; Malhotra 1977). The in-place concrete performance is difficult to quantify due to variation in the properties caused by variable construction practices and curing conditions, but it is essential for determining the safety of a structure and from the client's perspective, necessary for ensuring adherence to specified quality.

The quality of concrete is often measured for compressive strength using standard concrete cylinders which are made alongside the infrastructure with the same concrete. However, the concrete cylinders only represent the quality of the concrete, which includes the batching, mixing, transportation, and sampling (Suprenant 1995). Thus, engineers and researchers often question the correlation between the performance of a structure and the results of cylinder testing, particularly due to both the different placement and compaction procedures and the variable conditions caused by both temperature and moisture content during concrete hydration. A common method for evaluating the in-place concrete performance is through core testing. Cores, which are samples drilled from the concrete structure, can provide a more accurate estimate of the in-place concrete properties and indicate defects resulting from construction techniques and environmental conditions during hydration. However, core testing is typically completed only after the results of cylinder testing on day 28 fall below the specified day 28 design strength or when more accurate verification of the structure's performance is required for acceptance purposes.

1.2 Research Significance

Extracting cores at earlier ages, than day 28, is not common practice as it is evident from the limited amount of research data available on early age concrete coring. For certain infrastructure and concrete types, the Ontario standards allow for cores to be taken between 7 and 10 days and the cores are then held in a laboratory environment until testing on day 28. In many situations, coring is often specified at ages greater than 14 days, but with many modern high performance concretes which undergo hydration more quickly, it may be possible to extract and test cores at earlier ages.

The performance of concrete infrastructure is most often specified by its day 28 properties which can become a limiting factor in construction sequencing if work must be delayed to ensure the concrete

properties adhere to specifications on day 28. This is particularly critical in cast-in-place concrete infrastructure which may require the closure of traffic lanes for periods of time. In prefabrication plants, where quick turn-around time is desired for production of large concrete elements, knowledge of the early age in-place concrete performance can allow products to be assessed and accepted more quickly to increase production rates and confidence in the delivered product. Thus, cores at early age can be used for acceptance of the concrete for a given infrastructure to improve construction or production timelines, provided that there is a well-established understanding of that concrete relating to its 28 day performance.

1.3 Research Objectives

The purpose of this research project is to explore the feasibility of extracting and testing cores from various highway infrastructure, typical to Ontario, at ages earlier than the common testing on day 28 for quality control purposes. The experimental work on various structures has been conducted to address the following objectives:

- Develop an understanding of the behaviour of concrete in the structure during the early stages of hydration up to day 28 using cores extracted from various structures and modern concrete types. Evaluate the performance of the cores using test results for compressive strength, electrical resistivity, rapid chloride permeability, density, and air void system.
- Investigate the feasibility of extracting and testing cores on day 3 and day 7 and develop relationships between early core testing and core test results on day 28.
- Determine the relationship between the properties of cores and standard concrete cylinders.
- Investigate any differences in performance of cores:
    - extracted vertically and cores extracted horizontally.
    - extracted at different heights of the web of a girder.
- Investigate the relationship between the test results of electrical resistivity measurements and the common rapid chloride permeability measurements for the tested concrete types.

2 Literature Review

This chapter provides a background of research related to this project and highlights the missing information that will be covered through the project. The discussion will include an understanding of the basics of concrete, a description of factors affecting the in-place performance of concrete, the differences between concrete cores and cylinders, and previous research of cores extracted and tested at ages earlier than day 28.

2.1 Background to Literature Review

2.1.1 Components of a concrete mixture

Portland cement concrete is a mixture primarily composed of cement, water, aggregates, and air and involves an exothermic chemical reaction between cement particles and water which results in a paste that binds the aggregates together and hardens with time to form a product called concrete (Kosmatka et al. 2011). In addition to the essential components of concrete mentioned above, modern concretes also contain chemical admixtures which are chemical products that modify the normal properties of concrete (Neville 2011). The production of Portland cement is energy and material intensive which requires the use of raw materials from quarries and extremely elevated temperatures to create (Neville 2011). In light of the environmental impact and cost associated with cement production, modern concreting practice has introduced the use of supplementary cementitious materials (SCMs) which replace part of the Portland cement used in a concrete mixture. The quality of the concrete is dictated by the quality of the materials used and the effectiveness of the paste in coating the aggregate particles to ensure adequate bond between aggregates.

2.1.2 Hydration, Setting, and Hardening

Production of concrete involves an exothermic reaction between the water and cement called hydration. As the hydration reaction proceeds, the compounds that make Portland cement begin to form several new compounds, with calcium silicate hydrate (C-S-H) being of greatest importance. The calcium silicate hydrate constitutes approximately 50 to 60 percent of the volume of solids in a completely hydrated cement paste and often dictates the properties of the concrete such as setting, hardening, and strength (Kosmatka et al. 2011; Mehta 1986). The C-S-H continues to develop and contact the aggregates in the mixture until the C-S-H hardens to form a composite product. It must be noted that the entire cement particle does not react immediately and that as the C-S-H is formed from the cement particle, the rate at which the water can further react with the unhydrated cement is

reduced. Therefore the rate of hydration reduces over time, but slowly continues through the lifetime of the concrete (Neville 2011).

2.2 Factors Affecting In-Place Concrete Performance

2.2.1 Concrete Mix Composition

The type and quality of the materials used in a concrete mix will dictate the type of concrete and the performance of the structure. This section will investigate the components of cementitious materials and the w/cm ratio which have a major role on the properties of a concrete mixture. The total cementitious materials content in a concrete mix includes the Portland cement as well as the SCMs. The composition of the cementitious materials plays a major role in hydration and the structure of the hardened concrete which affects the strength and durability of concrete.

2.2.1.1 Cementitious Materials

There are many types of Portland cements available and each one has been designed for a specific purpose. Two Portland cements which are commonly used in Ontario infrastructure, and of relevance to the present project, are a general use (GU) cement, also known as ordinary Portland cement (OPC), and a high early strength (HE) cement. The two cements are chemically similar, but the one difference is that the HE cement has been ground finer than GU cement and so initiates the hydration reaction more quickly resulting in an earlier high strength (Bentz, Sant, and Weiss 2008). As a result of the more rapid hydration, the temperature created by the heat of hydration of a concrete with HE cement is higher than one mixed with GU cement.

The second component are the supplementary cementing materials (SCMs) used in concrete mixtures. The reaction of the SCMs takes place in the water-filled pores between the cement particles, thereby, partially filling the pores and reducing the porosity. This, in turn, increases the strength and decreases the permeability of the concrete (Hassan, Cabrera, and Maliehe 2000). The three most commonly used SCMs are fly ash, silica fume, and ground granulated blast furnace slag (slag).

Fly ash is a byproduct of coal combustion that is produced from mineral impurities which are cooled and solidify into small spherical particles of glass (Mehta 1986). Fly ash reacts more slowly than Portland cement and therefore compared to an OPC concrete can have lower compressive strengths at earlier ages, equivalent compressive strength on day 28, and larger compressive strengths after 28 days (Hassan et al. 2000). The Ontario specifications allow fly ash to be used in a dosage up to 25% by mass of the total cementitious material for a concrete mix (OPSS.PROV 1350 2016).

Silica fume is a byproduct of silicon and iron-silicon production and solidifies in very small spherical particles when cooled (Kosmatka et al. 2011). The quality that distinguishes silica fume from other SCMs is that it has a very high fineness and the composition is usually more than 85% silicon dioxide making it extremely reactive with the products of hydration to form more calcium silicate hydrate (Kosmatka et al. 2011). The fineness of silica fume allows it to react more quickly resulting in higher early day compressive strengths compared to an OPC concrete (Hassan et al. 2000). However, the rapid reaction leads to more water being consumed at a faster rate which, in effect, reduces the workability of the concrete significantly. Therefore, silica fume is often limited to 5 to 10% by mass of the total cementitious materials and is commonly used in Canada in a blended mix with GU cement at 8 - 9% by mass (Kosmatka et al. 2011; Neville 2011). Silica fume is often used in high-strength concrete and in concretes requiring a high degree of impermeability.

Slag is a byproduct of iron production and is itself a hydraulic cement having a similar composition to Portland cement, but not in the same proportions (Neville 2011). Although the slag is a hydraulic cement, it requires alkalinity to initiate the reaction. Consequently, the Portland cement begins to hydrate first producing an alkaline solution initiating the reaction of the slag. The Ontario specifications allow slag to be used in a dosage up to 25% by mass of the total cementitious material for a concrete mixture (OPSS.PROV 1350 2016). Similar to the strength growth of concrete containing fly ash, the slag concrete mixture will have lower early day strengths compared to an OPC concrete since the strength at early ages is provided by the cement hydration occurring first (Khatri, Sirivivatnanon, and Gross 1995). However after day 28, research has shown that adding slag to concrete even up to 40% by mass can decrease the porosity making the concrete denser and resulting in higher compressive strengths (Cheng et al. 2008).

2.2.1.2 Water to Cementitious Materials Ratio

The properties of the concrete are strongly related to the amount of water used relative to the total amount of cementitious material used, commonly referred to as the water to cementitious material (w/cm) ratio. Generally, as the w/cm ratio is decreased, the strength of the concrete is increased, provided the concrete is adequately consolidated (Neville 2011). The workability of the concrete is decreased when the w/cm ratio is decreased which causes issues with appropriately consolidating the concrete (Figure 2.1).

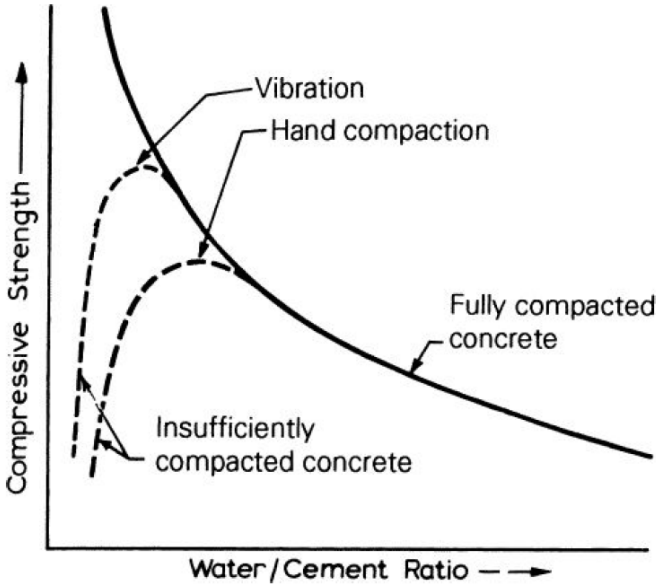

Figure 2.1 Influence of water to cement ratio on the compressive strength of concrete (Neville 2011)

It is often undesirable to have a high w/cm ratio since it leads to the hardened concrete containing many capillary pores from the remaining unreacted water resulting in lower compressive strength (Neville 2011; Powers 1958). Therefore, a compromise must be reached between attaining a desired workability which requires a higher w/cm ratio and achieving a desired strength with a lower w/cm ratio. Many modern concrete mixtures use a low w/cm to achieve high strength, but these lower w/cm ratios can lead to difficulty in consolidating the concrete. In order to achieve a workable concrete with lower w/cm ratios, water reducing admixtures are added to the concrete to improve the workability of the concrete without increasing the w/cm ratio (Kosmatka et al. 2011; Neville 2011). It is important to also note that these low w/cm ratio concrete mixes must be supplemented with adequate wet curing due to the reduced amount of water which can result in shrinkage cracking. Curing is further discussed in Section 2.2.3.

2.2.2 Concrete Age

The concrete properties are typically characterized by their 28 day values, specifically the 28 day concrete compressive strength. The chemical reaction between cement and water continues throughout the lifetime of the concrete, but most of the reaction occurs during the first month after which the strength gain is much slower (Mehta 1986; Neville 2011). In modern cements and concrete mixtures,

most of the strength is gained during the first 7 days and the relation between the 7 day and 28 day performance can be established to make decisions about construction sequencing (Neville 2011).

The strength development of the concrete is based on the degree of hydration achieved. This is affected not only by time, but also by the temperature created during hydration (heat of hydration) which is dependent on the concrete mixture composition and the ambient temperature. It has been found that higher internal temperature during curing results in a higher early strength, but also leads to lower 28 day strength compared to the same concrete cured at lower temperature (Mehta 1986; Shideler and Chamberlin 1949). The higher temperature accelerates the rate of hydration, causing more rapid early strength gain, but a more porous structure and, therefore, a lower compressive strength (Goto and Roy 1981; Shideler and Chamberlin 1949).

2.2.3 Curing: Moisture Condition and Temperature

Concrete hydration progresses and the concrete continues to gain strength provided that the concrete has adequate moisture available and is maintained at an appropriate temperature. The hydration reaction consumes the water, which effectively reduces the relative humidity within the concrete and when the relative humidity drops below 80%, hydration will stop (Kosmatka et al. 2011; Neville 2011). In addition to the water consumed during hydration within the concrete, the water near the surface of the concrete is exposed to evaporation which leads to drying and thermal gradients that make the concrete susceptible to surface cracking (Aitcin 1999). Thus, following the placement of concrete, it is desirable to maintain the concrete in saturated state and in an appropriate temperature through a process called curing.

Curing is the process of maintaining moisture content and temperature in concrete at an appropriate level for a suitable time period after placement to allow the concrete to develop desired properties (Kosmatka et al. 2011). Figure 2.2 shows that moist curing concrete, even for a duration of 3 days, can have a significant benefit on the compressive strength of the concrete (Neville 2011; Price 1951). In essence, there is no one unique way to employ curing and many methods of curing are available. The curing regime, which includes the moisture condition and temperature, must be designed to suit the concrete mix, structure size and type, and placement conditions. One simple and low cost curing approach is to apply wet fabrics, such as burlap, to the concrete surfaces and maintain the fabrics continuously moist during the curing period. The fabrics are often also covered with a polyethylene tarpaulin which acts as a moisture barrier to prevent the moisture from escaping.

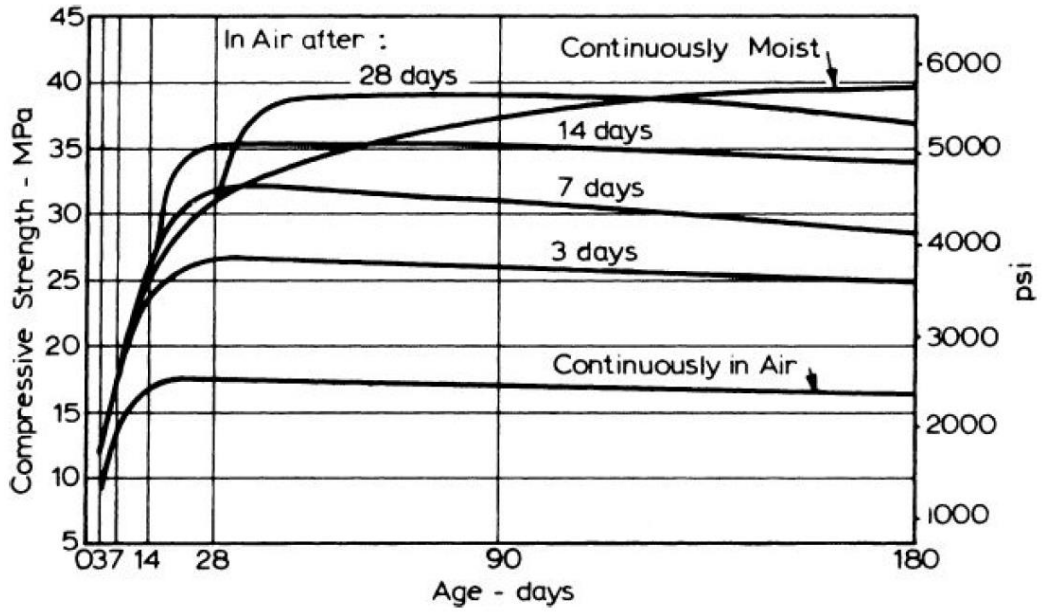

Figure 2.2 Influence of moist curing on the strength of concrete
(Price 1951)**;** Adapted by (Neville 2011)

Curing is particularly important in high performance concretes with low w/cm ratios in which the water is quickly consumed during hydration. Without the additional water provided through curing, the concrete will undergo drying shrinkage and crack. Aitcin (1999) concluded that wet curing of high performance concrete from time of setting until day 7 divided the shrinkage in the concrete by a factor of 2 compared to a non-cured concrete.

In addition to the temperature generated by hydration, the ambient temperature of the curing environment also has a significant effect on the concrete. As it was already stated, an increased temperature from heat of hydration will cause rapid early strength gain and similarly providing a heated curing environment will increase the rate of hydration. In certain concrete production facilities it is desired for the concrete to have adequate early day strength to increase the production rate. In these circumstances, curing can take place using elevated temperatures to reach desired strengths in the desired time, however, two things must be kept in mind. Firstly, higher temperatures at early age cause higher early age strength, but will result in a lower day 28 strength compared to the same concrete cured at lower temperatures due to the increased porosity created by poorly structured calcium silicate hydrate (Goto and Roy 1981). Secondly, it has been found that, as the internal concrete temperature begins to exceed 70°C in early stages during hydration, either due to heat of hydration, curing, or both combined, a phenomenon referred to delayed ettringite formation (DEF) can cause deterioration in the

long term performance of the concrete subjected to moisture (Taylor, Famy, and Scrivener 2001). The deterioration due to DEF is in the form of expansion which causes the concrete to crack due to the internal pressure caused by the DEF expansion (Diamond 1996; Taylor et al. 2001). Therefore the maximum temperature of the concrete must be controlled and the Ontario specifications limit the internal concrete temperature to 60°C for precast bridge elements (SSP 999F31 2016) and to 70°C for cast-in-place concretes and high-performance concretes (OPSS.PROV 904 2014; OPSS.PROV 909 2016).

2.2.4 Placement and Consolidation

The performance of the concrete structure not only relies on the quality of the concrete batched, but also the ability to adequately consolidate or compact the concrete in the formwork such that the concrete throughout the structure remains relatively uniform. Consolidation is the process of moulding the concrete within the formwork and around any reinforcement during placement in order to eliminate the pockets of entrapped air which are estimated to constitute approximately 5 to 20 percent of air (Mehta 1986; Suprenant 1995). The process of consolidating concrete for cylinders uses hand rodding, or tapping with a steel rod to settle the concrete into the cylindrical mould. The process for consolidating concrete in structures uses internal and/or external vibrators which create movement and settlement of the mixture, thereby forcing the entrapped air up and out of the concrete. An internal vibrator is typically called a poker or pencil vibrator and is placed directly into the concrete and slowly moved up and down to force the air bubbles up to the surface (Mehta 1986). External vibrators, or form vibrators, are rigidly attached onto the outside of the formwork and once the concrete is placed into the formwork, the vibrators are activated to shake the entire formwork, consolidate the mixture, and force air bubbles out through the top (Mehta 1986). They are frequently used on thin or heavily congested elements to ensure the concrete completely coats the reinforcement and to remove trapped air around the reinforcement. It is important to remember that it is not possible to remove all of the air from the concrete and continuing to apply vibration can lead to over-vibration which causes segregation of the aggregates and paste (Neville 2011). In large or tall concrete pours, it is not possible to place all the concrete from the same batch and, therefore, it is placed in uniform horizontal layers. The concrete needs to be adequately consolidated prior to the next layer being placed which should be done as quickly as possible such that the concrete in the layer below is still in a plastic state, otherwise a plane of weakness, “a cold joint“, can be formed (Mehta 1986).

2.2.5 Type of Structure and Variation within the Structure

The design of concrete infrastructure is often based on the assumption that once the concrete is hardened it is relatively homogenous throughout. However, as a result of several processes which include batching, transport, placement, curing techniques, and ambient environment, the material performance of the concrete in the constructed element will vary. The variation is further increased in the construction of large structures which require many batches or many truck loads. Understanding of the effect of the processes which create variation in concrete infrastructure is beneficial for making decisions about the performance and acceptance for a given concrete.

The effect of concrete variation has been studied in tall members, such as columns or walls, where the strength at the top of column is often considered to be lower than the strength at the bottom of the column. Bartlett and MacGregor (2000) attribute this to both the vertical migration of water resulting in a higher w/cm ratio near the top, and to the greater compaction experienced in the bottom of the member due to the weight of the concrete present higher in the form. Khoury et al. (2014) found that laboratory columns, 1.2 m tall, made with high strength concrete had up to 20 percent lower core strength at the top of the column compared to the middle and bottom of the column. Bartlett and MacGregor (1994) found that the top region of columns was up to 14% weaker than the middle region, while the bottom region was up to 9% stronger than the middle region.

Another variable is the direction of casting and, in particular, the effect of loading direction with respect to casting direction. This issue arises due to a weak plane at the interface between the aggregate and the cement paste, referred to as the interfacial transition zone (ITZ). The ITZ is particularly weak on the underside of an aggregate where more water is trapped resulting in a larger local w/cm ratio and, therefore, a more porous and weak interface (Suprenant 1985). In Figure 2.3 it seen that if a core is extracted horizontally (Core B), the weak plane of the ITZ becomes parallel with the loading direction when testing the core.

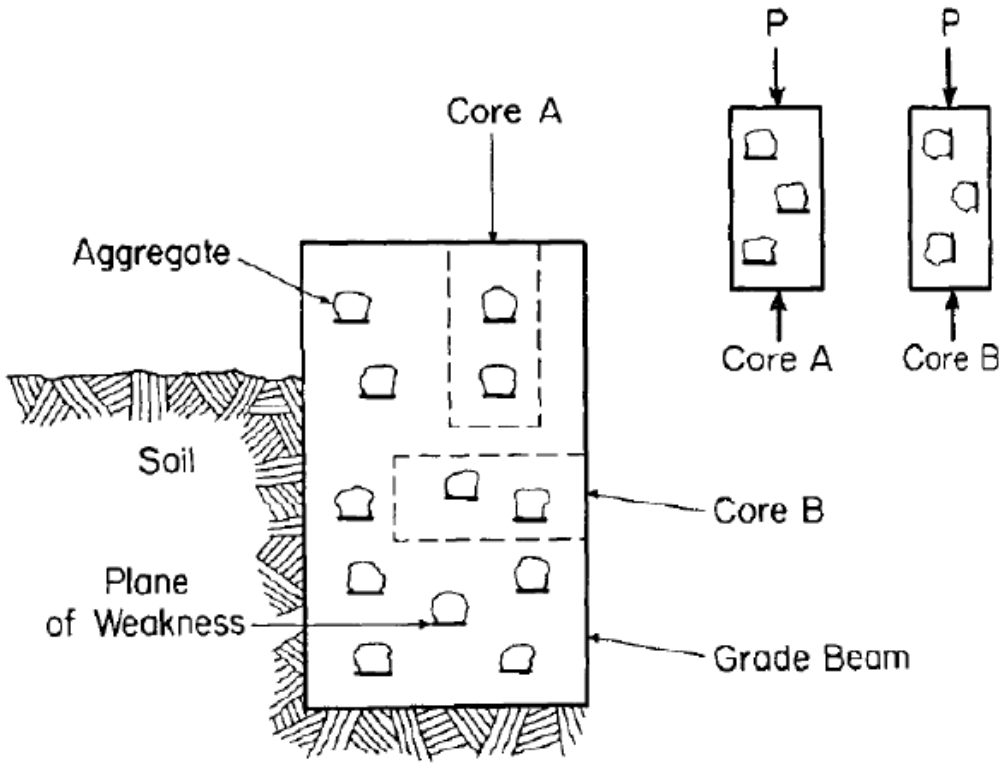

Figure 2.3 Effect of Coring Direction with respect to Casting Direction
(Suprenant 1985)

Various conclusions have been drawn from research on the comparison of horizontal and vertical cores and no real consensus has been reached. Suprenant (1985) found that vertical cores are 4 to 8 percent stronger than horizontal cores. Similarly, Carroll et al. (2016) found that vertical cores were approximately 4 percent greater than horizontal cores. On the other hand, Bartlett and MacGregor (1994) found the strength of cores taken horizontally and vertically did not differ significantly. The current practice in industry is to neglect the difference due to coring orientation (Suprenant 1995).

2.3 Concrete Structures: Cylinders and Cores

The strength of concrete, specifically, the compressive strength is generally accepted as its most important property. This is because, in reinforced concrete structures, the concrete is generally designed to carry a majority of the compressive forces and the compressive strength is evaluated by uniaxial compression tests for standard concrete cylinders (Bartlett and MacGregor 2000).

Concrete cylinders are small samples, typically 100 mm diameter and 200 mm tall, which are made alongside the infrastructure with the same concrete. The cylinders are held in their casting moulds and

generally kept with the structure during the curing period, after which they are removed from their moulds and placed in a moist curing room or in a calcium hydroxide solution (also referred to as saturated lime water) until day 28. The standard compressive strength test is performed on day 28 to quantify the 28 day strength of the concrete. Thus, the concrete cylinders represent the quality of the concrete, which includes the batching, mixing, transportation, and sampling (Suprenant 1995). However, cylinders provide a limited knowledge of the performance of a structure particularly due to both the different compaction procedures and the variable curing conditions caused by both temperature and moisture content during concrete hydration. Therefore, the correlation between the performance of a structure and the results of concrete cylinder testing is open to question.

Many tests exist to quantify the in-place concrete performance, one of the most common methods being core testing (F. Michael Bartlett and MacGregor 1994). Cores, which are samples drilled from the concrete structure, can provide a more accurate estimate of the in-place concrete and indicate defects resulting from construction techniques and environmental conditions during curing. Core testing is typically completed following low strength results from cylinder testing and where more accurate verification of the structure's performance is required for acceptance purposes (Bartlett and MacGregor 2000). However, it is generally accepted that core test results tend to be lower than test cylinders as a result of variable construction practices and curing conditions as well as damage sustained while drilling the cores (F. Michael Bartlett and MacGregor 1994). Additionally, cores will contain aggregates at their outer face that have been cut through during drilling and these aggregates are not completely contained within the cement paste and can be pushed out during compression testing causing a reduced cross-sectional area leading to a reduced compressive strength (Yener and Chen 1984). The Canadian Standard, CSA A23.1 Cl.4.4.6.6.2.2 (CSA A23.1 / CSA A23.2 2015), states that the average strength of each set of three cores must be greater than or equal to 85% of the specified design strength and no single core result shall be less than 75% of the specified strength. Bartlett and MacGregor (Bartlett and MacGregor 2000) indicate that these values are just acceptance rules and that the actual ratio of core strength to cylinder strength is generally greater than 85%.

As described earlier, cores are often drilled and tested following a low strength result from concrete cylinders and so these tests are conducted at ages greater than 28 days. Extracting cores prior to day 28 is not very common as it is evident from the limited amount of research data available on early age concrete coring. Research by Ariöz et al. (2006) found that coring and testing on day 7 resulted in lower core to cylinder strength ratios, compared to day 28 and day 90 coring and testing, which they

attributed to damage from drilling at early age. Cores of 94 and 144 mm Ø were extracted from small beams measuring 250 x 300 x 650 mm. The various tested concrete mixes contained between 300 and 350 kg/m^3 of cement with a water to cement ratio of 0.6 (discussion on cement content and water to cement ratio is found later in Section 2.2.1). The concrete was of relatively low strength and the cylinder tests found that the concrete appeared to have 7 day strengths of approximately 18 MPa and 28 day strengths of approximately 24 MPa (Ariöz et al. 2006). Research by Szypula and Grossman (1990) investigated the in-place concrete performance of a concrete slab in a tall structure by conducting testing on a replicated laboratory slab. The slab was supported by shoring until complete shore removal on day 14 to simulate the construction sequence in the tall structure and induce flexural cracking in the slab due to self-weight. The concrete used in the slab contained approximately 300 kg/m^3 of cement with a water to cement ratio of 0.6. Some cores were extracted on day 2, while the slab was still fully supported by shoring, and the cores were moist cured alongside the cylinders and tested on days 3, 7, 14, 28, and 56. Cores were also taken on days 3, 7, 14, 28, and 56 to determine the effect of flexural cracking on the in-place concrete performance. The cylinder compressive strengths were higher than core compressive strengths at all ages during the testing period and the day 2 cored specimens recorded higher compressive strengths than cores extracted at later ages due to the reduced strength from flexural cracking (Szypula and Grossman 1990). The researchers concluded that reasonable results can be attained with coring at early age and testing on day 28 compared to cores taken at later dates when the concrete has been subjected to larger loading (Szypula and Grossman 1990). The studies presented by these authors used concretes which are not completely representative of modern concrete mixes which often use cement contents larger than 400 kg/m^3 and water to cement ratio as low as 0.3.

For certain infrastructure and concrete types, the Ontario Provincial Standard Specifications (OPSS) allow for cores to be taken between 7 and 10 days and the cores are then held in a laboratory environment until testing on day 28 (OPSS.PROV 1350 2016; OPSS.PROV 909 2016). However, testing of cores at early age is not conducted, but with many modern high performance concretes which undergo most of their hydration more quickly, it may be possible to extract and test cores at earlier ages for the acceptance of the concrete infrastructure.

3 Experimental Program

This chapter describes the design and procedures for the experimental testing completed. This includes the rationale for constructed structures, concrete mixes used, coring locations within each structure, and the testing conducted. The experimental program included structures built in the University of Waterloo (UW) Structures lab and structures built in three different precast concrete plants.

3.1 Laboratory Structures

The laboratory structures included two sets of beams and one set of girder webs. The formwork for the structures was constructed in the UW lab and concrete was delivered to the lab from local ready-mix concrete plants for each cast.

3.1.1 Beams – B1 and B2

3.1.1.1 Description

The beams were designed to replicate elements of a bridge, such as a large beam, the bridge deck, or an abutment, which would allow for full 200 mm long cores to be extracted. The B1 and B2 beams were constructed to represent cast-in-place and precast non-prestressed bridge elements, respectively. The beams were dimensioned 650 mm x 600 mm x 2100 mm and consisted of minimal steel reinforcement since the structure would only be exposed to self-weight forces when moved around the lab and it was important to allow for adequate space to extract many cores. Four identical beams were constructed for each set of B1 and B2 beams to retrieve the desired number of cores required for testing. The beam design is shown in Figure 3.1.

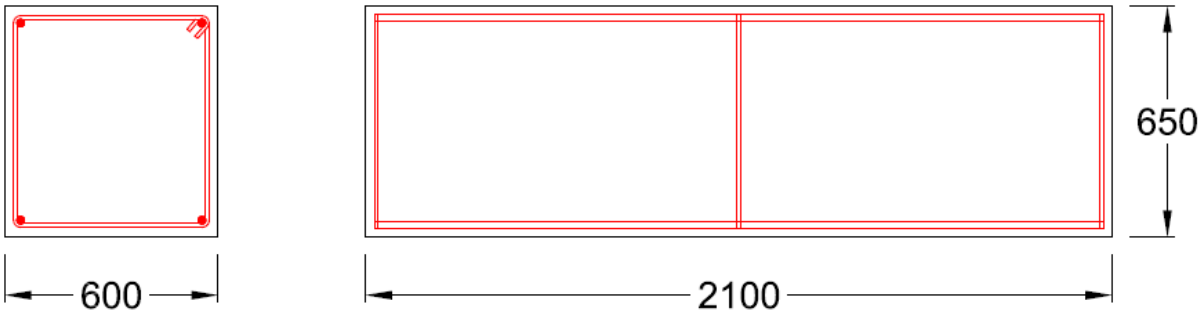

Figure 3.1 Beam Dimensions and Reinforcement Layout

The formwork was constructed using 19 mm formply board and form oil was applied to inside surface of formwork to allow for easier removal of formwork after casting. A temperature probe was placed inside the center of one of the beams to monitor the temperature during concrete hydration, as shown in Figure 3.2.

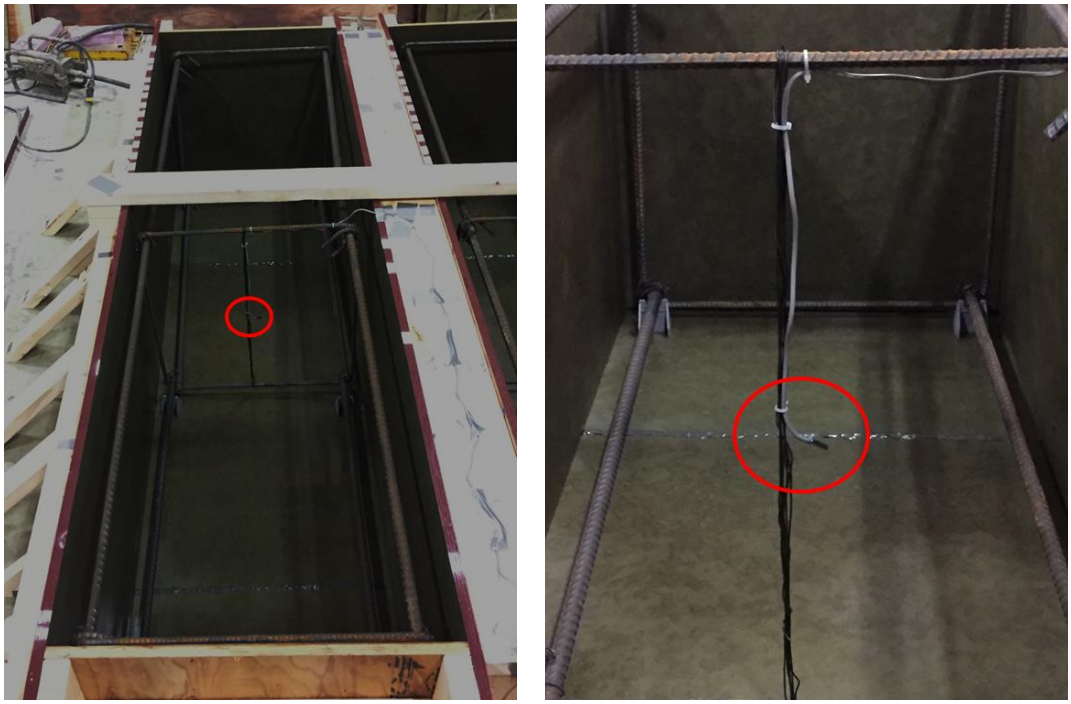

Figure 3.2 Temperature probe location for B1 beam

3.1.1.2 Concrete Mix Designs

The concrete mix chosen for B1 beams was a typical 30 MPa concrete used in Ontario bridge elements such as large beams, bridge decks, abutments, or pier caps. The mix contained Portland cement with a 9% cement replacement of ground granulated blast furnace slag (slag) for a total cementitious content of 350 kg/m^3, a w/cm ratio of 0.41, and used a 19 mm nominal maximum aggregate size, complying with OPSS guidelines (OPSS.PROV 1350 2016). At the time of casting, the fresh concrete had a slump of 90 mm and an air content of 4.8%.

The concrete mix chosen for B2 beams was a 50 MPa concrete mix containing silica fume to achieve a low permeability structure with high strength at early age. The concrete mix was proprietary and only limited information was provided. The mixture contained a blended cement, GUb-SF, which contains 8%, by weight, of silica fume blended with the Portland cement. The target w/cm ratio was 0.35 and a

19 mm nominal maximum aggregate size was used in the mixture. At the time of casting, the fresh concrete had a slump of approximately 200 mm and an air content of 6.0%.

3.1.1.3 Casting, Curing, and Coring

Both sets of beams were cast indoors, but bay doors were open at the time of the cast to provide clearance for the concrete truck. B1 beams were cast on a March morning with an outdoor temperature of approximately -8°C and a light snow. B2 beams were cast on a May morning with an outdoor temperature of 10 °C. The formwork was filled in half-height lifts and consolidated using two pencil vibrators. During each cast, concrete for the cylinders was taken from two wheel barrow loads, one near the start of the cast and the second midway through the cast. Following the surface finish, the beams were covered with presoaked burlap and plastic tarpaulin to prevent moisture loss while curing. Due to the requirement of coring many samples as early as day 3, the B1 beams did not achieve the 4 days of wet curing as required by OPSS.PROV 1350 (OPSS.PROV 1350 2016) and B2 beams did not achieve the required 7 days of curing as per OPSS.PROV 1350 (OPSS.PROV 1350 2016) and SSP 999 (SSP 999F31 2016), but were maintained uncovered in the laboratory environment at room temperature after 3 days of curing. Cylinders were kept in their plastic moulds until demoulding on day 3. They were then placed in calcium hydroxide solution until their respective testing days.

The beams were designed to extract cores from two orientations: parallel and perpendicular to the casting direction. Therefore, cores were taken from the top (parallel) and from the side (perpendicular) of the beam. It is important to note that it is reported in the literature there was no difference found between the physical horizontal or vertical drilling, provided that the drill was adequately mounted to the structure (Neville 2001). Therefore, it was decided to simplify the coring process and rotate the beams to vertically core the horizontal cores.

Coring and testing was completed on days 3, 7, and 28 for both sets of beams. Due to the large number of cores required on any given day, a clamping assembly was developed using steel bars and rods to ensure the drill bases were appropriately fastened to the beams for coring, as shown in Figure 3.3. All coring was completed using two water-cooled drills with two diamond tipped coring barrels.

Figure 3.3 Coring drill clamping assembly for UW lab beams

The core samples were still attached at their bottom after coring and a chisel was used to gently break the core out of the core hole and a steel wire was used to extract the core. This process is shown in Figure 3.4, as well as the bottom of the core after breaking.

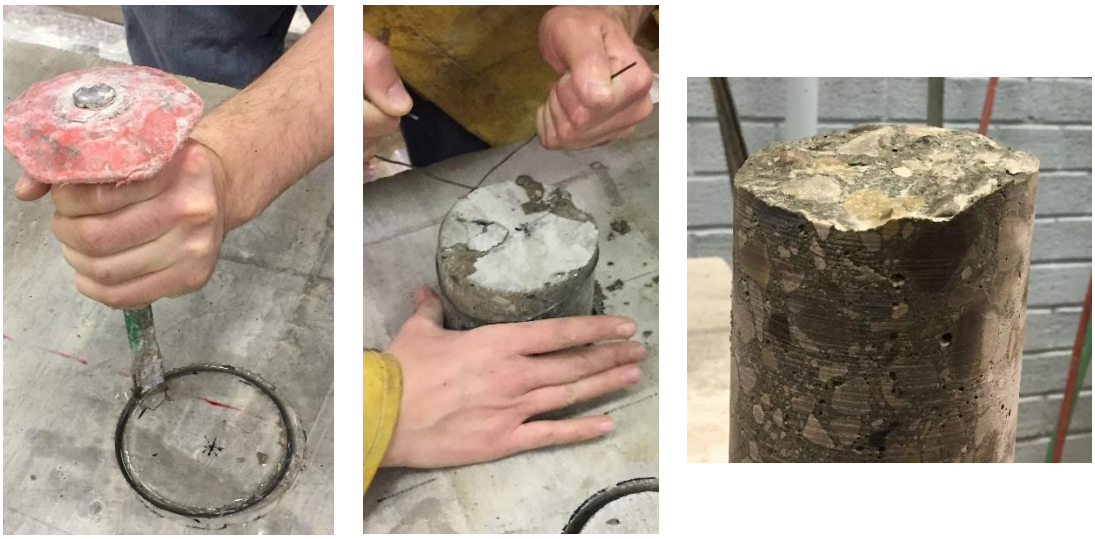

Figure 3.4 Core Removal Process

The beams were to be re-used for coring on their other faces on future days within the testing period, therefore core holes were plugged (Figure 3.5) to prevent moisture loss from the structure. Pipe plugs of 100 mm diameter were tightened within each core hole and maintained until the end of the testing period.

Figure 3.5 Plugged core holes for reduction in moisture loss

3.1.1.4 Coring Outline and Core Labelling

The beams were designed to allow for up to 16 cores to be extracted from both the top (vertical cores) and sides (horizontal cores) of the beam. Since the beams were quite large and difficult to quickly rotate due to lab constraints, coring on any particular day was carried out on three of the four beams, with "horizontal" cores taken from two beams and "vertical" cores from the third beam. The complete coring layout of a single beam is shown in Figure 3.6.

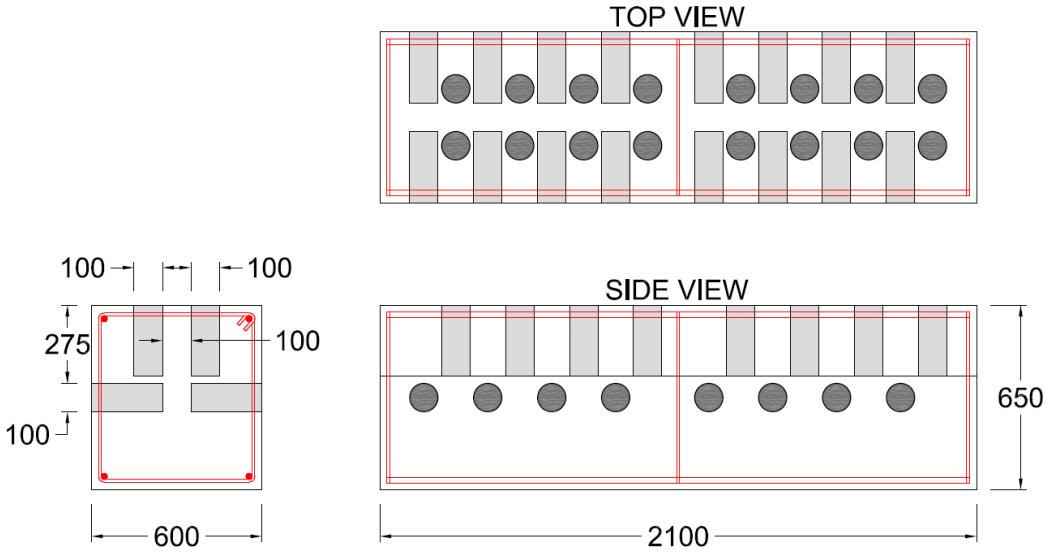

Figure 3.6 Coring Layout for B1 Beams

Each core was individually labelled to track the date and location from which it was taken. The cores were then grouped for testing and examples of the labelling scheme used for beam cores and cylinders are shown in Table 3.1 and Table 3.2. The first part corresponds to specimen type, i.e. B1 or B2. The second part corresponds to coring direction relative to placement, V for vertical coring and H for horizontal coring. The third and fourth parts correspond to coring day and testing respectively, 3-28 for day 3 coring and day 28 testing.

Table 3.1 Examples of Core Labels for B1 and B2 Beams

Element Type	Orientation	Day Coring	Day Testing	Core Label
B1	V	3	3	B1-V-3-3
B2	H	7	28	B2-H-7-28

Table 3.2 Examples of Cylinder Labels for B1 and B2 Beams

Element Type	Day Testing	Cylinder Label
B1	3	B1-3-Cyl
B2	28	B2-28-Cyl

3.1.2 Girder Web – G1

3.1.2.1 Description

The girder webs were designed to represent the web of large prestressed concrete girders with web heights of approximately 1.6 meters. The congestion of prestressing strands in these girders results in cores being extracted from a particular region within the web and the purpose of this study was to evaluate the variation in concrete performance along the height and length of the structure. The girder webs were cast vertically and cores were extracted horizontally with respect to placement at the top and bottom regions of the web. The web of these highway girders is often thinner than 200 mm preventing the standard length/diameter (L/D) ratio of 2.0 for 100 mm diameter cores. The webs were designed with a thickness of 180 mm and cores were cut to provide 100 mm Ø cores with an L/D ratio of 1.5 as well as 75 mm Ø cores with an L/D ratio of 2.0.

For this study, the girder webs were not prestressed. However, they were reinforced using 2 mats of 10M bars in a grid with adequate spacing for extracting cores. This grid was intended to replicate regions of the girder which would contain congestion from small stirrup spacing. The design consisted of minimal steel reinforcement since the structure would only be exposed to self-weight forces when

moved around the lab. Four identical girder webs were constructed and the design is shown in Figure 3.7.

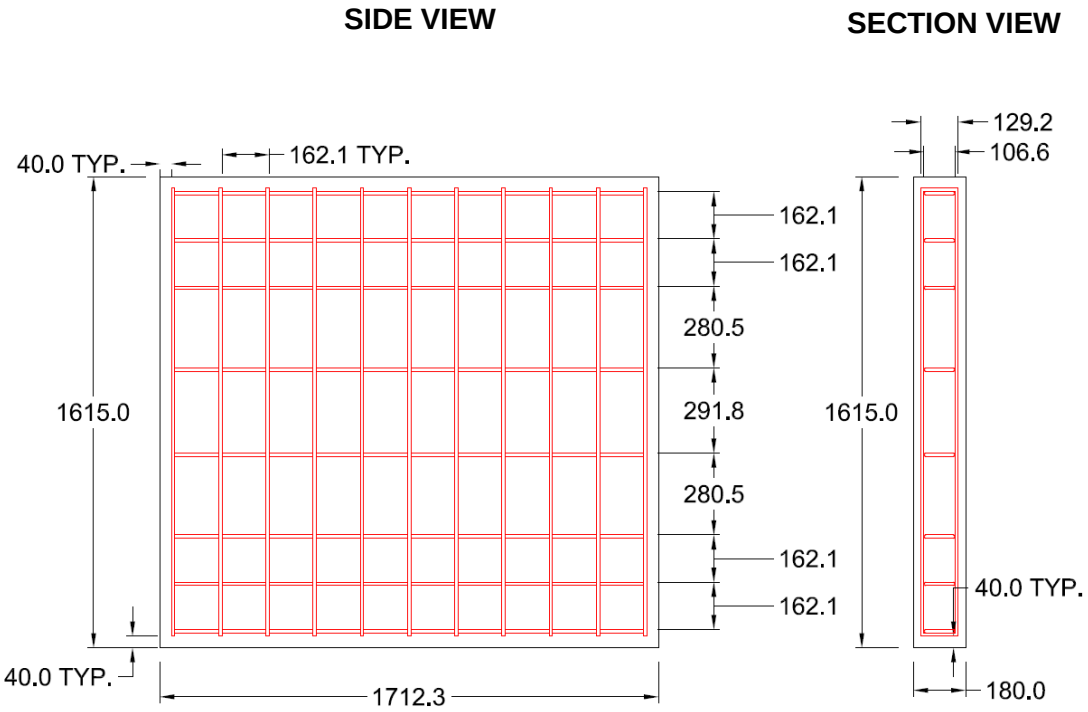

Figure 3.7 G1 Girder Web Design and Reinforcement Layout

The formwork and casting set up were designed to withstand the concrete pressure acting along the height of the girder web. It was constructed using 19 mm formply as the surface material and reinforced with sawn lumber along its height. Form oil was applied to the inside surfaces of the formwork to allow for easier removal of formwork after casting. The full formwork set up is shown in Figure 3.8. The temperature during concrete hydration was monitored using 9 probes in a grid pattern within one of the girder webs. The locations of probes P1 through P9 are indicated in Figure 3.9.

Figure 3.8 Constructed Formwork for G1 Girder Webs

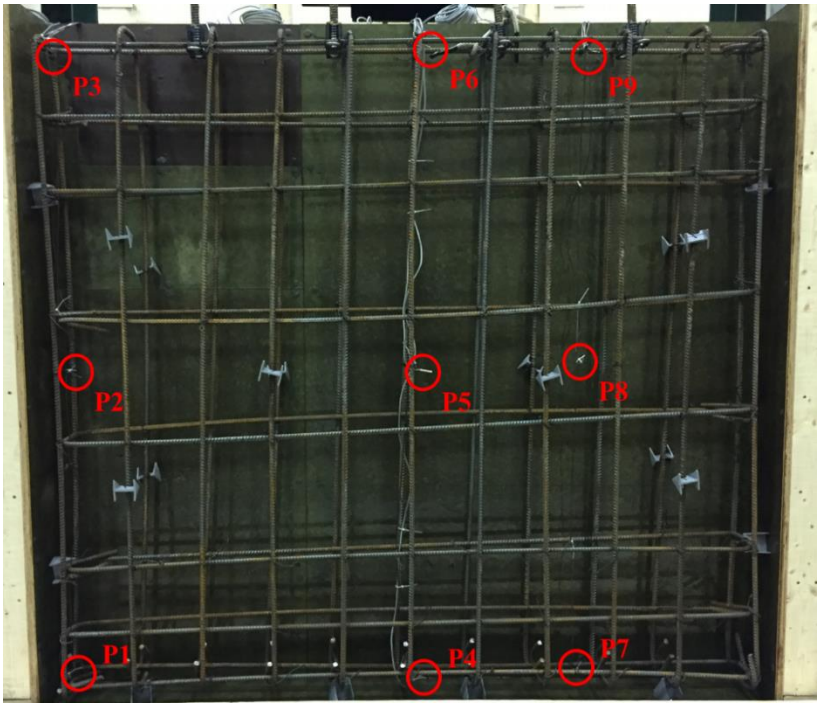

Figure 3.9 Temperature Probe Layout for G1 Girder Web

3.1.2.2 Concrete Mix

The concrete mix chosen for the G1 girder webs had a specified design strength of 60 MPa and contained 80% GU cement and 20% slag for a total cementitious content of 600 kg/m^3, a w/cm ratio of 0.28, and 13 mm nominal maximum aggregate size. This mix was chosen as a possible alternative to the typical design mix which contains high early (HE) cement. At the time of casting, the concrete had a slump of 210 mm, air content of 4.2% and a temperature of 15.6°C.

3.1.2.3 Casting, Curing, and Coring

Similar to the beams, the girder webs were cast indoors with the laboratory bay doors open at the time of pour to provide clearance for the concrete truck. The girder webs were cast on a November morning with an outdoor temperature of approximately -10°C. The girder formwork was filled in 1/3 volume lifts and consolidated using pencil vibrators. Concrete for the cylinders was taken from two wheel barrow loads, one near the start of the cast and the second midway through the cast. The curing and demoulding procedure for the girder webs and cylinders was the same as for the beams.

Coring and testing was carried out on days 3, 7, and 28. All coring was completed using two water-cooled drills which were attached with embedded anchors within the girder webs. The girder webs were placed flat on plywood boards and coring was conducted in a vertical orientation as shown in Figure 3.10. The girder webs were cored through the web thickness and the purpose of the plywood boards underneath was to prevent popout of the core on the opposing side. The two previously used 100 mm diameter coring barrels were inspected and confirmed to be in sufficiently good condition for further coring during this testing. Additionally, two new 75 mm diameter coring barrels were used. The coring was divided evenly between the four coring barrels over the three coring days and coring barrels were inspected each time to assess their condition. No coring issues were encountered on days 3 and 7, but on day 28 coring, 3 of the 40 cores were not able to be used due to contact with steel reinforcement during drilling.

Figure 3.10 Anchored coring drill for coring of G1 girder webs

3.1.2.4 Coring Outline and Core Labelling

The girder webs were designed to allow coring of two rows of 10 cores each near the top and bottom of the web for a total of 40 cores on each coring day. In each row, both 75 mm and 100 mm diameter cores were extracted as shown in Figure 3.11. Some of the cores were extracted and tested on the same day and the remaining cores were placed in calcium hydroxide solution until testing on day 28. In order to obtain an adequate representation of the concrete, cores were selected at random along the length of the girder to form a subset of 3 cores rather than 3 cores from the same region. For example, on day 3, the 100 mm Ø cores, T1, T5, and T8 were tested as a subset (Figure 3.11).

Examples of the labelling scheme used for G1 girder web cores and cylinders are shown in Table 3.3 and Table 3.4. The first part corresponds to specimen type, i.e. G1 for first girder structure studied. The second part corresponds to diameter size of the core, 100 mm or 75 mm. The third part corresponds to coring location in the girder web, T for top of specimen and B for bottom of specimen. The fourth and fifth parts correspond to coring day and testing respectively.

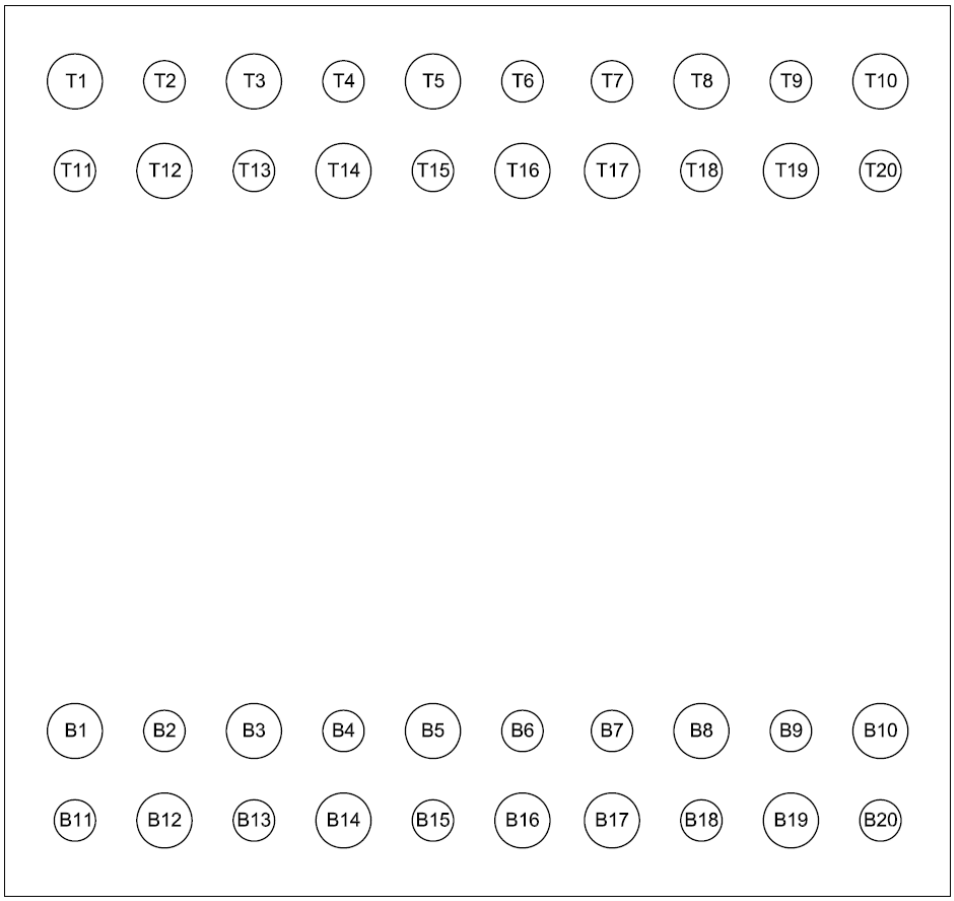

Figure 3.11 Core Location Labelling for G1 Girder Webs

Table 3.3 Examples of Core Labels for G1 Girder Webs

Element Type	Diameter	Top / Bottom Core	Day Coring	Day Testing	Core Label
G1	100	T	3	3	G1-100-T-3-3
G1	75	B	7	28	G1-75-B-7-28

Table 3.4 Examples of Cylinder Labels for G1 Girder Webs

Element Type	Day Testing	Cylinder Label
G1	3	G1-3-Cyl
G1	7	G1-7-Cyl
G1	28	G1-28-Cyl

3.2 Prefabricated Structures

The prefabricated structures included three different structures from three different precast plants to evaluate and compare the results to those achieved in laboratory structures. The structures were constructed, cast, and cored at the precast plant locations. For two of the structures, cores were brought back to the UW lab for testing. For the third structure, testing was completed at the precast plant and at the MTO lab and results were provided to the researchers. The prefabricated structures also provided different concrete mixtures than those from ready-mix plants which were used in the UW lab structures.

3.2.1 Girder Web – G2

3.2.1.1 Description

Similar to the girder webs constructed in the UW lab, a prefabricated girder web section was constructed and cast vertically to represent the web of a large precast prestressed concrete girder. Cores were extracted from the top, middle, and bottom of the girder web to evaluate the variation in concrete performance as a function of the height. The web had a thickness of 160 mm and therefore 75 mm Ø cores with an L/D ratio of 2.0 were used for the study. Four cores with a 100 mm diameter were extracted for RCP and AVS testing as this is the required core size for these tests and the length is unimportant. The girder web was not prestressed, but was reinforced using a single mat of 15M bars in a grid with adequate spacing for extracting cores. The design and reinforcement layout are shown in Figure 3.12.

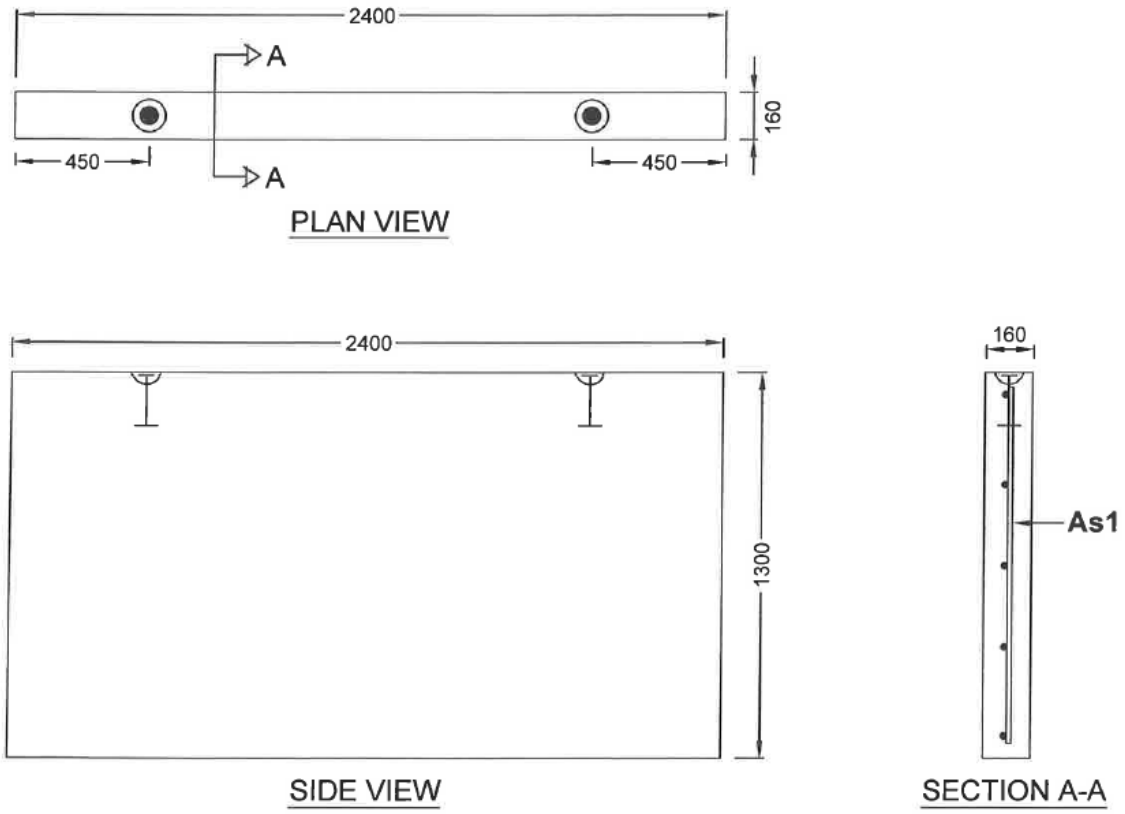

Units: mm

Figure 3.12 G2 Girder Web Design and Reinforcement Layout

The formwork was made of steel forms welded together. The reinforcement cage was lowered into the formwork and plastic rebar chairs were used to achieve approximately 60 mm cover from the two large walls of the web. The temperature during concrete hydration was monitored using 9 probes in a grid pattern attached to the reinforcement cage (Figure 3.13).

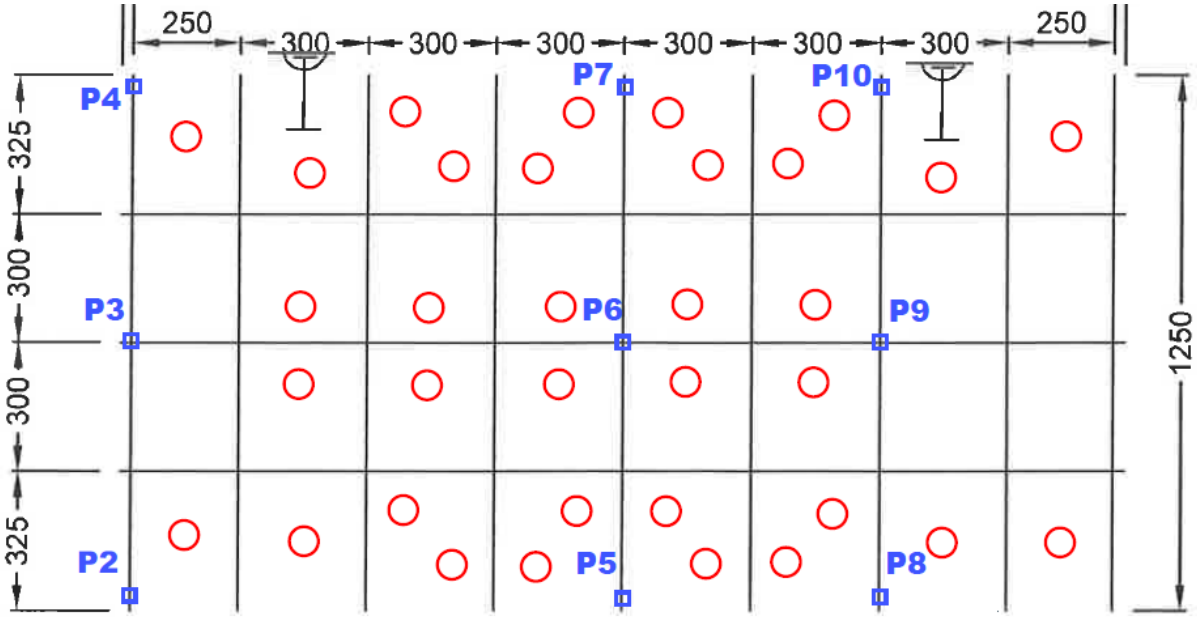

Units: mm

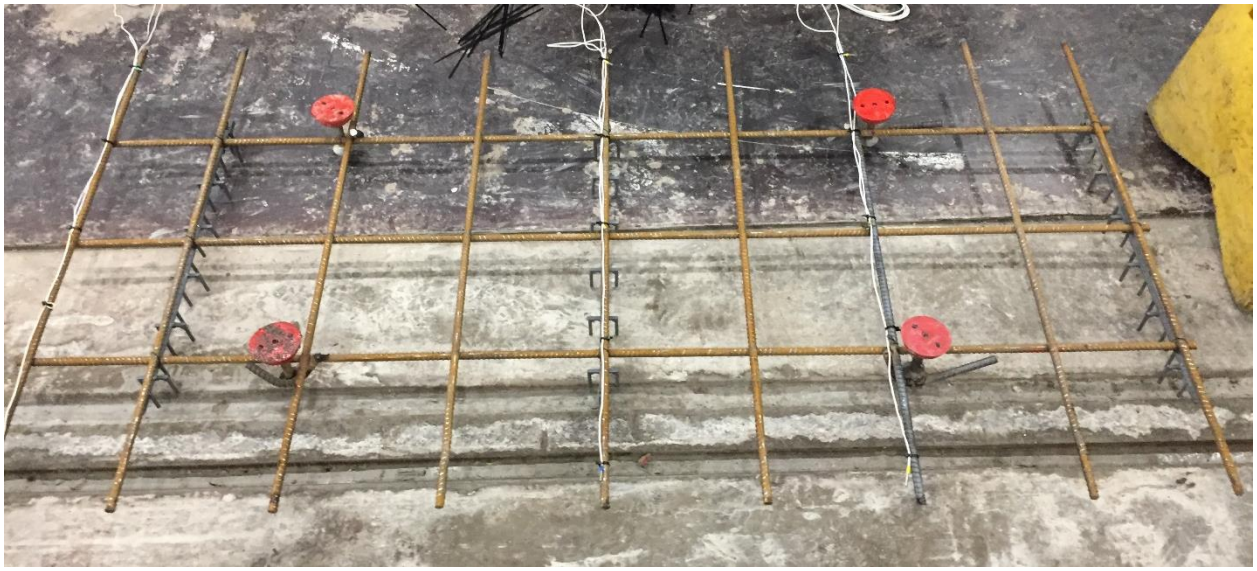

Figure 3.13 Temperature Probe Layout for G2 Girder Web

3.2.1.2 Concrete Mix

The concrete mix contained HE cement typical of that used in large prestressed concrete girders. The design strength at 28 days is 60 MPa; however, the precast plant mixes are typically designed to have very high day 1 strength to allow faster production. This particular mix contained a very high cementitious material content of approximately 630 kg/m^3 of combined HE cement (75%) and slag (25%), a low w/cm ratio of 0.32, and used 13 mm nominal maximum aggregate size. At the time of casting, the concrete had a slump of 225 mm and a temperature of 23.5°C.

3.2.1.3 Casting, Curing, and Coring

The girder web was cast inside the precast plant and consolidated using a pencil vibrator. Concrete for cylinders came from the start of the cast. The exposed top surface of the girder web was covered with presoaked burlap and two layers of plastic tarpaulin following the cast. The formwork was removed 18 hours after casting and placed in a steam kiln two hours later as per this precast plant's curing regime for their girders. The girder web was maintained in the steam kiln for 7 days of curing, except for the temporary removal on day 3 for coring. The steam curing used was intended to provide 100% saturation within the kiln during the curing period and no heat was introduced. Following the completion of 7 days of curing, the girder web was placed outdoors until the end of the 28 day testing period.

Coring and testing were completed on days 3 and 28 and cores were extracted using one water-cooled drill with a diamond tipped coring barrel. The girder web was placed flat on blocks, the drill was vacuum attached to the web, and coring was completed vertically through the thickness of the web. Since there was no support below the girder web, there was a small amount of popout on the back ends of the cores. Immediately after wet coring, the cores were placed in plastic bags and delivered to the UW lab for testing. Core holes were not plugged or grouted following day 3 coring and were left exposed to the elements. The effect of this exposure to variable temperature and moisture on the test results of the cores taken on day 28 is discussed in Sections 4.2, 4.3, and 4.4.

3.2.1.4 Coring Outline and Core Labelling

Core locations were separated into subsets for testing purposes and randomly spread along the length of the girder web. For example, as can be seen in Figure 3.14, cores extracted on day 3 and tested on day 3 (represented by solid blue circles) were from locations T1, T6, and T10. Cores had a diameter of 75 mm and an L/D ratio of 2.0 with the exception of the cores for RCP and AVS testing (represented with solid green solid circles in Figure 3.14). Core locations T4, M1, and B3 were additional spare cores in the event of issues during coring. Since there were no issues encountered, the additional cores were not

extracted. Examples of the labelling scheme used for G2 girder web cores and cylinders are shown in Table 3.5 and Table 3.6.

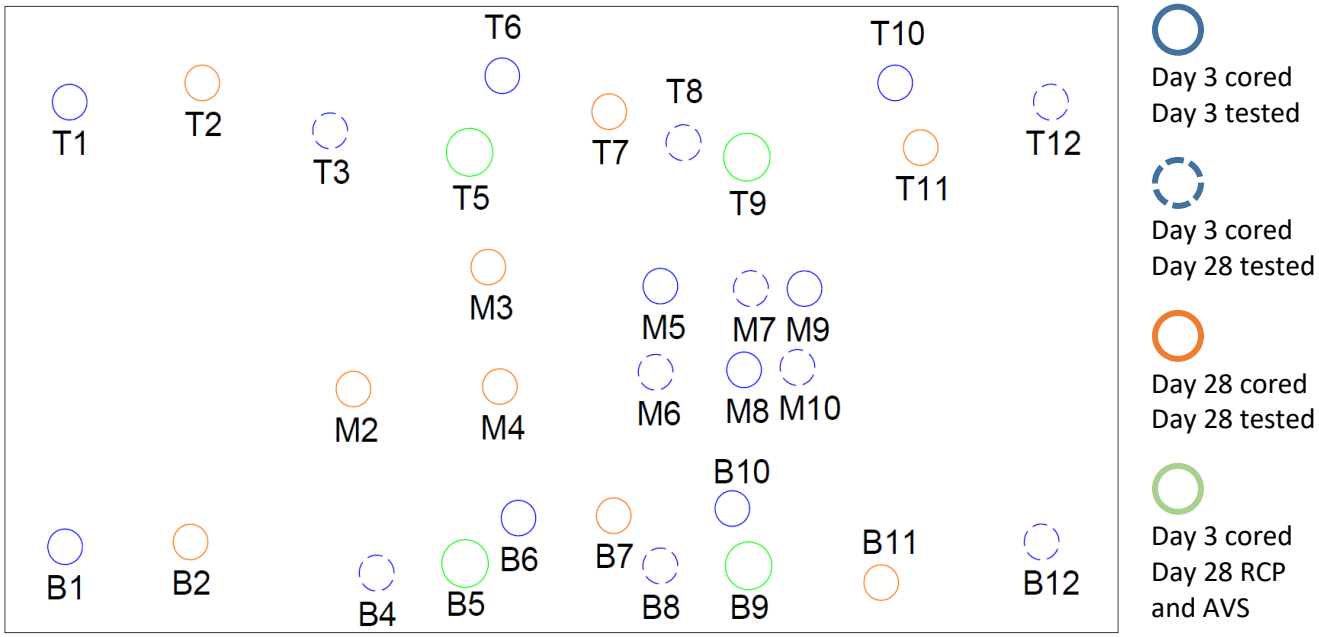

Figure 3.14 G2 Girder Web Core Locations Colour Coded by Day Cored and Tested

Table 3.5 Examples of Core Labels for G2 Girder Web

Element Type	Top / Bottom Core	Day Coring	Day Testing	Core Label
G2	T	3	3	G2-T-3-3
G2	M	3	28	G2-M-3-28
G2	B	28	28	G2-B-28-28

Table 3.6 Examples of Cylinder Labels for G2 Girder Web

Element Type	Day Testing	Cylinder Label
G2	3	G2-3-Cyl
G2	28	G2-28-Cyl

3.2.2 Girder – G3

3.2.2.1 Description

The third girder structure was a true girder complete with flanges. The girder was not reinforced and only contained deeply embedded lifting anchors. The G3 girder was 2 meters tall and 4 meters long and the cross sectional design is shown in Figure 3.15. The formwork was made using typical girder section steel forms. The temperature during concrete hydration was monitored using 3 probes along the length at the mid-height of the girder (Figure 3.16).

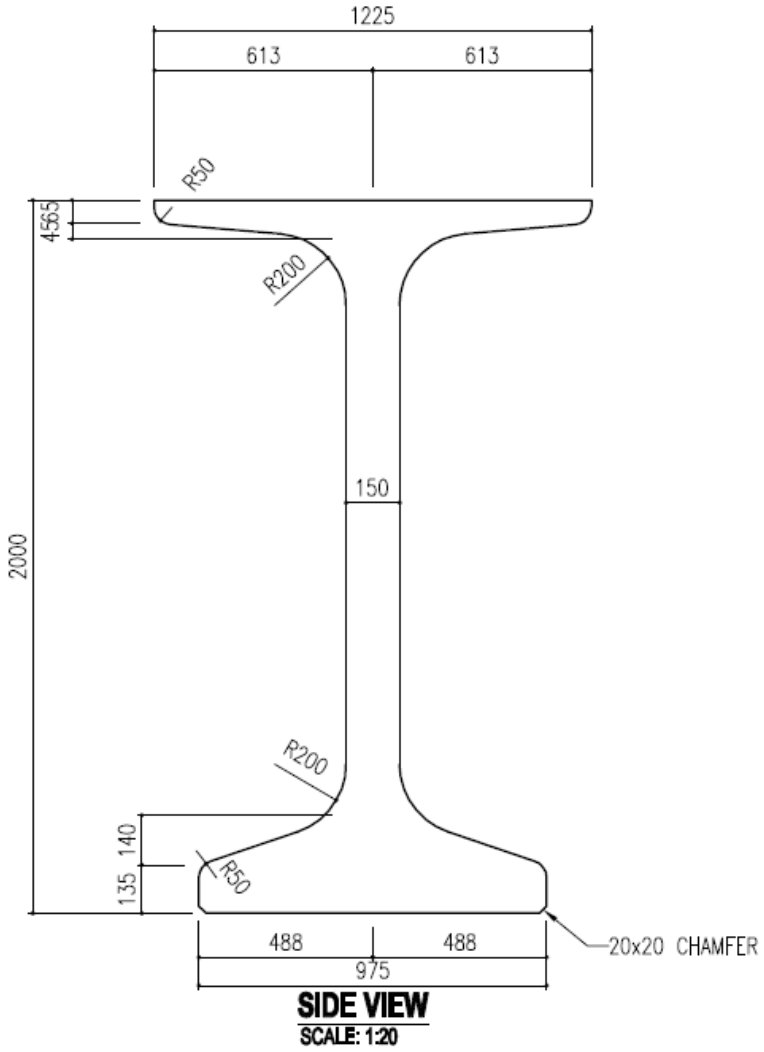

Units: mm

Figure 3.15 G3 Girder Web Design

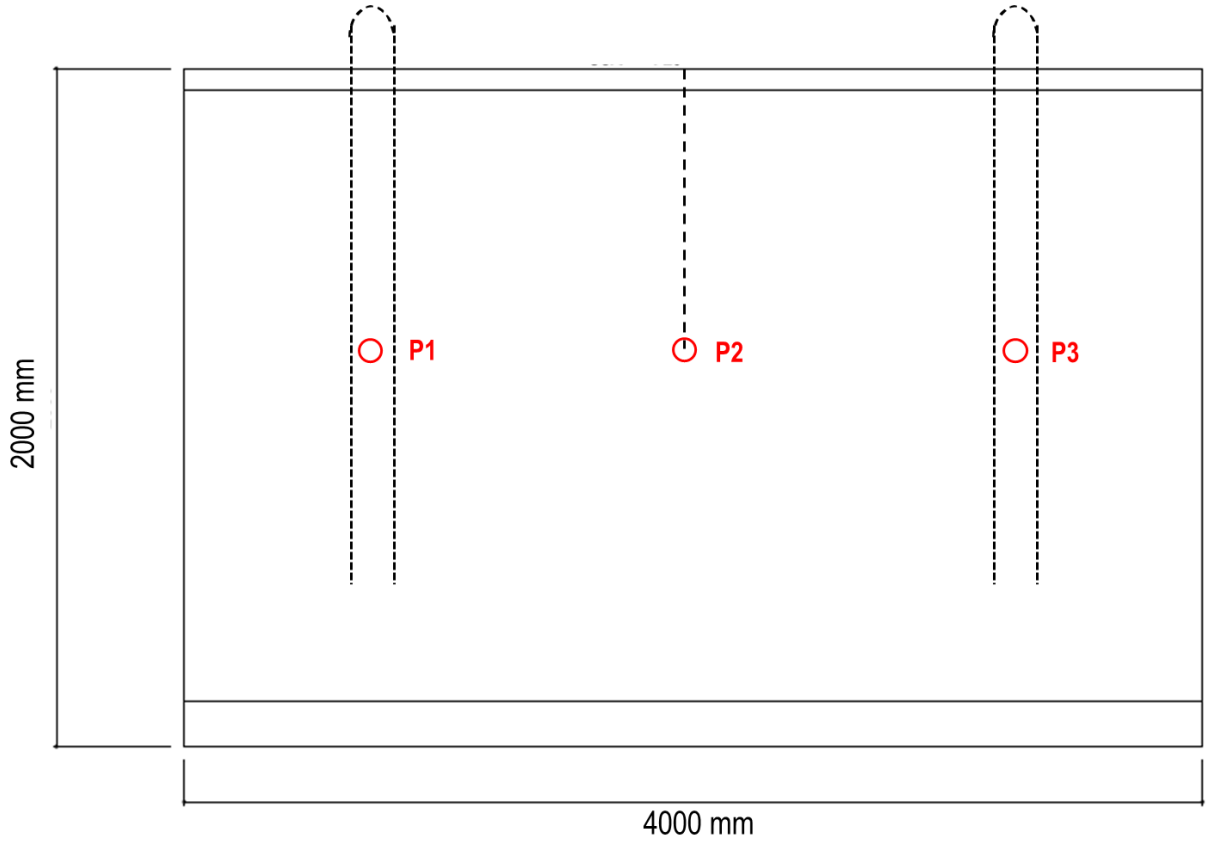

Figure 3.16 Temperature Probe Layout for G3 Girder

3.2.2.2 Concrete Mix

The concrete mix used for the G3 girder had a specified day 28 design strength of 55 MPa and contained a combination of GU cement (74%), silica fume (7%), and fly ash (19%) for total cementitious content of 475 kg/m3, a w/cm ratio of 0.24, and a 13 mm nominal maximum aggregate size. At the time of casting, the concrete had a slump of 220 mm and a temperature of 24.5°C.

3.2.2.3 Casting, Curing, and Coring

The girder was cast inside the precast plant and consolidated using pencil vibrators as well as 1 external vibrator mounted to the formwork. Following the cast, the top of the formwork was covered with presoaked burlap and large tarps were used to cover the entire structure for heated steam curing. The steam curing involved introducing hot steam at a regulated temperature for approximately 6 to 8 hours until the internal concrete temperature approached specification limits and then allowing the temperature to slowly decrease. Due to the requirement of coring many samples on day 3, the beams did not achieve the required 7 days of curing as per OPSS.PROV 1350 (OPSS.PROV 1350 2016) and SSP

999 (SSP 999F31 2016), however, the beams were maintained inside the precast plant slightly below room temperature after 3 days of curing. Cylinders were kept in their moulds with the girder during heated curing and demoulded on day 3. The cylinders were then placed into water (not calcium hydroxide solution).

Cores were taken on days 3 and 28 using one water-cooled drill with a diamond tipped coring barrel. Special mounting bolts were drilled into the structure in order to attach the drill to the girder and coring was completed horizontally for web cores. Testing was conducted on days 3 and 28. Core holes were not plugged or grouted following day 3 coring and were left exposed to the plant environment.

3.2.2.4 Coring Outline and Core Labelling

Due to some miscommunication, the desired core locations were not achieved on day 3. Instead, on day 3, cores were extracted vertically from the top flange, horizontally at the mid-height of the web, and vertically from the bottom flange (Figure 3.17). On day 28, cores were extracted from the same locations as day 3 in addition to horizontal cores from both the top and the bottom of the web. Examples of the labelling scheme used for G3 girder cores and cylinders are show in

Table 3.7 and Table 3.8.

Figure 3.17 Day 3 Core locations in G3 Girder

Table 3.7 Examples of Core Labels for G3 Girder

Element Type	Top / Bottom Core	Day Coring	Day Testing	Core Label
G3	TF	3	3	G3-TF-3-3
G3	T	28	28	G3-T-28-28
G3	M	3	28	G3-M-3-28
G3	B	28	28	G3-B-28-28
G3	BF	3	3	G3-BF-3-3

Table 3.8 Examples of Cylinder Labels for G3 Girder

Element Type	Day Testing	Cylinder Label
G3	3	G3-3-Cyl
G3	28	G3-28-Cyl

3.2.3 Valve Chamber – VC

3.2.3.1 Description

The last prefabricated structure was a valve chamber box, which was not a bridge element, but the concrete used in the chamber is the same as other bridge elements constructed at this particular precast plant. The valve chamber consisted of 4 rectangular walls 254 mm thick and was approximately 2270 mm tall as shown in Figure 3.18.

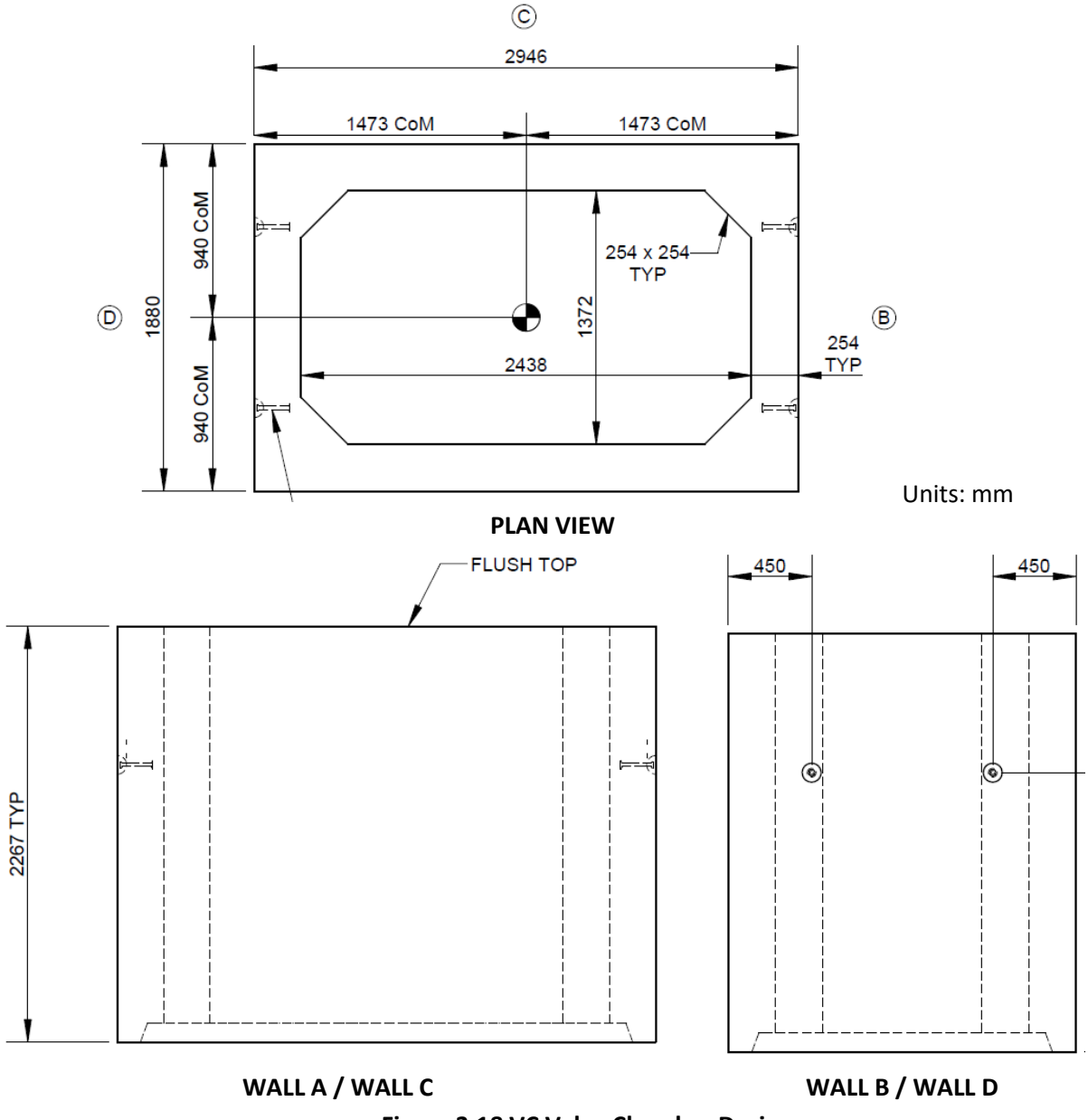

Figure 3.18 VC Valve Chamber Design

The VC chamber contained minimum reinforcement using 15M bars in a grid with adequate spacing for extracting cores. The formwork was made from large steel sections clamped and bolted together. The reinforcement cage was lowered into the formwork and plastic rebar chairs were used to achieve desired cover on each wall. The temperature during concrete hydration was monitored using 4 probes along the centre line in Wall D with 3 probes along the centre thickness of the wall and 1 probe near the concrete surface at the mid-height of the wall (Figure 3.19).

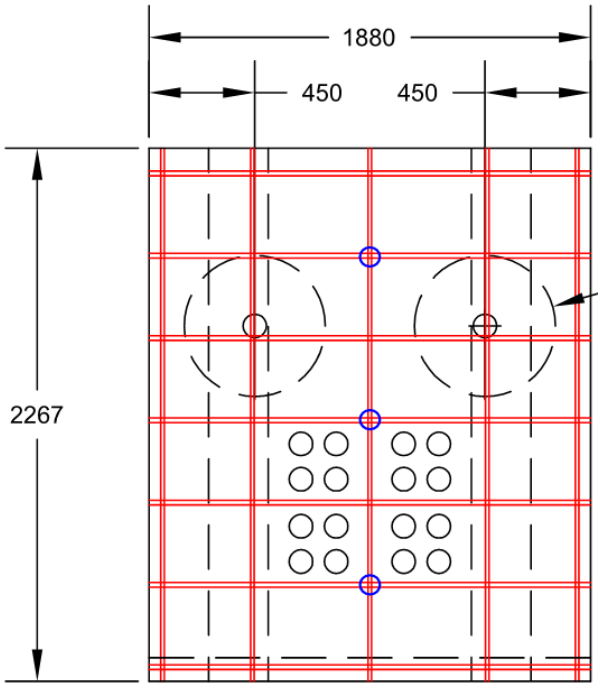

WALL D

Figure 3.19 Temperature Probe Layout for VC Chamber

3.2.3.2 Concrete Mix

The concrete mix used for the VC chamber was a self-consolidating concrete (SCC) containing HE cement and 25% slag. The design strength of the mix at 28 days is 40 MPa; however, a minimum day 1 average cylinder strength of 20 MPa is desired for this concrete to remove the structure from its formwork. The cast required 3 batches to complete and the average cementitious content and average w/cm ratio between the 3 batches were 480 kg/m^3 and 0.36, respectively. At the time of casting, fresh concrete properties were tested from the first batch and the concrete had a slump flow diameter of 580 mm, air content of 7.9%, and a temperature of 20.1°C.

3.2.3.3 Casting, Curing, and Coring

The valve chamber was cast inside the precast plant using 3 batches due to the capacity of the mixer. The time between pouring of batches into the formwork was approximately 5 minutes. The first two batches filled most of the formwork with the third batch completing a small portion of approximately 100 mm at the top. All three batches were poured at the centre of Wall A and since the concrete was an SCC mix, the concrete freely flowed around the perimeter of the formwork and no vibration was required for consolidation. The exposed top surface of the chamber was covered with an insulated tarpaulin until the chamber was removed from its formwork 18 hours after casting with no additional curing applied. The valve chamber did not require a longer curing period which was common with the previous structures since it was not a bridge element, but if the testing were to be repeated, it would be recommended to match the curing used for typical bridge elements using OPSS.PROV 1350 (OPSS.PROV 1350 2016) and SSP 999 (SSP 999F31 2016). The valve chamber was placed outdoors approximately 45 hours after casting and was exposed to the elements for the remainder of the testing period during March which included freezing periods and winter-like weather. Cylinders were kept in their moulds with the valve chamber until transporting to the UW lab and demoulding on day 3. The cylinders were then placed into a tub with calcium hydroxide solution.

Following the removal of the chamber from the formwork, the joints between the batches were visible on the concrete surface, in particular, between the second and third batches. However, since coring was completed closest to the mid-height of the chamber, the joint between the first and second lifts is of more importance. The joint was least apparent on Wall A which was closest to the pouring location (Figure 3.20a) and most apparent on Wall C which was the opposite side (Figure 3.20b). The side walls (B and D) also showed the joints between batches. It appears that the concrete blended well at the pouring location due to the gravity of falling concrete, but did not blend at the furthest location from pouring which may be one of the limitations of using SCC.

(a) Wall A – Pouring location

(b) Wall B

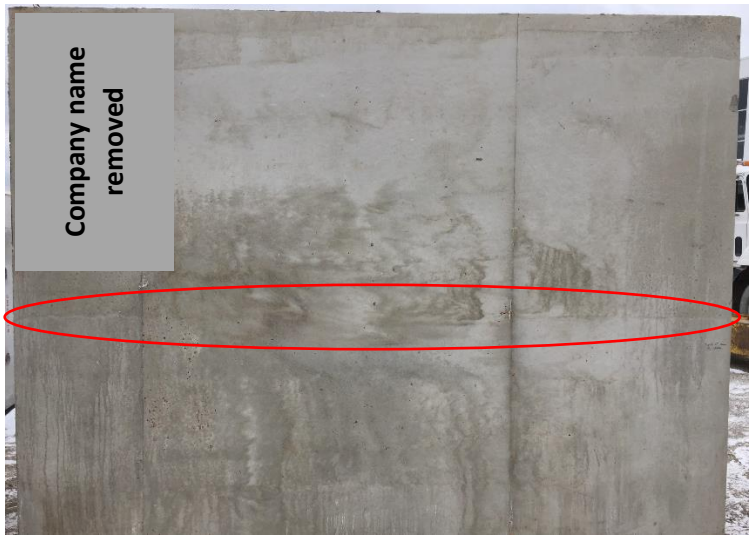

(c) Wall C – Opposite end from pouring location

(d) Wall D

Figure 3.20 Joints between concrete batches in VC Chamber cast

Coring drills were horizontally attached to the walls of the valve chamber using post-installed anchors to adequately secure the drill base and coring was completed through the thickness of the wall. After coring, the cores were placed inside plastic bags and transported to the UW lab. Core holes were plugged at both ends using the same procedure for B1 and B2 beams to prevent moisture loss from the structure for coring on future days.

3.2.3.4 Coring Outline and Core Labelling

Coring was completed on all four walls of the valve chamber, but only those from the two smaller walls (B and D) were used for the data in this thesis. Wall D was cored on days 3 and 14 and Wall B was cored on days 7 and 28 (Figure 3.21). The coring drill barrel had an outer diameter of 100 mm and, therefore, the cores had a diameter of 94 mm and were trimmed to an L/D ratio of 2.0. Cores were extracted around the mid-height of the chamber with cores being taken from both batches of the poured concrete. Examples of the labelling scheme used for VC cores and cylinders are shown in Table 3.9 and Table 3.10.

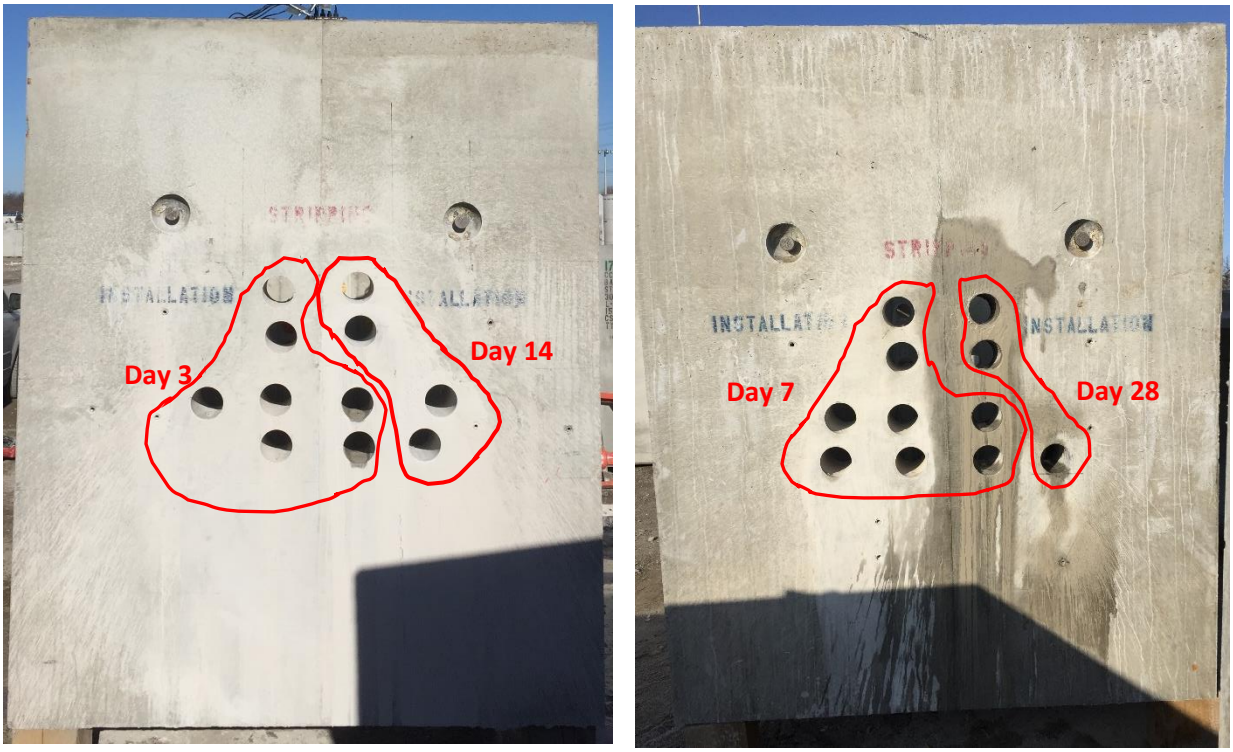

Wall D – Day 3 and 14 coring

Wall B – Day 7 and 28 coring

Figure 3.21 VC Chamber Core Locations

Table 3.9 Examples of Core Labels for VC Chamber

Element Type	Day Coring	Day Testing	Core Label
VC	3	3	VC-3-3
VC	7	7	VC-7-7
VC	28	28	VC-28-28

Table 3.10 Examples of Cylinder Labels for VC Chamber

Element Type	Day Testing	Cylinder Label
VC	3	VC-3-Cyl
VC	7	VC-7-Cyl
VC	28	VC-28-Cyl

3.3 Testing Procedure

3.3.1 Sample Preparation

The lab structures were cored in the UW lab and, therefore, no transportation was involved in sample preparation. Immediately after coring, cores were cut using a concrete saw to their appropriate length based on desired L/D ratio and the ends were ground to ensure two flat, parallel surfaces for testing. The prefabricated structures were cored at their respective plants and then cores were transported back to the lab for testing. Cores from the G2 and VC structures were placed in plastic bags, transported to the UW lab where they were cut to their appropriate length and the ends were ground. Some of the cores from the G3 girder were cut and ground at the plant for testing at the plant. The remaining G3 cores were wrapped in bubble wrap and shipped to an MTO lab where they were cut to length and end-ground. Cylinders for all testing were end-ground to an L/D ratio of 2.0. The cored lengths and cut lengths of all tested cores are shown in Figure 3.22 and the cutting and grinding process of cores is shown in Figure 3.23.

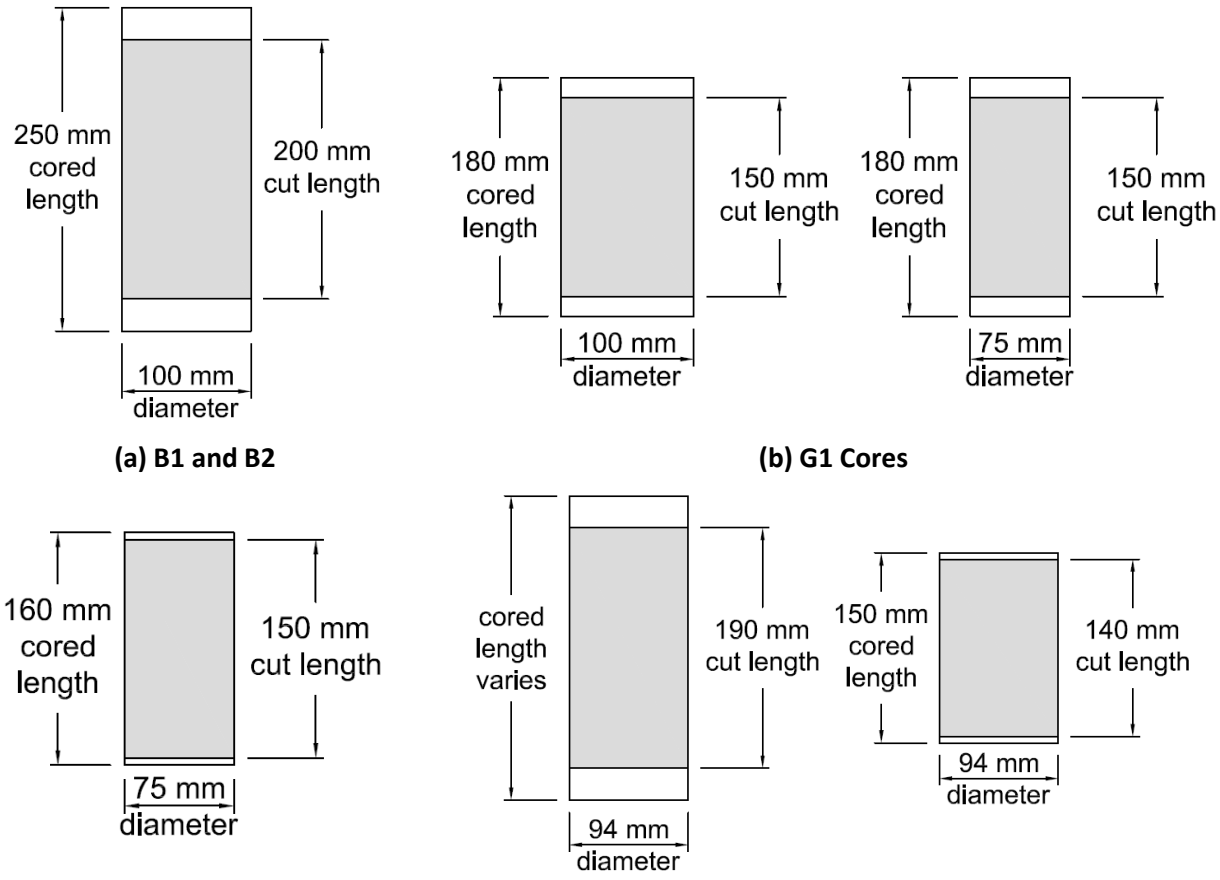

(a) B1 and B2 **(b) G1 Cores**

(c) G2 Cores **(d) G3 Cores and VC Cores (left only)**

Figure 3.22 Cored Lengths and Cut Lengths of all Tested Cores

Figure 3.23 Cutting and end-grinding of cores

3.3.2 Conditioning

The cores which were not being tested on the same day as coring, were cut and end-ground, and then placed in a tub containing calcium hydroxide solution (lime water) to maintain a fully saturated state of the cores (Figure 3.24). The cylinders were kept in their moulds until day 3 and then placed in the calcium hydroxide solution alongside the cores.

Figure 3.24 Sealed and Soaked Conditioning of Cores

3.3.3 Sample Characteristics

Prior to testing, the cores and cylinders were measured and weighed to quantify the dimensions and mass of each sample in order to determine the approximate cross-sectional area for compressive strength calculation and to determine the approximate volume for the sample density. A digital caliper was used to measure the diameter and length of each core and cylinder. The diameter was taken using an average of two readings at right angles to each other at approximately the mid-height of the sample as per CSA A23.2-9C (CSA A23.1 / CSA A23.2 2015) and the length was taken using an average of two readings at right angles to each other. The samples were then placed on a scale to determine their mass and the approximate density of each sample was then calculated by dividing the mass by the approximate volume of the sample. Lastly, the cores and cylinders were thoroughly inspected and documented to determine the presence of imperfections which include, but are not limited to the presence of voids, surface ridges from poor coring, or poor consolidation during cylinder rodding.

3.3.4 Rapid Chloride Permeability Testing

The concrete's ability to resist chloride ion penetration was determined using the rapid chloride permeability (RCP) test outlined in the Ministry of Transportation Ontario Lab Testing Manual, LS-433 (LS-433 2011) and the American standard, ASTM C1202 (ASTM C1202-12 2012). Cores and cylinders were sent to an MTO lab where two 50 mm samples were cut from each core and cylinder and two RCP tests were conducted. The RCP test is completed on day 28 and, therefore, only cores extracted on days 3, 7, and 14 were used for RCP testing. The RCP test set-up is shown in Figure 3.25 and an example of a tested set of samples is shown in Figure 3.26.

Figure 3.25 Rapid Chloride Permeability Test Set-up

Figure 3.26 Rapid Chloride Permeability Test Samples from B2 Beams

The OPSS 1350 (OPSS.PROV 1350 2016), OPSS 909 (OPSS.PROV 909 2016), and SSP 999 (SSP 999F31 2016) guidelines provide the following acceptance criteria for concrete used in Ontario infrastructure. For concretes containing silica fume the average charge passed must be no more than 1000 Coulombs and, all other concretes, no more than 2500 Coulombs. Concretes exceeding these values can be subjected to payment adjustments by the contractor or supplier or even removal and replacement in the event that the RCP results exceed 2000 Coulombs for concrete containing silica fume and 3500 Coulombs for all other concretes.

3.3.5 Electrical Resistivity testing

An alternative to the RCP testing procedure is an electrical resistivity measurement of the concrete. The bulk resistivity of the concrete can be measured using a uniaxial method where the concrete samples is placed between two parallel metal plates (electrodes) with moist sponge contacts at the interfaces to ensure an electrical connection. An AC current is applied between the electrodes and the potential difference is measured (Layssi et al. 2015). The resistivity, ρ, is calculated using a relationship between the resistance, R, and a geometry factor, k, which depends on the length and cross-sectional area of the sample being tested (Equation 1). The bulk resistivity measurement set-up is shown in Figure 3.27.

$$\rho = R \times k\ [k\Omega \cdot cm] \quad (1)$$

Figure 3.27 Bulk Resistivity Measurement

The electrical resistivity measurements of the cores were performed on the same day as core extraction. The cores were removed using a wet coring process, followed by cutting and grinding using wet processes. Prior to recording the electrical resistivity, both cores and cylinders were kept in a bucket of water for approximately 5 minutes and then placed between the two electrodes of the resistivity meter to record the measurement.

3.3.6 Compression Testing

After the samples were measured, described, and tested for electrical resistivity, they were tested for compressive strength following CSA A23.2-9C – Compressive Strength of Cylindrical Concrete Specimens (CSA A23.1 / CSA A23.2 2015). The samples were tested in a hydraulic compression testing machine (Figure 3.28), using the loading rates specified in CSA A23.2-9C. Peak loads of each sample were recorded, as well as the failure type.

Figure 3.28 Hydraulic Compressive Testing Machine in the UW Lab

3.3.7 Air Void Analysis

The hardened concrete air content was determined using an air void system (AVS) analysis following the procedure outlined in LS-432 (LS-432 2017) and ASTM C457 (ASTM C457/C457M-12 2012). The B1 concrete is validated according to the OPSS 1350 (OPSS.PROV 1350 2016) guideline which specifies the minimum air content must be 3.0% and the maximum spacing factor must be 0.230 mm. The remaining concretes which are representative of precast style structures are validated according to the OPSS 909 (OPSS.PROV 909 2016) and SSP 999 (SSP 999F31 2016) guidelines which involve precast concrete structures and specify the minimum air content must be 3.0% and the maximum spacing factor must be 0.200 mm. The AVS analysis for each tested sample provided the results for air content as a percentage, spacing factor as a length, paste content as a percentage, and specific surface as a reciprocal length. The spacing factor is defined as a parameter related to the maximum distance in the cement paste between air voids which in simpler terms relates to the distance water would need to travel in the paste before entering an air void (ASTM C457/C457M-12 2012; Portland Cement Association 1998). The specific surface is defined as the surface area of the air voids divided by their volume and a larger specific surface typically indicates a greater number of small air bubbles which is better for freeze-thaw durability (ASTM C457/C457M-12 2012; Portland Cement Association 1998).

4 Experimental Results

4.1 Hydration Temperature Profiles

It is important to distinguish the differences between the lab structures and the prefabrication plant structures to understand the effects of temperature on the hydration of the concrete. The prefabrication plants are much larger than the UW lab and many operations occur throughout the day resulting in bay doors remaining open or frequently being opened. There will be more airflow movement past the structure which can result in faster cooling rates. The ambient temperature through the plant is not as steady as it is in the lab and can vary during the day, which can cause the structure to be subjected to some outdoor temperatures. Instead of the wood formwork used in the lab, the plant formwork was made of steel which has greater heat conduction and can cause the temperature during hydration to dissipate more quickly than through wood. The combination of these effects results in lower hydration temperatures which can be particularly favourable for the larger structural elements being constructed at the plants.

4.1.1 Laboratory Structures

The temperature change due to heat of hydration for B1 and B2 beams is shown in Figure 4.1 and Figure 4.2. The center of the B1 beam reached 41°C after approximately 36 hours and the center of the B2 beam reached 56°C after approximately 26 hours. The concrete for B2 beams contained silica fume which caused a faster reaction as well as the higher hydration temperature compared to the concrete for B1 beams. Unfortunately only one thermocouple was used in the beams and it would have been beneficial to place more along the length. During the B2 beam cast, thermocouples were also placed inside some concrete cylinders to measure the difference between the much larger beams and the cylinders. In Figure 4.2, it is seen that the cylinders peaked at approximately 24°C and then began to follow the ambient temperature after 24 hours. Based on the temperature profiles of the cylinders from the B2 concrete, it is safe to assume the cylinders from the B1 concrete would not have exceeded 24°C since the B1 concrete contained a lower total cementitious content and would have a lower heat of hydration temperature than the B2 concrete. This leads us to conclude that the difference in temperature between the center of the B1 beam and the cylinder would be approximately 15°C compared to the difference between the B2 beam and the cylinders which is close to 30°C. This effect of temperature on the early and late day compressive strength is discussed in Chapter 4.2. Both sets of beams were stripped of their formwork after 72 hours (3 days) and the sharp dip in the temperature

profile of the B2 beam is due to the beam being cored close to the thermocouple with a water-cooled drill on day 3.

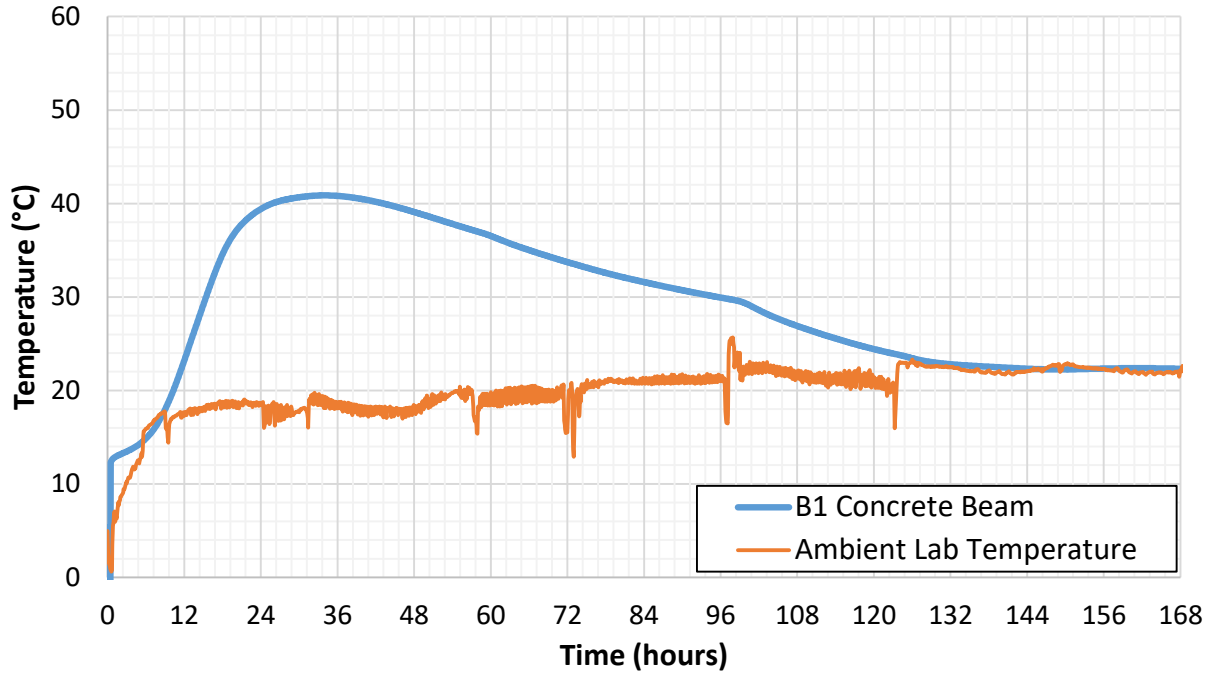

Figure 4.1 Temperature Profile for B1 Beam

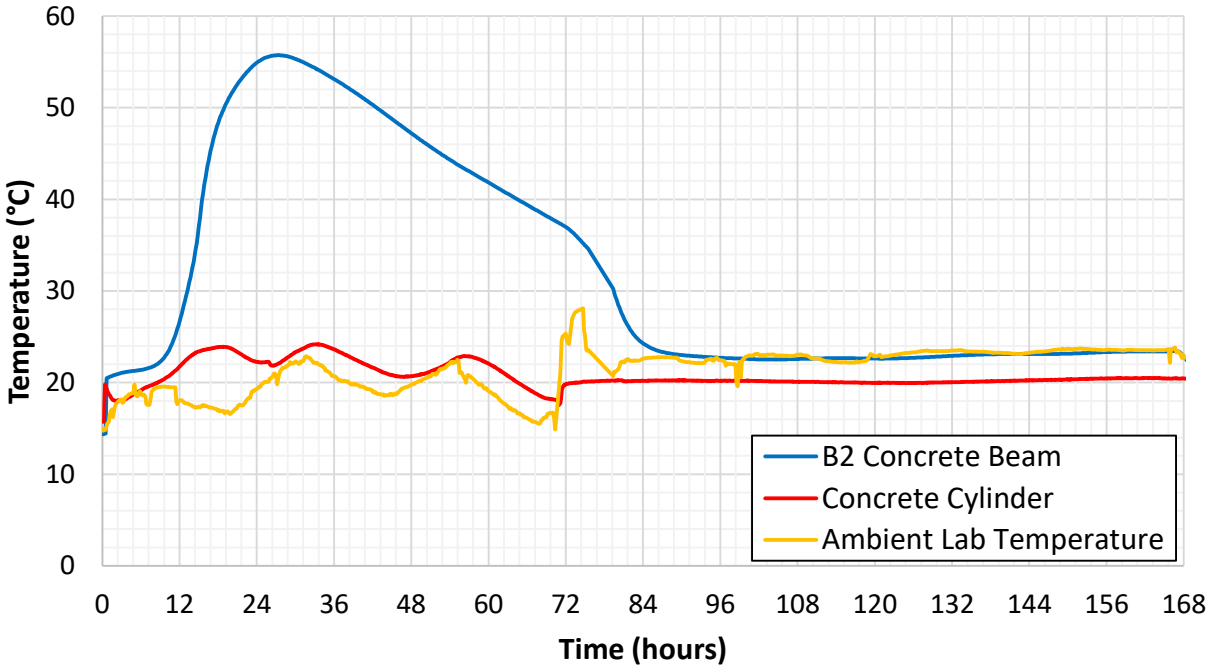

Figure 4.2 Temperature Profile for B2 Beam

The center (P5) of the G1 girder web reached approximately 57°C compared to the bottom left corner (P1) which only achieved 41°C (Figure 4.3). There is also a difference in time to reach the temperature peak. The thermocouple probes located closer to the edges (P1, P3, P4, P7, and P9) reached their respective peaks after approximately 14 hours compared to the approximately 20 hours for those located closer to the middle of the web (P2, P5, P6, and P8). Due to the wooden formwork and relatively steady ambient lab temperature, the girder web took approximately 96 hours (4 days) to cool to room temperature. The structure was removed from its formwork after 72 hours and since the webs are fairly thin, the heat dissipation was relatively uniform after formwork removal. It is also seen that slightly higher temperature peaks were recorded at the top of the girder web than near the bottom. This indicates that there was more thermal loss through the base of the formwork (which was made of 3 layers of 19 mm plywood on top of the concrete floor) compared to the top of the girder which was covered with soaked burlap and a tarpaulin.

The concrete cylinder with a much smaller volume only reached 31°C and had cooled to room temperature all before 24 hours. As a result we can expect the cylinders to have hydrated at a much slower rate compared to the structure and this effect is reflected in the discussion of compressive strength in Chapter 4.2.

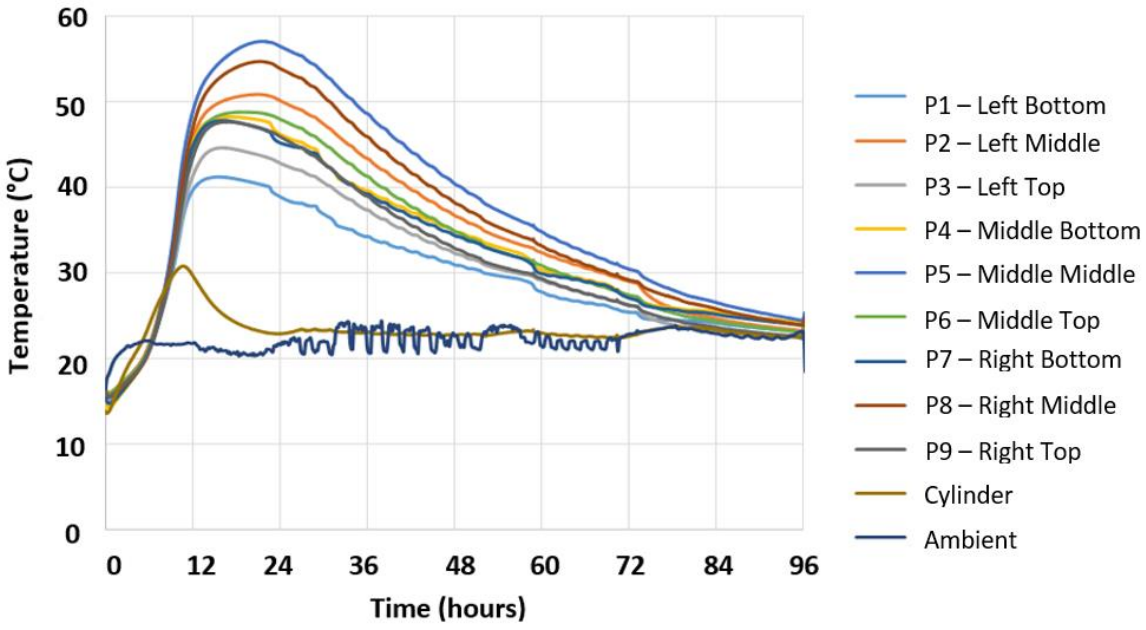

Figure 4.3 Temperature Profile for G1 Girder Web

4.1.2 Prefabrication Plant Structures

The G2 girder produced at Precast Plant #1

The G2 girder web was similar in size to the G1 girder web, however it was approximately 20 mm thinner and was cast in steel formwork. As it is seen in Figure 4.4, the center of the web reached 49°C compared to the center of the G1 web which reached 57°C. There was approximately 15 to 20°C difference between the center of the web and the bottom corner. Unlike the G1 girder, the G2 girder web reached maximum hydration temperature after approximately 10 hours in all locations measured. The formwork was stripped from the G2 web after approximately 20 hours and all the probes returned to the ambient lab temperature shortly after 24 hours. The increase seen in the ambient temperature is the result of the ambient temperature probe being placed inside a plastic covering along with the data logger case to protect the case from being damaged.

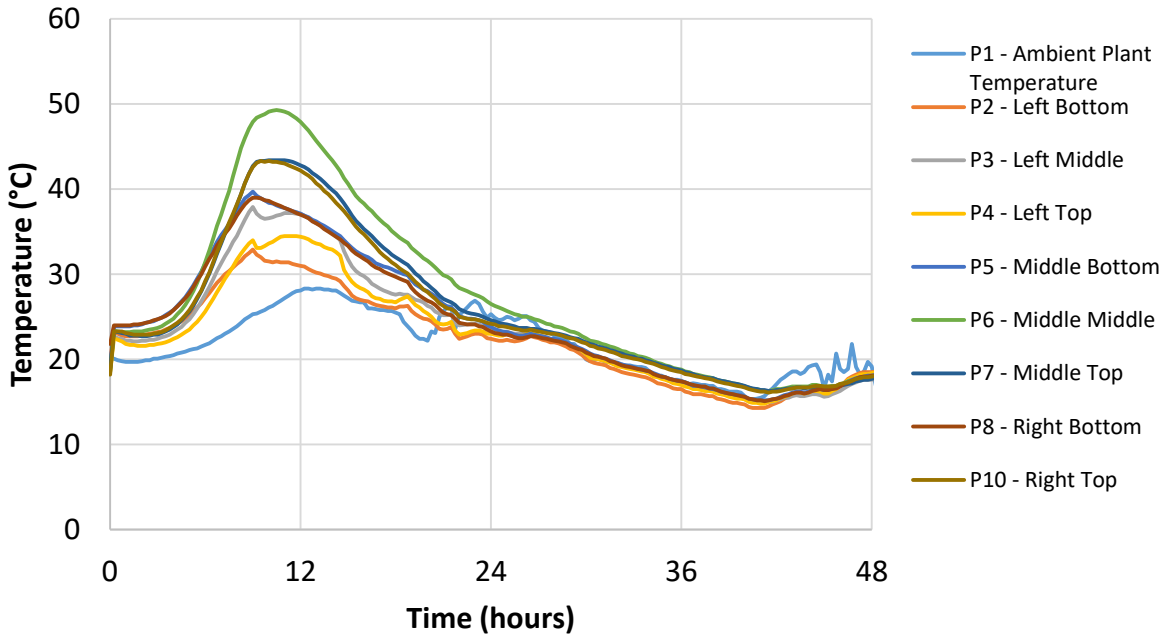

Figure 4.4 Temperature Profile for G2 Girder Web

The G3 girder produced at Precast Plant #2

The G3 girder was the only structure subjected to heat curing which is represented by the 'Heated Ambient Temperature' profile in Figure 4.5. Based on the difference between the temperature profiles of the north (P1) and south (P2) ends of the girder, it appears that the heat was introduced near the

south end of the structure causing a faster and higher hydration temperature peak in the concrete on the south end. It is also seen that the center of the girder had a slightly delayed peak temperature following the heat curing. The first peak of the girder center at approximately 50°C is attributed to the cement hydration on its own with the second peak at approximately 60°C relating to the additional heat introduced through curing. The temperature of the structure cooled to the ambient plant temperature after approximately 48 hours. The formwork was stripped after 72 hours.

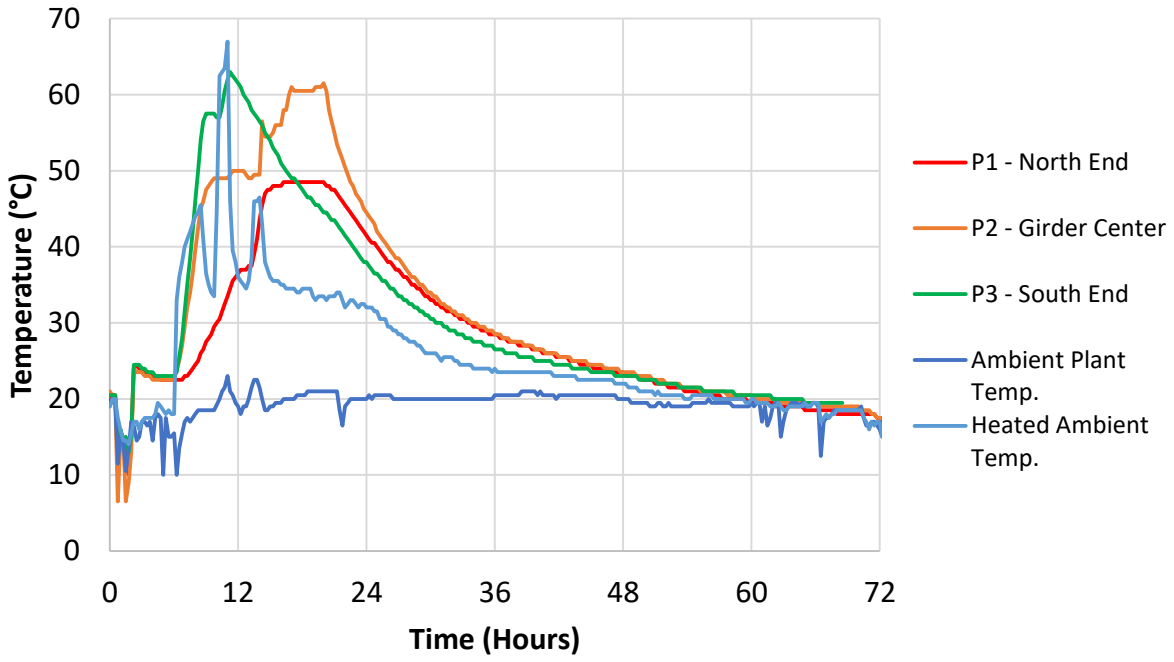

Figure 4.5 Temperature Profile for G3 Girder

The Valve Chamber VC cast at Pre-Cast Plant #3.

The variation within the VC chamber between center and edges was less than 10°C with the center of the wall reaching 42°C after approximately 14 hours (Figure 4.6). The VC chamber was covered with an insulating tarpaulin after casting which explains the smaller variation between the top thermocouple probe (P1) and center probe (P2). The formwork was set up such that the concrete was approximately 500 mm above the plant floor and as a result there was less thermal loss through the bottom. These factors aided in ensuring a more uniform temperature along the height of the structure during casting. A thermocouple was also placed inside the concrete near the surface to measure the variation through the thickness of the wall. The difference between these two locations (P2 and P3) was approximately 5°C. The structure was stripped of its formwork approximately 18 hours after casting and was kept inside the

plant until being placed outside 45 hours after casting, which is seen in the drop in temperature in Figure 4.6.

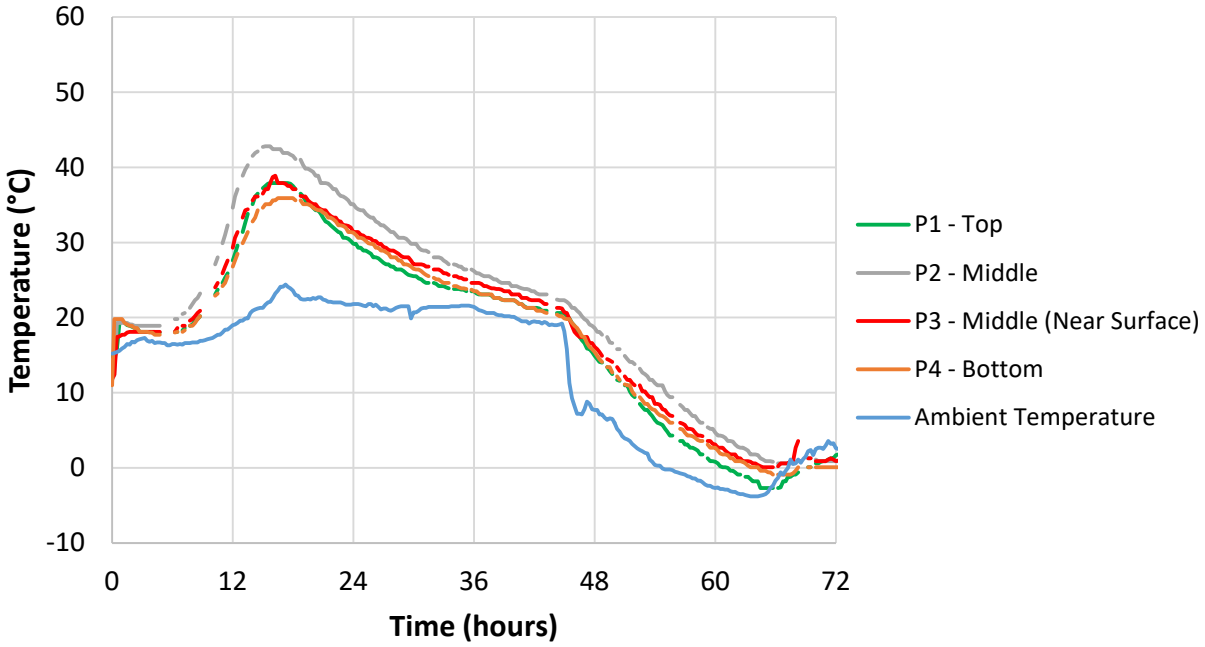

Figure 4.6 Temperature Profile for VC Chamber

4.2 Compressive Strength

In the following figures, the data points refer to an average of three (3) samples with error bars indicating one standard deviation above and below the average compressive strength.

4.2.1 Cylinder Strengths from Tested Concrete Mixtures

The strength of the cylinders represent the quality of the concrete produced and, in all cases of the mixtures used for testing in this research, the day 28 compressive strength of the cylinders was greater than the specified 28 day design strength (Table 4.1). The results in Figure 4.7 show that all mixes were equal to or great than the specified design strength by day 7 and in the case of the two mixes containing HE cement (G2 and VC), the specified design strength was exceeded as early as day 3. These two mixes experienced only a small increase in strength between day 7 and day 28. This behaviour is different from the two mixes containing silica fume (B2 and G3) which experienced early strength gain, but also continued to gain strength between day 7 and day 28. In the case of B2 concrete, the day 7 strength was approximately 50 MPa (equal to the specified 28 day design strength) and the strength increased to almost 70 MPa on day 28. The G1 and G2 mixes which contained very large cementitious content

behaved quite similarly between day 14 and day 28, but the G2 mix with HE cement experienced a more rapid reaction up to day 14 compared to the GU cement mix.

Table 4.1 Summary of Tested Concrete Mixtures

Name	Day 28 Design Strength, f'c (MPa)	Average Day 28 Cylinder Strength (MPa)	Total cementitious content (kg/m^3)	Cement Type	SCM Types
B1	30	39.7	350	GU	Slag (9%)
B2	50	67.8	Not provided	GU	Silica fume (8%)
G1	60	73.8	600	GU	Slag (20%)
G2	60	73.2	630	HE	Slag (25%)
G3	55	80.6	475	GU	Silica fume (7%) and Fly ash (19%)
VC	40	56.8	480	HE	Slag (25%)

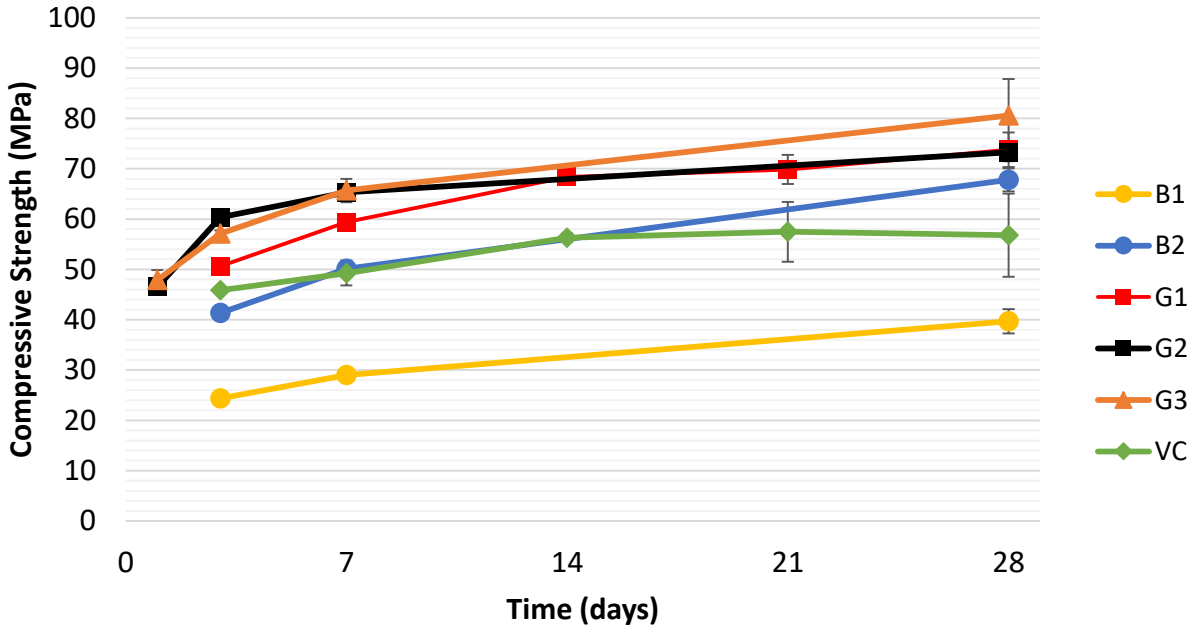

Figure 4.7 Cylinder Compressive Strengths from All Concrete Mixtures Tested

4.2.2 Cores from B1 Beams

Some researchers found that the vertical cores had a stronger compressive strength than the horizontal cores (Carroll et al. 2016; Suprenant 1985) and others found no difference at all (F Michael Bartlett and MacGregor 1994). In the case of the B1 beams, the horizontal cores were, in fact, slightly greater in

compressive strength than the vertical cores, as shown in Figure 4.8. The horizontal cores were, respectively, between 17%, 6%, and 12% stronger than the vertical cores on days 3, 7, and 28.

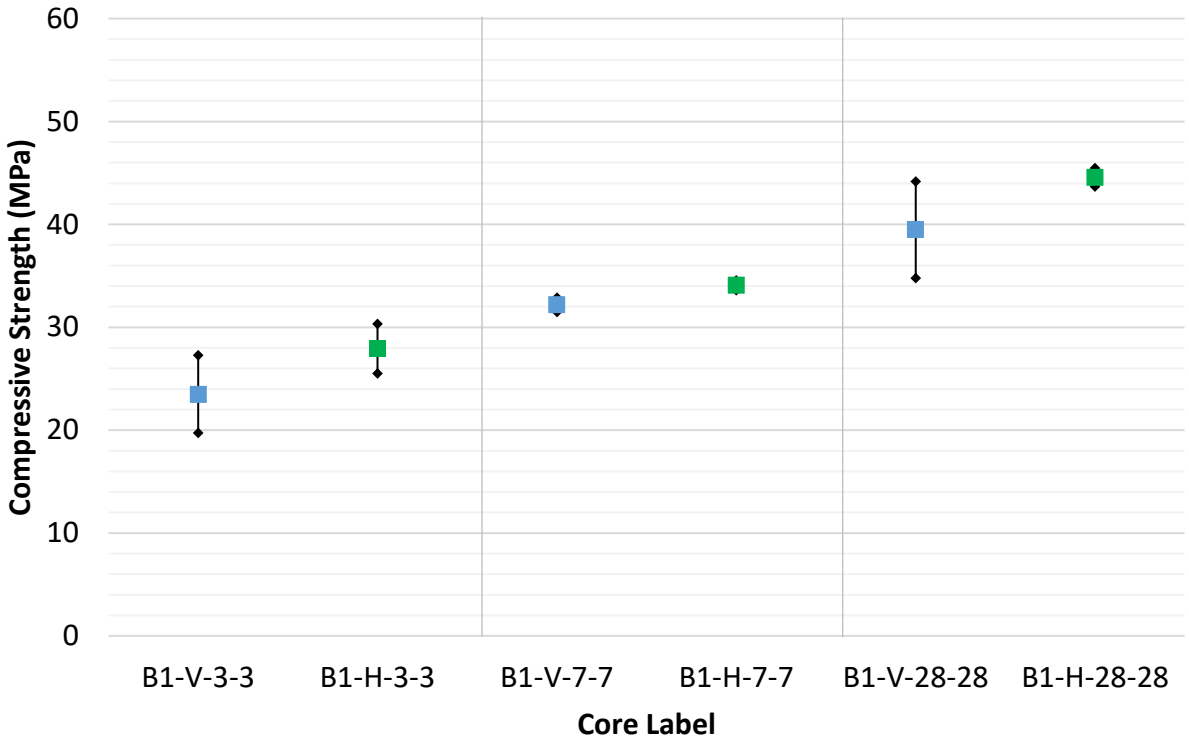

Figure 4.8. Compressive Strengths of Cores from B1 Beams on Days 3, 7, and 28

One reason for this is that the cores were not in the same plane, the horizontal cores being from the mid height of the beam, approximately 300 mm from the top surface of the beam, while the vertical cores were taken from the top 250 mm of the beam (Figure 4.9). Although the difference in height is not very large between the vertical and horizontal cores, it is believed that the middle section of the beam developed a stronger matrix of hydration products due to the increased temperature.

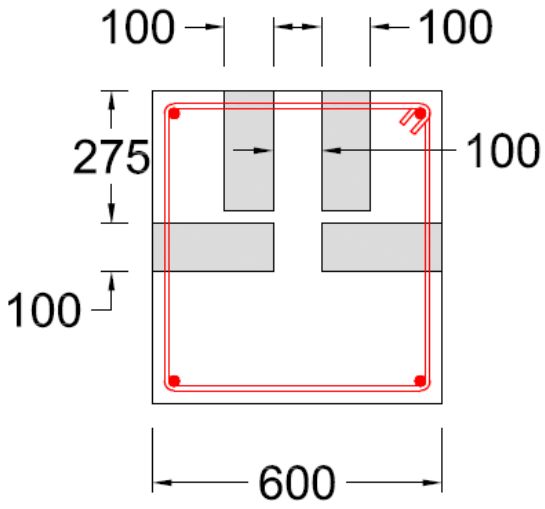

Figure 4.9 Cross section of B1 beam with coring locations

Comparing the results of the cores to the results of the cylinders, the vertical cores have similar strength to the cylinders (Figure 4.10). The horizontal cores, however, experienced a slightly higher temperature due to heat of hydration and resulted in higher compressive strengths than the cylinders on day 3, 7, and 28.

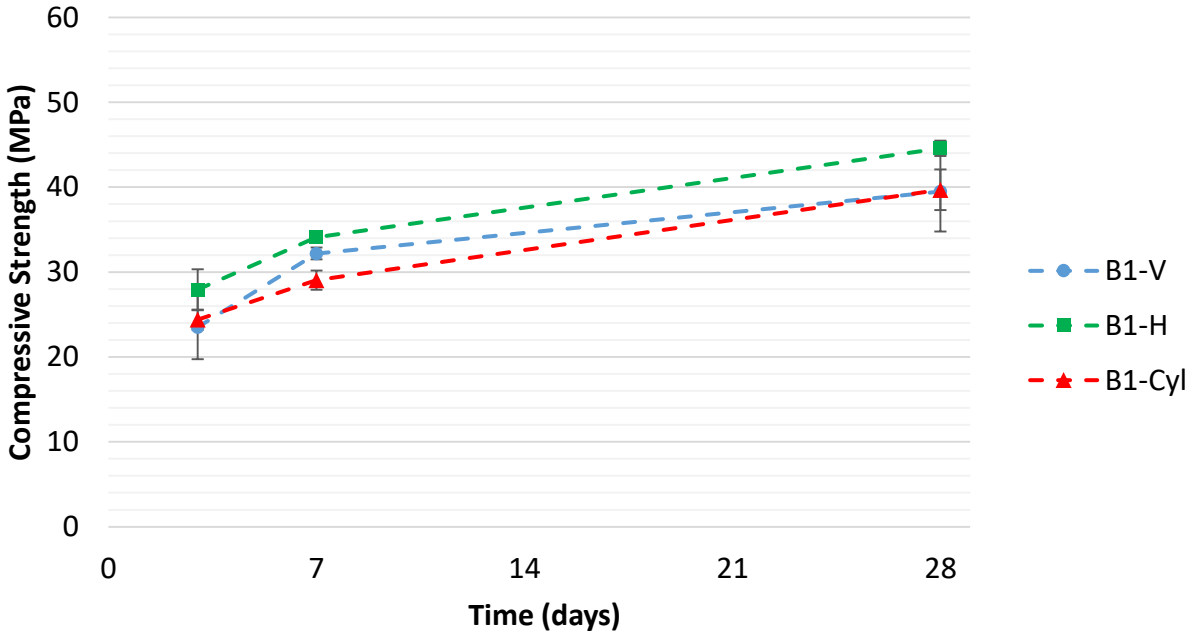

Figure 4.10. Comparison of B1 Core and Cylinder Compressive Strengths for Days 3, 7, and 28

4.2.3 Cores from B2 Beams

Similar to the findings of the B1 cores, the horizontal B2 cores had a higher compressive strength than the vertical B2 cores. The horizontal cores were stronger by 7% on day 3, 6% on day 7, and 9% on day 28.

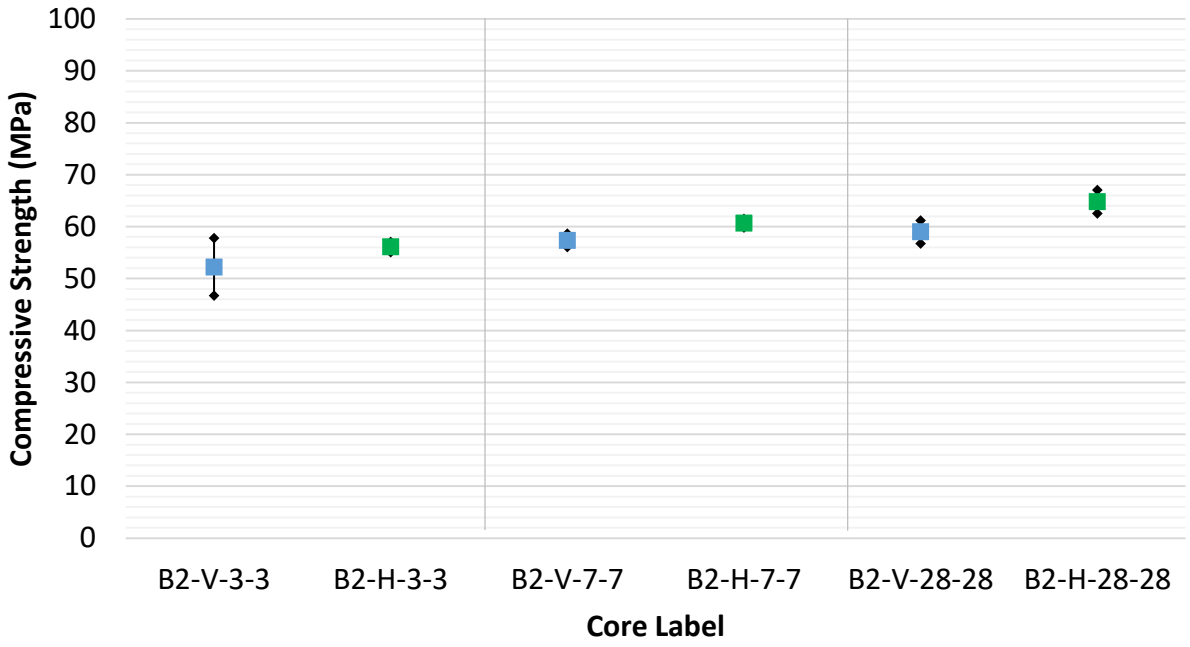

Figure 4.11 Compressive Strengths of Cores from B2 Beams on Days 3, 7, and 28

Comparing the strengths of the cores to those of the cylinders, the effect of high early temperature during hydration results in higher core strengths on days 3 and 7, but lower core strengths on day 28. The center of the beam recorded a maximum temperature of 56°C during hydration and was still above 30°C on day 3 compared to the cylinders which had a maximum temperature of 24°C and quickly returned to the ambient lab temperature in less than 24 hours. The increased heat in the structure resulted in a quicker reaction and, therefore, a high early strength. Additionally, the cylinders were maintained in a fully saturated state in lime water between day 3 and day 28 which allowed the unhydrated cement and silica fume particles in the cylinders to continue to react while the concrete in the beam was wet cured until day 3 and then remained in the lab environment for the duration of the testing period. It is for these reasons that cores extracted at later ages typically have lower strength results compared to the 28 day cylinder strengths. However, it is seen that there is little strength gain between day 7 and day 28 in both horizontal and vertical cores and as the strength of the cores on day 7 is greater than the specified design strength, earlier acceptance of the concrete is possible.

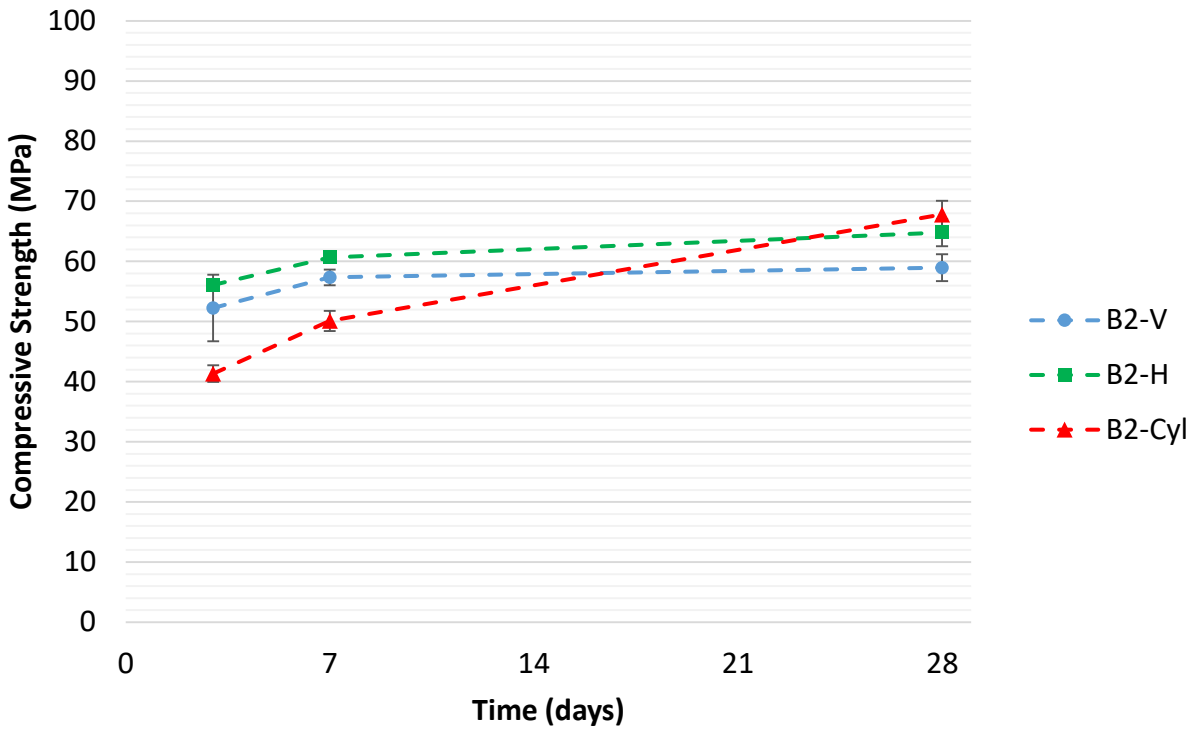

Figure 4.12 Comparison of B2 Core and Cylinder Compressive Strengths for Days 3, 7, and 28

4.2.4 Cores from G1 Girder Webs

In tall structures it is generally assumed that, because of settling in the plastic state, the strength near the top of the structure will be lower than the strength at the bottom. The G1 girder webs were designed to replicate the size of web used in common larger girders. They were 1600 mm tall and cores were extracted at the top and bottom of the web with a height difference greater than 1000 mm on average. In contrast to the general assumption, the cores from the top of the web were slightly greater than those from the bottom on days 3 and 7 and the strengths were approximately equal on day 28 (Figure 4.13 and Figure 4.14). It is important to note that the 100 mm cores, which have a L/D ratio of 1.5, were factored by 0.96 according to CSA A23.2-9C (CSA A23.1 / CSA A23.2 2015) and no other factors were used.

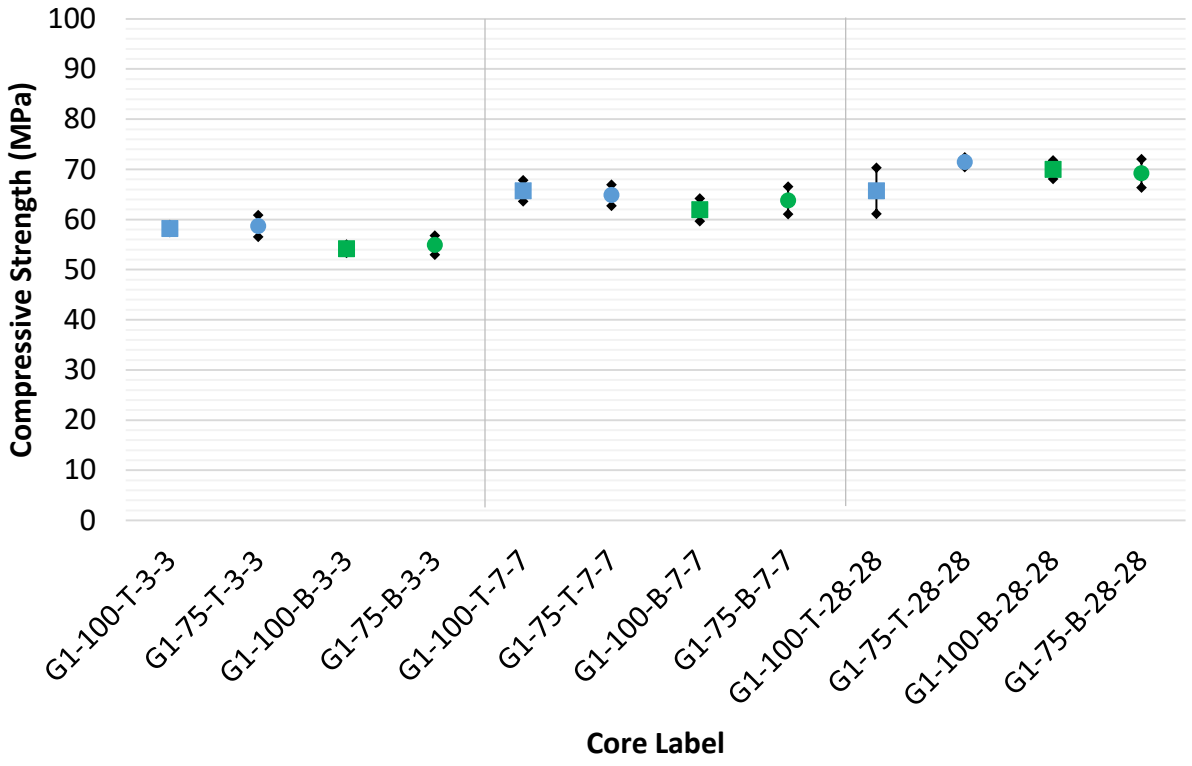

Figure 4.13 Compressive Strengths of Cores from G1 Girder Webs on Days 3, 7, and 28

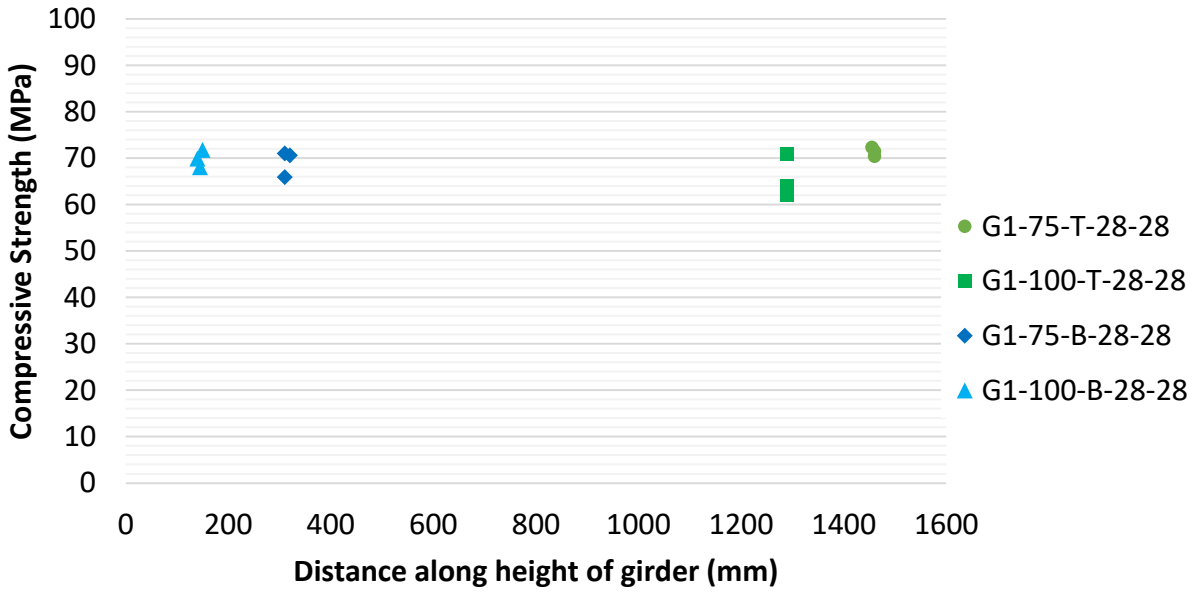

Figure 4.14 Day 28 Compressive strength of individual cores versus height of G1 Girder Webs

Figures similar to Figure 4.14 for days 3 and 7 for variation in compressive strength along the height as well as variation along the length of the girder are found in Appendix A. The temperature in the top of the girder was slightly higher than those near the bottom and caused higher early strength in the top of the web compared to the bottom. However on day 28, the compressive strength was approximately equal between the top and bottom of the web.

Comparing the strengths of the cores to those of the cylinder, the previously encountered trend due to the effect of temperature during hydration is seen. The cylinders which reached a maximum temperature of 30°C compared to the almost 48°C reached in the web resulted in higher compressive strengths of the cores on days 3 and 7, but lower core strengths on day 28. Again, as the day 7 strength of the cores is greater than the specified design strength, earlier acceptance of the concrete in the structure is possible.

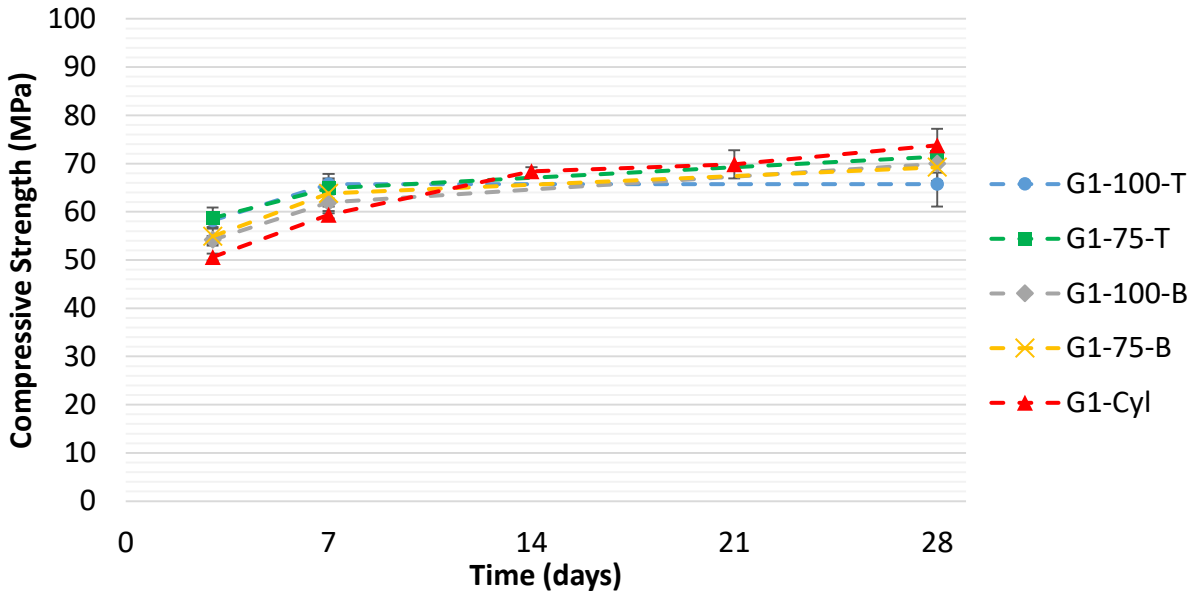

Figure 4.15 Comparison of G1 Core and Cylinder Compressive Strengths for Days 3, 7, and 28

4.2.5 Cores from G2 Girder Web

After cores were extracted from the G2 structure, large voids were found in the cores taken from the top section, medium sized voids were found in the cores from the middle section, and few small voids were found in the cores from the bottom section of the girder web. It was evident that the structure was not adequately consolidated during the cast. As a result of these voids, the density of the top cores was lower than the middle and bottom cores and consequently the compressive strength varied considerably (Figure 4.16).

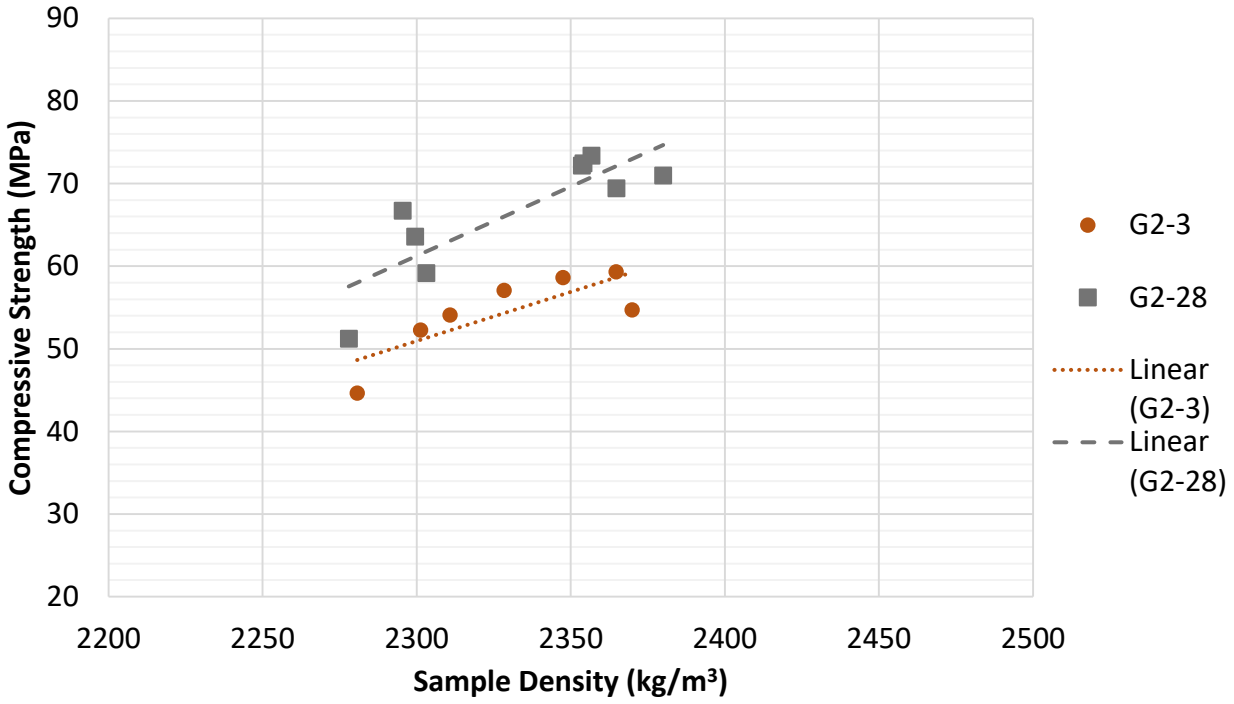

Figure 4.16 Compressive Strength versus Density of G2 Cores

The presence of these large voids was found to have a significant effect on the strength of the concrete and it is difficult to distinguish how much of the effect was related to the voids on their own and how much was related to the variation along the height. The compressive strength was lowest in cores from the top section of the girder and highest in cores from the bottom. The variation in compressive strength along the height of the G2 girder web is shown in Figure 4.17 and Figure 4.18 for day 3 and day 28, respectively. The cores from the middle section tended to be closer in strength to the bottom cores than to the top cores which is related to fewer and smaller voids present in the middle cores. Of the core results from day 28, 1 middle core and 1 top core are below the specified 60 MPa design compressive strength. However, neither of these cores failed the CSA A23.1 Clause which states that the average strength of three cores must exceed 85% of the specified design strength and no single core test result shall be less than 75% of the specified design strength (CSA A23.1 / CSA A23.2 2015).

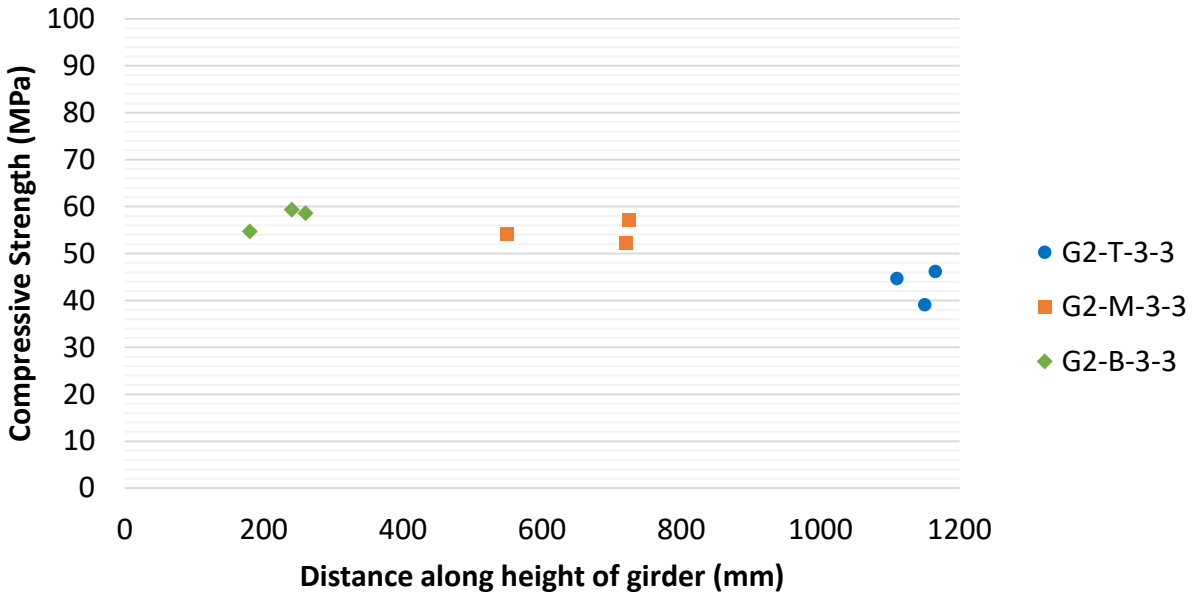

Figure 4.17 Day 3 Compressive strength of individual cores versus height of G2 Girder Web

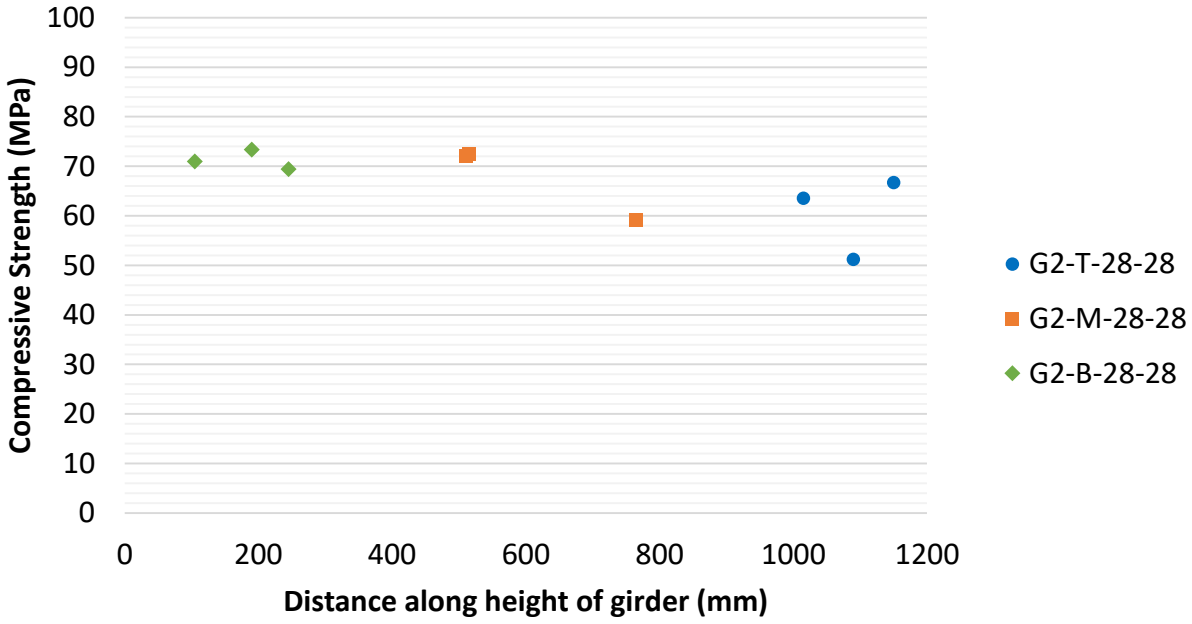

Figure 4.18 Day 28 Compressive strength of individual cores versus height of G2 Girder Web

On both day 3 and day 28, the cylinders had a slightly higher compressive strength than any of the cores taken from the structure (Figure 4.19). This trend is different from that observed in the lab structures since the higher temperature at hydration resulted in higher day 3 compressive strengths in the cores from lab structures. The middle and bottom core compressive strengths are close to those of the

cylinders, but the results of the top cores are much lower. The lower strength in the top cores can be concerning since it is common to use the cylinders strengths on day 1 to decide if the concrete has reached adequate transfer strength for cutting pretensioned strands. It is understood that the presence of the large voids in the top cores was the primary factor in the lower compressive strengths, however, unlike in the lab structures, the cylinders have shown to have higher compressive strengths than the cores from the structure, at early age and on day 28.

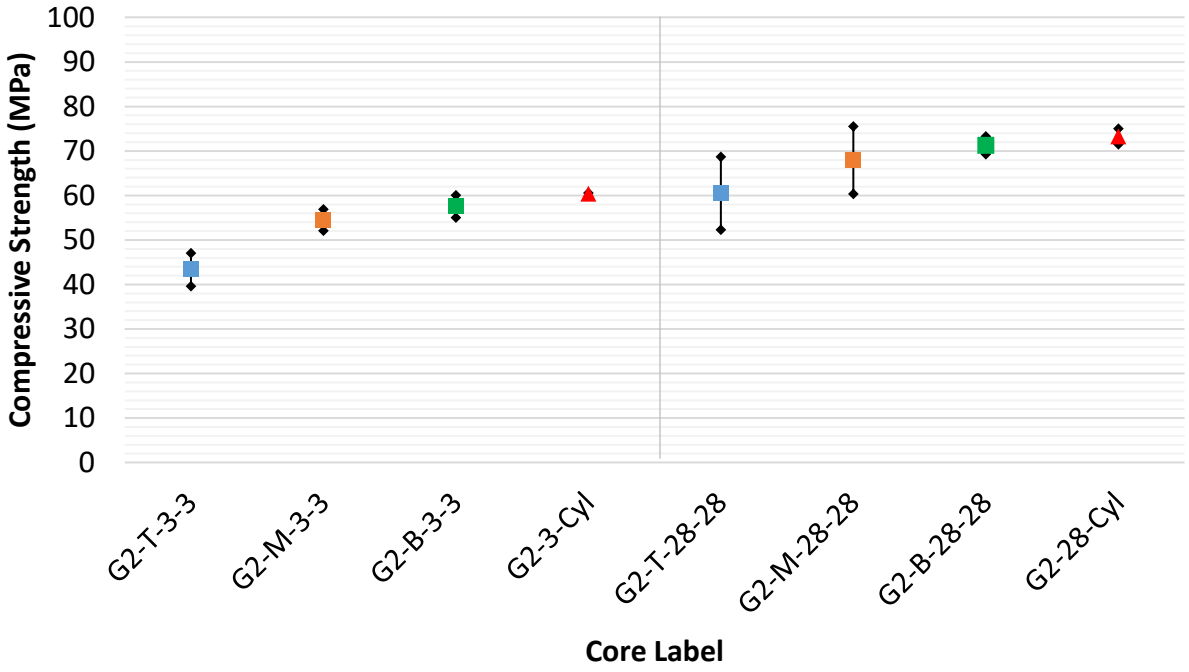

Figure 4.19 Comparison of G2 Core and Cylinder Compressive Strengths for Days 3 and 28

4.2.6 Cores from G3 Girder

Cores were taken from the top flange, bottom flange, and mid-height of the web on days 3 and 28 and additional cores were taken from the top and bottom of the web on day 28. All of the cores extracted from the web and some of the cores extracted from the flanges were not able to be cut to an L/D ratio of 2 and therefore were cut to have as long a length as possible and were then factored according to CSA A23.2-9C (CSA A23.1 / CSA A23.2 2015). The results of compressive strength on days 3 and 28 (corrected to L/D of 2) are shown in Figure 4.20. The first concern noticed was the much lower strength of the middle of the web on day 3 compared to both top and bottom flanges and to the cylinders. The cores were not available for inspection and there was no information provided regarding the presence of voids or damage in the cores from drilling operations. The thermocouples used inside of the structure

were only placed inside the web of the structure and the temperature within the flanges is not known, but it is expected that the temperature would be higher in the flanges due to the greater volume of concrete. This may be one factor which caused a greater strength on day 3 in the cores from the flanges. However, on day 28, the middle cores had a comparable strength to the bottom flange cores and exceeded the strengths of the top flange cores. The additional cores from the top and bottom of the web on day 28 were found to also have higher compressive strength than both the top and bottom flanges and it is likely the result of higher temperatures during hydration in the thicker flange compared to the web which caused a lower day 28 strength in the cores from the flanges.

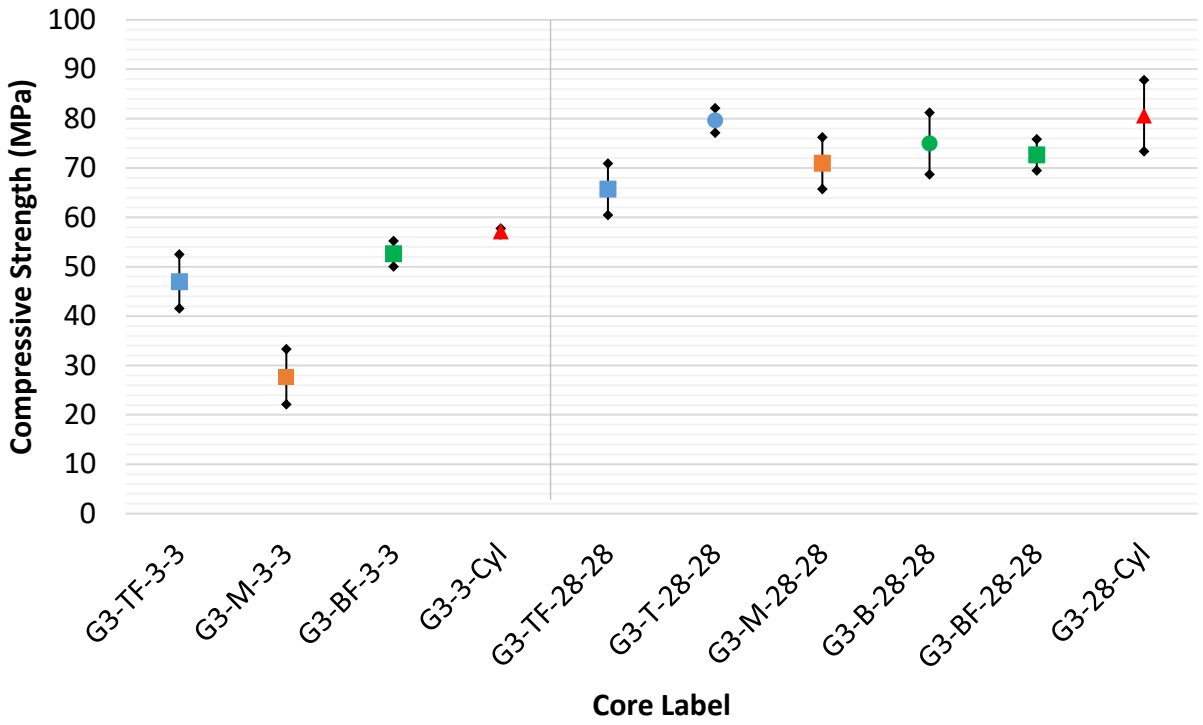

Figure 4.20 Comparison of G3 Core and Cylinder Compressive Strengths for Days 3 and 28

Similar to the G2 girder and contrary to the lab structures, the cylinders had slightly higher compressive strengths than the cores on both day 3 and day 28. The lab structures tended to have higher compressive strengths on earlier coring days as a result of the increased temperature during hydration compared to the cylinders, but this effect is not observed in the prefabricated structures.

4.2.7 Cores from VC Valve Chamber

Cores were extracted from the valve chamber on days 3, 7, and 28 at the mid-height of the walls and the compressive strengths of the cores and cylinders are shown in Figure 4.21. The VC structure had been placed outside by day 2 and exposed to the elements which included periods of freezing weather. This resulted in a reduction of the rate of hydration and the structure experienced little strength gain between day 3 and day 28. The structure had a specified design strength of 40 MPa and due to the HE cement used in the concrete mixture, the structure achieved this strength as early as day 3, but only had a slight increase in strength by day 28. The cylinders which were maintained indoors in calcium hydroxide solution between day 3 and day 28 experienced greater strength gain by day 28.

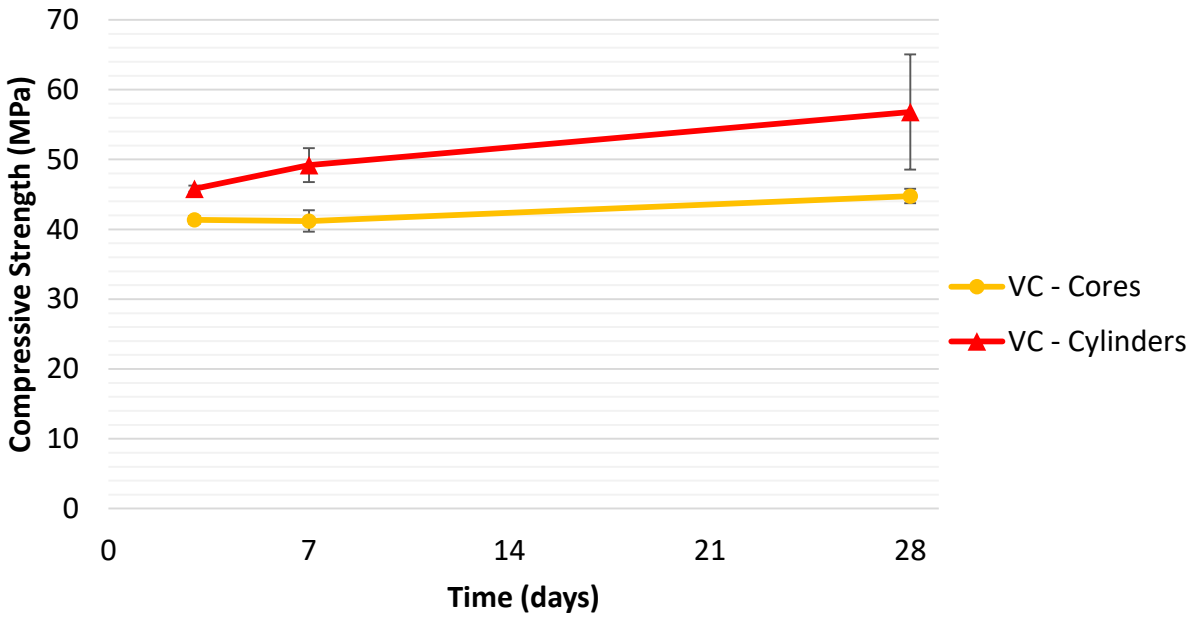

Figure 4.21 Comparison of VC Core and Cylinder Compressive Strengths for Days 3, 7, and 28

4.3 Rapid Chloride Permeability

Recalling the RCP test limitations set by the Ontario Provincial Standards discussed in Section 3.3.4, the B2 beams containing silica fume are limited to 1000 Coulombs for acceptance and all other concretes are limited to 2500 Coulombs. Failed test results are indicated by highlighted values in the tables presented throughout this section. It is important to note that only a small number of samples could be tested at a given time and due to a small sample size only certain conclusions can be made regarding the comparisons.

Vertical and horizontal B1 cores extracted on days 3, 7, and 14 were tested for RCP and the results are shown in Table 4.2. The B1 concrete did not contain silica fume and, therefore, the acceptance criteria limits the average test result to 2500 Coulombs or less. The results indicate that each of the vertical cores failed the RCP test while the three horizontal cores just met the acceptance criteria. As it was discussed in the literature section, using SCMs in the concrete mix reduces the porosity and permeability. The B1 concrete mix, which had a target to contain 25% slag, only contained 9% slag which can be one of the reasons for the poor RCP test results. Based on the results of the B1 cores, the horizontal cores would be accepted while the vertical cores would be subjected to payment adjustments by the supplier.

Table 4.2 RCP Test Results for B1 Beams

Label	Test 1	Test 2	Test Average
B1-V-3-28	2733	2823	2778.0
B1-V-7-28	2725	2809	2767.0
B1-V-14-28	2875	2872	2873.5
B1-H-3-28	2642	2246	2444.0
B1-H-7-28	2271	2510	2390.5
B1-H-14-28	2474	2493	2483.5

The RCP results for vertical and horizontal B2 cores extracted on days 3, 7, and 14 are shown in Table 4.3. The horizontal cores were found to have more favourable RCP test results, similar to the results from the B1 cores. The B2 concrete contained silica fume and its influence is very apparent in the low charge passed through B2 cores where no core even exceeded 400 Coulombs. Thus, both the vertical and horizontal cores are found to be acceptable according to the OPSS criterion.

Table 4.3 RCP Test Results for B2 Beams

Label	Test 1	Test 2	Test Average
B2-V-3-28	387	333	359.6
B2-V-7-28	393	378	385.9
B2-V-14-28	401	369	385.0
B2-H-3-28	331	332	331.1
B2-H-7-28	344	352	347.8
B2-H-14-28	314	306	309.9

The RCP results for top and bottom G1 cores extracted on days 3 and 7 are shown in Table 4.4. The top cores recorded slightly greater RCP test results which is likely related to the increased paste content in the top section of the girder web due to settling. Although from the same concrete, the day 3 and day 7

cores were extracted from two different girder webs and the consolidation between the two webs could have varied. The day 3 top core passed the most charge resulting in a failed test result, while the accompanying bottom core passed the least charge. This may indicate that the web cored on day 3 was vibrated slightly more than the web cored on day 7 resulting in a greater paste content in the top section of the web. The variation between the top and bottom cores from day 7 is relatively small compared to the variation in cores from day 3.

Table 4.4 RCP Test Results for G1 Girder Webs

Label	Test 1	Test 2	Test Average
G1-T-3-28	2456	2835	2645.3
G1-T-7-28	2230	2199	2214.7
G1-B-3-28	1843	2227	2034.7
G1-B-7-28	2040	2241	2140.4

Top and bottom G2 cores were extracted on day 3 for RCP testing and the results are shown in Table 4.5. The top core recorded a less favourable RCP test result than the bottom core which is related to the poor consolidation of the G2 structure, but both readily met the OPSS criterion.

Table 4.5 RCP Test Results for G2 Girder Web

Label	Test 1	Test 2	Test Average
G2-T-3-28	1667.4	1485.9	1576.6
G2-B-3-28	1353.9	1355.4	1354.7

The VC chamber was constructed using concrete containing HE cement with 25% slag, similar to the G2 girder, however, the G2 concrete contained a greater total cementitious content compared to the VC concrete mix. It would be expected that the VC structure would have a more favourable RCP test result due to the lower total cementitious content, but due to the poor curing of the VC structure, the G2 cores passed less charge than the VC cores. The results of the RCP test for VC cores are fairly consistent regardless of coring day and all three cores passed the RCP test (Table 4.6). Although the day 3 core experienced the least time outdoors and most time with additional curing in calcium hydroxide solution, the results indicate that there is little difference between the cores extracted at later days.

Table 4.6 RCP Test Results for VC Chamber

Label	Test 1	Test 2	Test Average
VC-3-28	1865	1829	1847.0
VC-7-28	1741	1712	1726.5
VC-14-28	1808	1921	1864.8

4.4 Electrical Resistivity

On day 3 testing, both cores and cylinders were not in a fully saturated state when recording the measurement. On day 7 and day 28 testing, the cylinders, which were cured in a tub of calcium hydroxide solution since day 3, were in a saturated state, while the cores extracted from the structure were not fully saturated. The level of saturation is known to impact the result of the resistivity measurement and, therefore, only relative comparisons are made between the results. In the following figures, the data points refer to an average of three (3) samples with error bars indicating one standard deviation above and below the average resistivity.

4.4.1 B1 Beams

The bulk resistivity for B1 cores and cylinders on days 3, 7, and 28 is shown in Figure 4.22. During the testing period, both the horizontal and vertical cores recorded slightly greater bulk resistivity compared to the cylinders. One reason could be due to the cores being less saturated than the cylinders, but overall, the difference in bulk resistivity between the cores and cylinders from the B1 beams is relatively small.

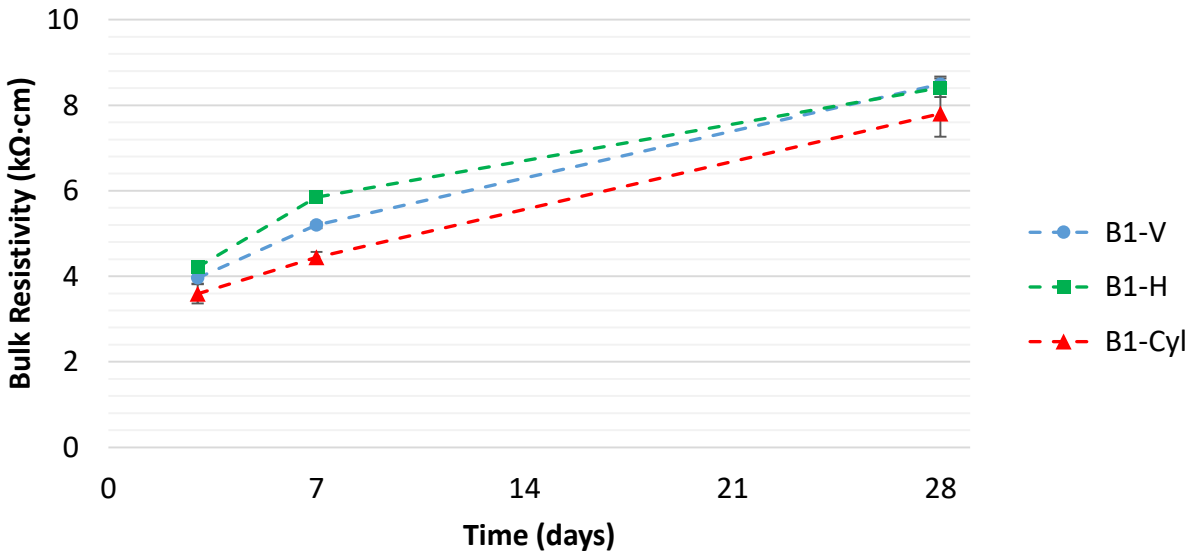

Figure 4.22 Comparison of B1 Core and Cylinder Bulk Resistivity for Days 3, 7, and 28

4.4.2 B2 Beams

The bulk resistivity for B2 cores and cylinders on days 3, 7, and 28 is shown in Figure 4.23. During the testing period, both horizontal and vertical cores recorded greater resistivity results than the cylinders, with the horizontal cores being slightly better than the vertical cores. These results compare well with

the results of the RCP tests of B2 cores and cylinders and indicate the low porosity and permeability of the B2 beams compared to the cylinders. The trend in the horizontal cores shown in Figure 4.23 indicates a low average resistivity on day 7. This outlier is due to the very low resistivity of one of the three cores, which was extracted from a corner of a beam exposed to cold drafts from the loading bay door during curing. Therefore, the resistivity of all cores extracted that day (day 7), and on all following testing days, was measured to determine the variation along the length of the beam. The results, shown in Figure 4.24, confirm the variation along the length of the beams with greater resistivity of cores extracted closer to the middle section of the beam. This variation was found to be less prominent by day 28 testing. Additional graphs of variation in resistivity along length of the beam are found in Appendix B.

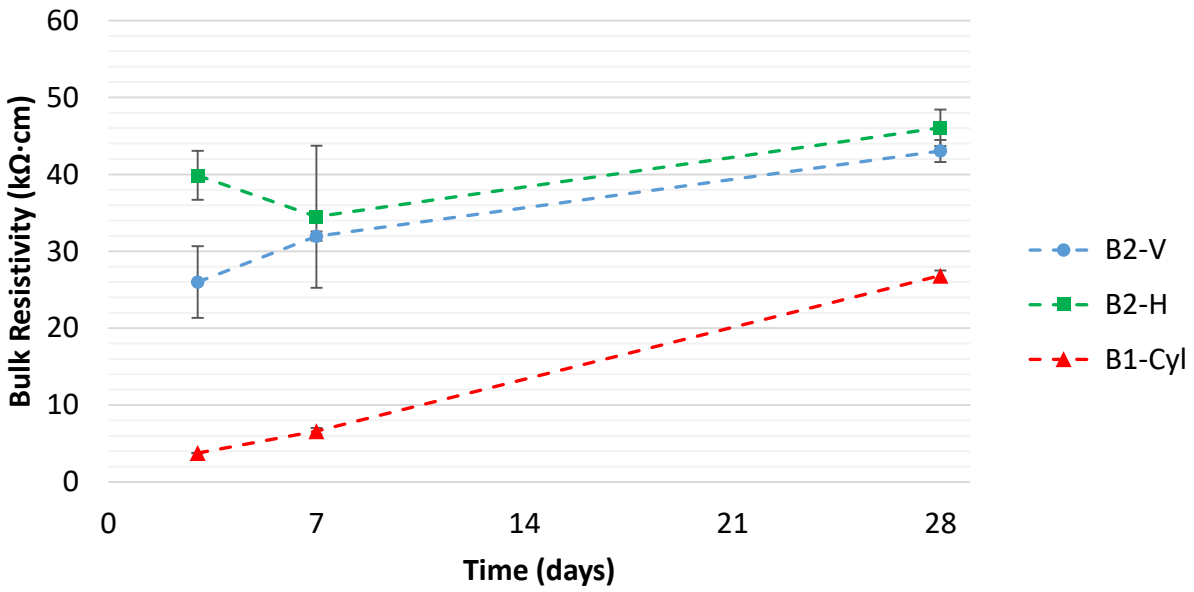

Figure 4.23 Comparison of B2 Core and Cylinder Bulk Resistivity for Days 3, 7, and 28

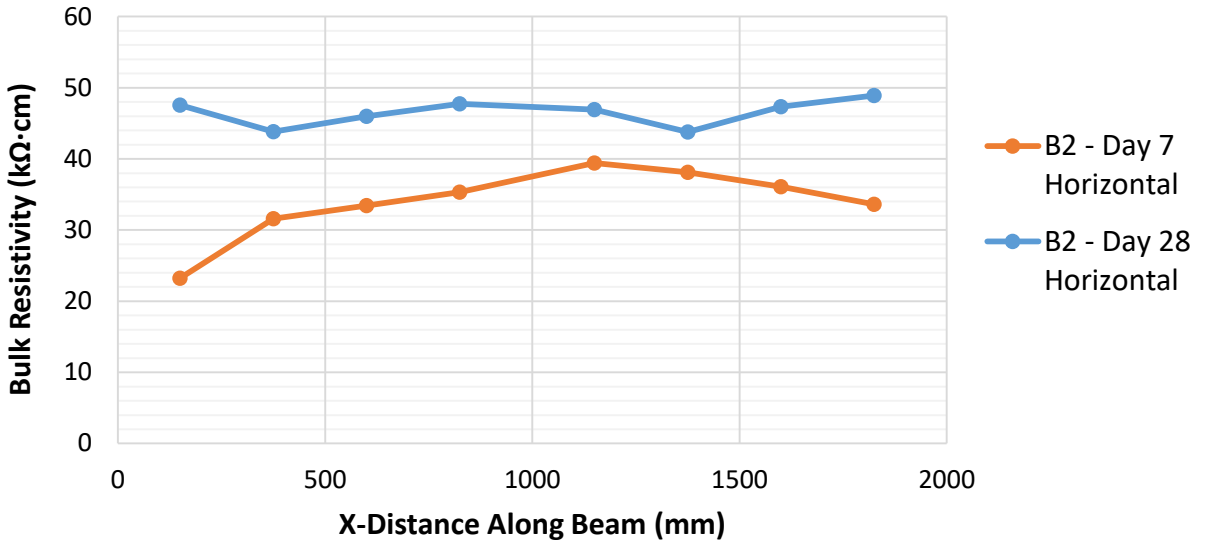

Figure 4.24 Variation of B2 Core Bulk Resistivity along Length of Beam on Day 7 and 28

4.4.3 G1 Girder Webs

The bulk resistivity for G1 cores and cylinders on days 3, 7, and 28 is shown in Figure 4.25. Similar to the results from B1 and B2 bulk resistivity, the G1 cores recorded higher bulk resistivity values compared to the cylinders. This is related to both the higher temperature during hydration of the structure as well as the less saturated state of the cores compared to the cylinders.

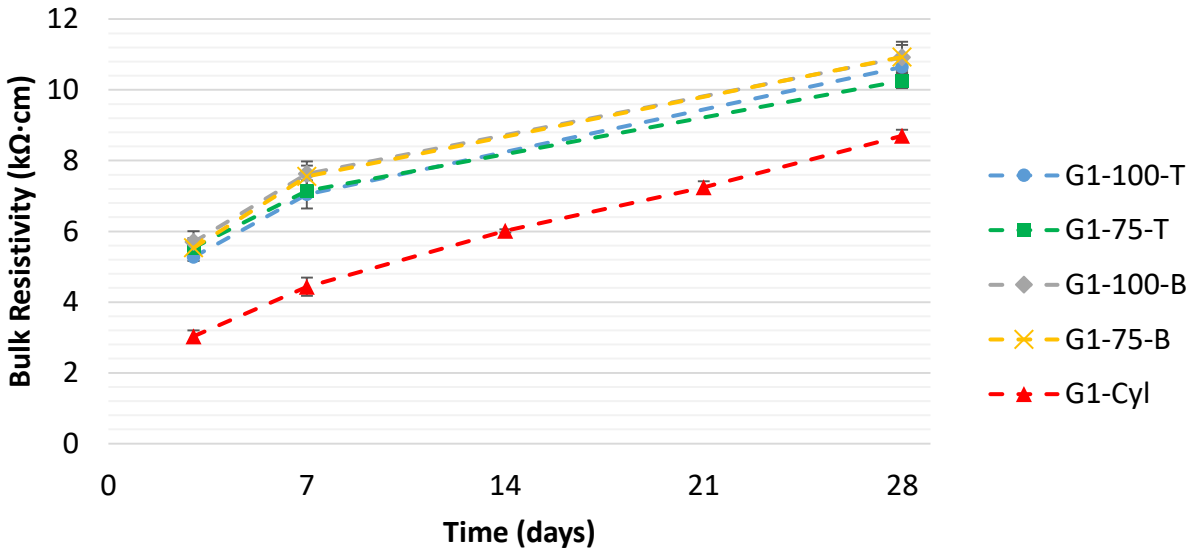

Figure 4.25 Comparison of G1 Core and Cylinder Bulk Resistivity for Days 3, 7, and 28

The variation in bulk resistivity along the length of the girder webs was measured to determine if a similar profile that was seen in the B2 beams would be found. The results shown in Figure 4.26, confirm that the variation along the length found in B2 beams is not found in the G1 girder webs. This could be due to the different behaviour of silica fume and slag in their respective mixtures. The first observation is that the GU and silica fume concrete had a significantly greater resistivity between 25 and 40 kΩ·cm on day 3 compared to the GU and slag concrete with a resistivity between 5 and 6 kΩ·cm. Due to the greater magnitude of resistivity, it is easier to identify variation in the results along the length of the B2 beams. Another factor can be the thinner section of the girder webs which can dissipate the heat more evenly and, therefore, a more uniform resistivity profile was found. The day 28 bulk resistivity profile shows more fluctuation which can be attributed to the varying saturation levels within the structure.

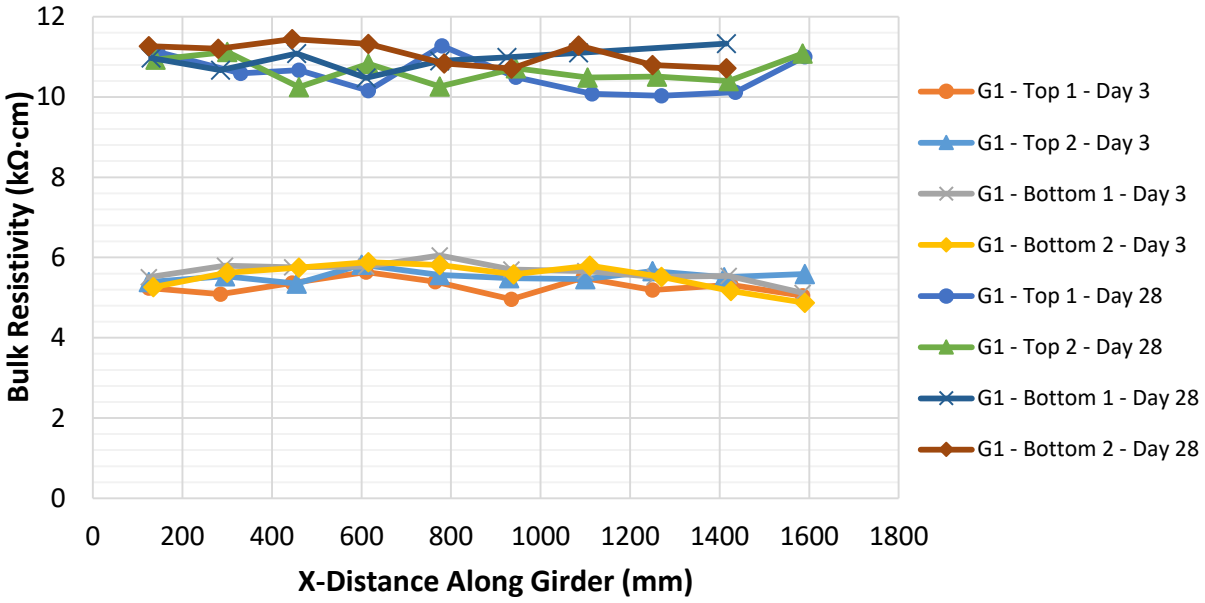

Figure 4.26 Variation of G1 Core Bulk Resistivity along Length of Girder on Day 3 and 28

4.4.4 G2 Girder Web

The bulk resistivity for G2 cores and cylinders on days 3 and 28 is shown in Figure 4.27. The resistivity within the structure is fairly similar at the top and bottom on both days 3 and 28 with the middle cores having a slightly greater bulk resistivity. This is partly related to the higher temperature developed within the middle section of the web during the hydration and is also affected by the location from which the cores were taken. The middle cores were not taken along the full length of the girder due to requirements for attaching the drill base to the structure. As a result, the three middle cores used on

days 3 and 28 were more closely spaced than the top and bottom core sets and a greater resistivity was found in the cores closer to the mid-length of the web.

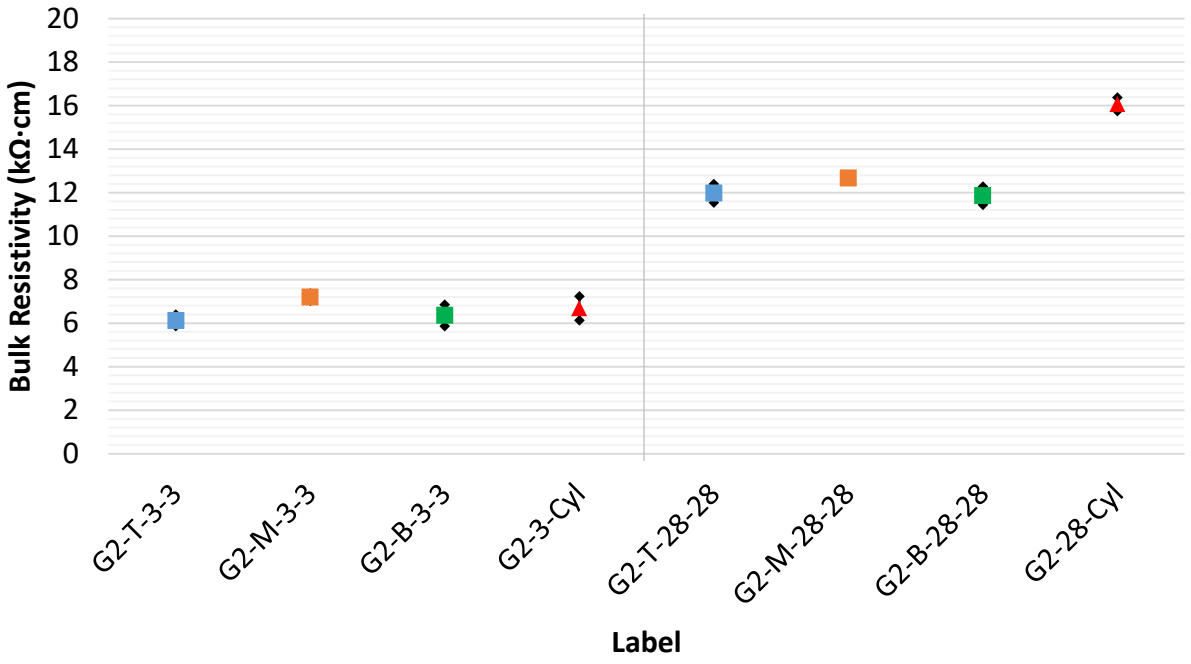

Figure 4.27 Comparison of G2 Core and Cylinder Bulk Resistivity for Days 3 and 28

Contrary to the results seen in lab constructed structures, the cylinders have fairly similar resistivity values to that of the cores on day 3 and exceed the resistivity of the cores on day 28. This is attributed to the fact that, compared to the lab structures which were left in their formwork until coring on day 3, the G2 girder was removed from its formwork after approximately 18 hours and placed in moist curing chamber until day 7. The temperature increase due to hydration was able to dissipate quicker from the G2 girder web and the development of a greater resistivity was reduced. The lower resistivity of cores extracted on day 28 can be attributed to the structure being exposed to the elements between day 7 and 28 which included a period of negative 10°C temperature and snowy conditions. Although the cylinders were in a more saturated state than the cores on day 28, the cylinders had more adequate curing conditions to allow for better hydration.

The values shown in Figure 4.28 indicate that a slightly greater resistivity was found in the cores closer to the centre of the girder. The thinner section of the G2 girder web was able to dissipate the heat from hydration more quickly resulting in only a slight variation along the length of the girder web. The bulk resistivity on day 28 is very variable due to the harsh curing environment between day 7 and day 28 in

addition to the core holes not being plugged to prevent moisture loss as was done with the lab structures.

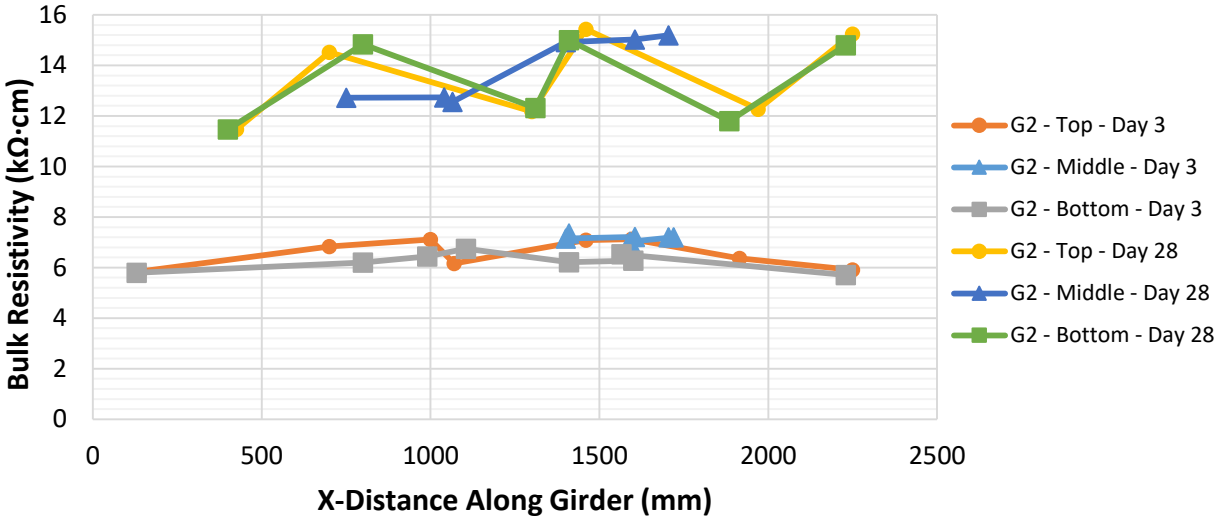

Figure 4.28 Variation of G2 Core Bulk Resistivity Along Length of Girder on Day 3 and 28

4.4.5 VC Chamber

The bulk resistivity for VC cores and cylinders on days 3, 7, and 28 is shown in Figure 4.29. As the structure spent more time exposed to the elements and variable temperature, there was only a slight increase in the resistivity during the 28 day period. In contrast, the cylinders, cured in solution at room temperature, exhibited a doubling of the resistivity from day 3 to day 28.

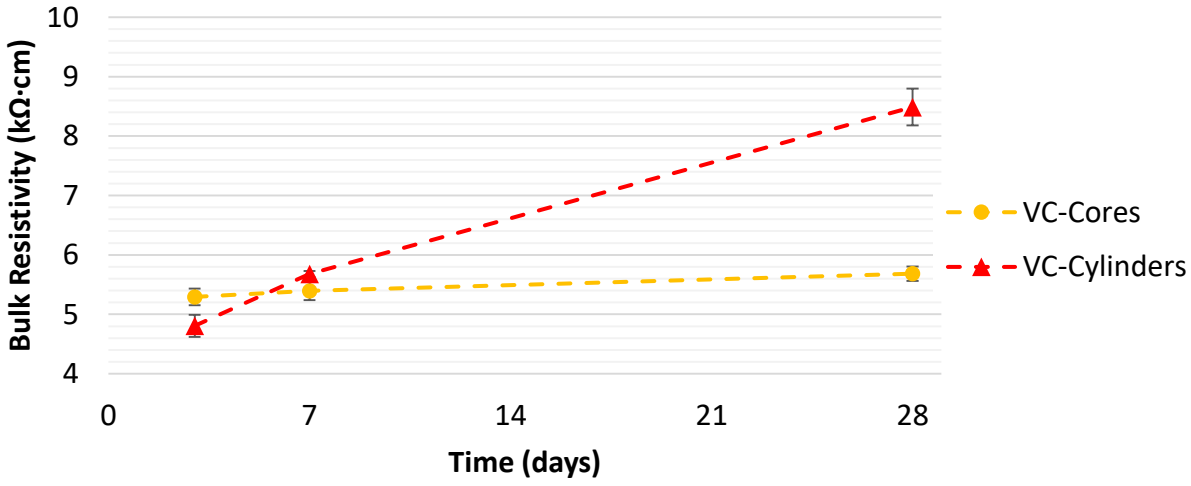

Figure 4.29 Comparison of VC Core and Cylinder Bulk Resistivity for Days 3, 7, and 28

4.5 Air Void System

The air content was measured on both the fresh and hardened concrete. The fresh concrete air content was measured during each cast and the results are shown in Table 4.7. The target air content for several mixes was not provided, but a typical air content of 5 to 8 percent is common for concrete infrastructure in Ontario. The results indicate that each of the mixes recorded desirable air content, however, the fresh concrete air content test does not account for the placement and in-place variations of the concrete.

Table 4.7 Fresh Concrete Air Content

Concrete Name	Target Air Content (%)	Fresh Concrete Air (%)
B1	Not provided	4.8
B2	Not provided	6.0
G1	Not provided	4.6
G2	Not provided	6.2
G3	5.0 – 8.0	6.0
VC	7.0	7.9

The results of the hardened concrete air void content are shown in Table 4.8. Similar to the RCP testing, only one core was able to be tested for AVS to represent a set and only certain conclusions can be drawn on the results from a small sample size. All samples passed the minimum air content requirement of 3.0%, but both G1 girder web samples failed the maximum spacing factor requirement which is indicated with the highlighted values in Table 4.8. The guidelines have adjustments for spacing factors exceeding the required 0.230 mm and 0.200 mm. The G1-B core which has a spacing factor greater than 0.200 and less than 0.250 mm and would be subjected to repair with a sealer material while the G1-T core exceeding 0.250 mm spacing factor would be rejected and need to be replaced according to OPSS 909 (OPSS.PROV 909 2016).

Table 4.8 Air Void System Results from Cores

Label	Air Content (%)	Spacing factor (mm)	Paste Content (%)	Specific Surface (mm^{-1})
B1-V	4.5	0.175	33.7	31.7
B1-H	4.8	0.163	33.0	32.9
B2-V	3.9	0.149	29.9	37.7
B2-H	6.3	0.162	32.3	28.9
G1-T	4.2	0.319	41.1	19.7
G1-B	3.3	0.238	34.9	27.2
G2-T	6.9	0.171	35.0	27.2
G2-B	5.3	0.197	34.0	26.5
G3-TF	10.2	0.115	27.1	23.0
G3-BF	10.6	0.144	26.6	17.4
VC	8.7	0.196	33.1	19.4

In both the B1 and B2 beams, cores for horizontal and vertical orientations were chosen from the same beam and from the same location along the length of the beam to have the closest comparison of results. However, the data do not provide further information on the reason for the horizontal cores having greater compressive strengths than the vertical cores. The results for B1 horizontal and vertical cores are very similar, but those for the B2 cores differ significantly.

The G1 top core had a higher air content than that of the bottom core despite the higher strength of the top core, which must, therefore be attributed to the greater paste content in the top of the girder.

The G2 top core had a higher air content than the bottom core, as expected because of the poor consolidation at the top of the girder.

The air void parameters of G3 cores are fairly similar between the top and bottom flange, but the measured air content is quite large. Since these structures are typically reinforced with many pretensioned strands and a certain procedure for using the external vibrator used for the heavily reinforced section, it is possible the G3 structure, which was not reinforced at all for this test, could have been over vibrated causing greater air content in the structure.

4.6 Density

The density of the cores and cylinders was approximated using the volume from the sample dimensions and the mass of the sample prior to compressive testing. Normal density concrete is defined as having a density between 2150 and 2500 kg/m^3 (CSA A23.1 / CSA A23.2 2015). All the concretes tested in this research were normal density concrete with densities in the range of 2300 to 2400 kg/m^3, however, the top cores in the G2 girder web and the top flange cores in the G3 girder had densities slightly lower than 2300 kg/m^3. In general, the density of the cylinders was slightly greater than that of the cores and is related to the more saturated state of the cylinders.

The results for the density of B1 cores and cylinders are shown in Table 4.9 and unfortunately the day 3 densities were not recorded and the values are not shown. The densities between the vertical and horizontal cores do not vary largely and is likely not a large contributor for the difference in compressive strength.

Table 4.9 Density of B1 Cores and Cylinders

Label	Average Density (kg/m^3)	COV
B1-V-7-7	2379	0.002
B1-H-7-7	2362	0.004
B1-V-28-28	2371	0.001
B1-H-28-28	2385	0.004
B1-7-Cyl	2380	0.006
B1-28-Cyl	2391	0.005

The densities for B2 cores and cylinders is shown in Table 4.10. On each of the testing days, the vertical cores have a slightly lower density than the horizontal cores, but the difference is relatively small and is likely not a contributor for the difference in the compressive strength.

Table 4.10 Density of B2 Cores and Cylinders

Label	Average Density (kg/m^3)	COV
B2-V-3-3	2346	0.003
B2-H-3-3	2375	0.003
B2-V-7-7	2357	0.006
B2-H-7-7	2368	0.012
B2-V-28-28	2347	0.004
B2-H-28-28	2353	0.004
B2-3-Cyl	2370	0.003
B2-7-Cyl	2387	0.013
B2-28-Cyl	2369	0.008

The results from the G1 cores (Table 4.11) show that the top cores had a slightly lower density than the bottom cores on each of the testing days and this can be related to the consolidation of heavier aggregates towards the bottom of the web.

Table 4.11 Density of G1 Cores and Cylinders

Label	Average Density (kg/m^3)	COV
G1-T-3-3	2354	0.004
G1-B-3-3	2365	0.005
G1-T-7-7	2358	0.004
G1-B-7-7	2376	0.003
G1-T-28-28	2353	0.003
G1-B-28-28	2357	0.003
G1-3-Cyl	2373	0.006
G1-7-Cyl	2362	0.007
G1-14-Cyl	2377	0.003
G1-21-Cyl	2384	0.003
G1-28-Cyl	2373	0.005

The variation in density was very apparent in the cores from the G2 girder web (Table 4.12). As it was previously explained, large voids were found within the top cores, medium voids were found within the middle cores, and few small voids were seen in the bottom cores. The result of these voids caused a reduced density in the top cores leading to a reduction in the compressive strength.

Table 4.12 Density of G2 Cores and Cylinders

Label	Average Density (kg/m^3)	COV
G2-T-3-3	2272	0.003
G2-M-3-3	2313	0.006
G2-B-3-3	2361	0.005
G2-T-28-28	2291	0.005
G2-M-28-28	2337	0.013
G2-B-28-28	2367	0.005
G2-3-Cyl	-	-
G2-28-Cyl	2346	0.006

The density results of the G3 cores (Table 4.13) indicate that the web had fairly good consistency from top to bottom with densities approximately 2400 kg/m^3. The top and bottom flanges have slightly lower densities and this was also apparent in the very high air content of above 10% in both the top and bottom flange cores as well as lower compressive strengths in these cores on day 28. It is interesting to see that the web cores recorded higher densities than the bottom flange cores which may explain the difficulty in consolidating the concrete into the bottom flange.

Table 4.13 Density of G3 Cores and Cylinders

Label	Average Density (kg/m^3)	COV
G3-TF-28-28	2283	0.005
G3-T-28-28	2399	0.008
G3-M-28-28	2397	0.007
G3-B-28-28	2411	0.014
G3-BF-28-28	2336	0.003
G3-28-Cyl	2367	0.005

The cores from the VC chamber were taken from the mid-height of the wall and the densities appear fairly consistent on each of the testing days (Table 4.14). The slightly increasing densities with time of the cylinders is likely the result of an increase in saturation with time and it plateaus around day 14.

Table 4.14 Density of VC Cores and Cylinders

Label	Average Density (kg/m^3)	COV
VC-3-3	2331	0.002
VC-7-7	2327	0.004
VC-28-28	2315	0.006
VC-3-Cyl	2319	0.005
VC-7-Cyl	2334	0.001
VC-14-Cyl	2355	0.005
VC-21-Cyl	2357	0.005
VC-28-Cyl	2357	0.008

5 Analysis and Discussion

5.1 Compressive Strength of Cores versus Specified Design Strength

The primary goal of core testing is to assess the adequacy of the concrete in the structure by comparing the results to the specified 28 day design strength. The results of cores from the tested structures show that the day 28 compressive strength of all the structures exceeded their specified design strength as shown in Figure 5.1. This even included the top cores from the G2 girder web which had a ratio of core strength to design strength of 1.01 despite the large internal void content of these cores.

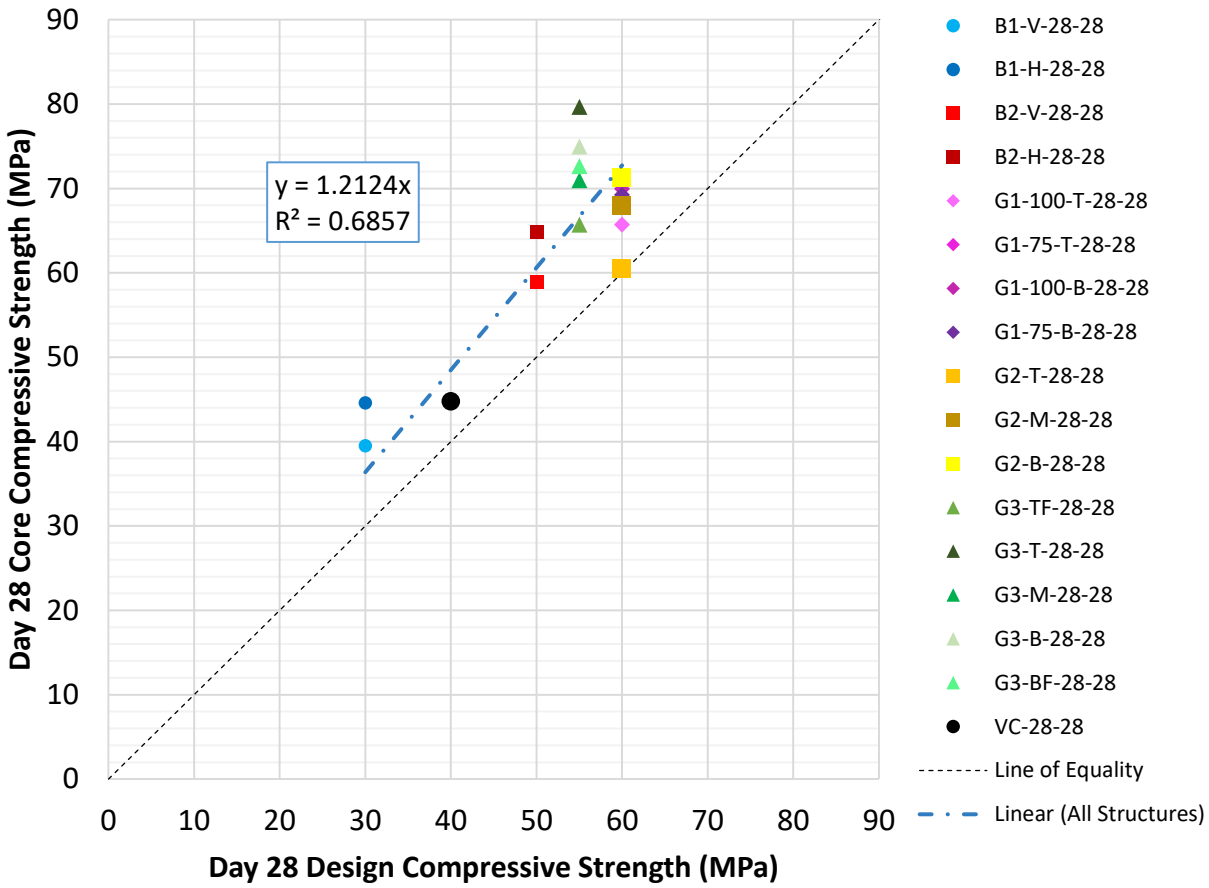

Figure 5.1 Day 28 Compressive Strength of Cores versus Specified Design Strength

The ratio of compressive strength on days 3, 7, and 28 to the day 28 specified strength is shown in Figure 5.2. The results indicate that the structures, on average, tend to have compressive strengths approximately 90%, 110%, and 120% of the specified 28 day design strength. In all cases, the design strength was met by day 7 and there was only a small increase in the ratio between day 7 and day 28.

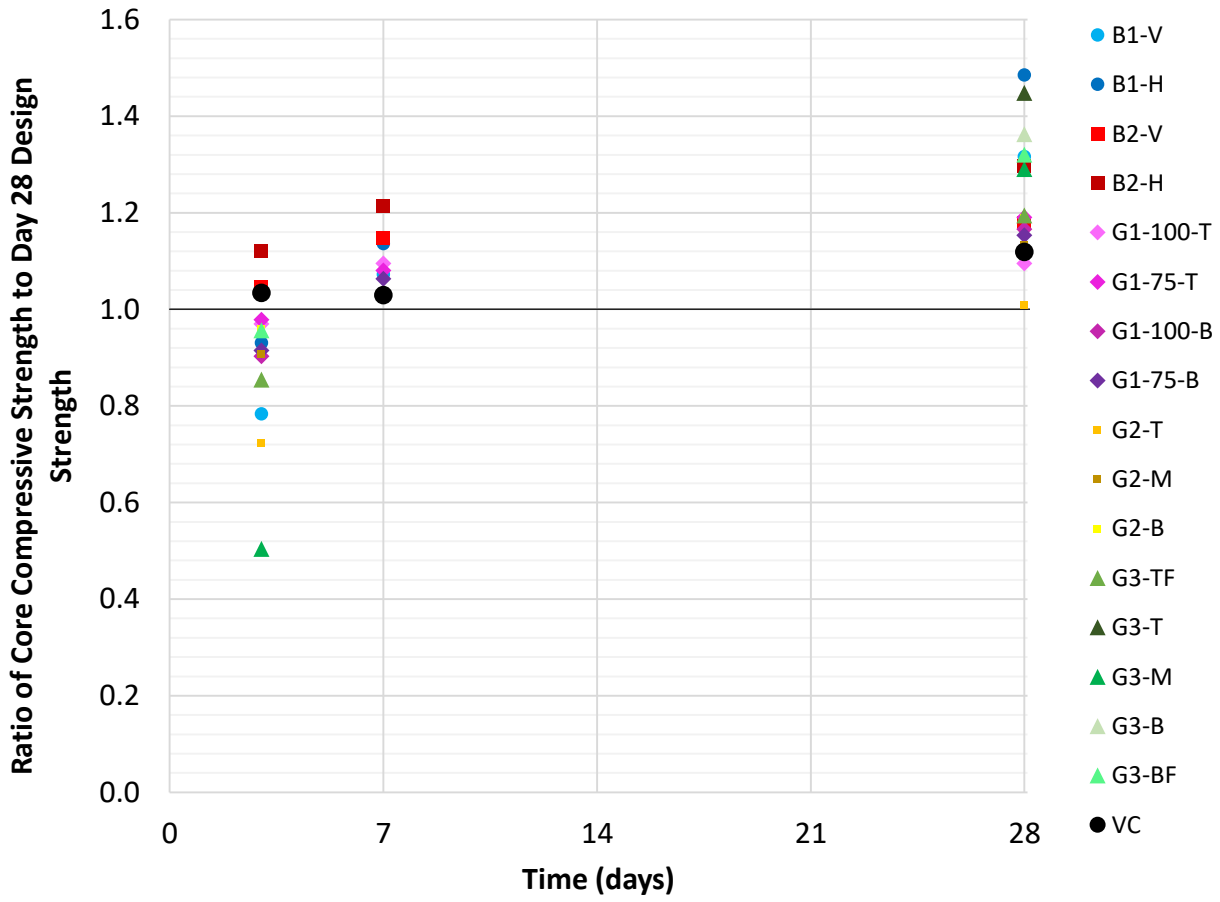

Figure 5.2 Compressive Strength on Day 3, 7, and 28 Relative to Day 28 Specified Strength

The ratio of the day 3 and day 7 compressive strengths relative to their day 28 strength is shown in Figure 5.3. The results indicate that, by day 3, and day 7, all the structures, except B1, attained approximately 80% and 90%, of their 28 day strength, respectively. The B1 beams, however, attained approximately 60% by day 3 and 80% by day 7 of their 28 day strength. These beams had the lowest specified design strength and the lowest total cementitious content of the structures tested. As a result, they had the slowest development in strength. The G3 middle web cores had a surprisingly low average compressive strength on day 3 (only 40% of their 28 day strength), but experienced a large increase in compressive strength between day 3 and day 28. These cores were not available for inspection and, therefore, an explanation of this deviating behaviour is not possible.

The results indicate that most of the concrete hydration had occurred by day 7 and the further strength development between day 7 and day 28 was limited. Based on these findings, compressive strength

acceptance of the structure based on core test results can occur as early as day 7 and in some cases even as early as day 3.

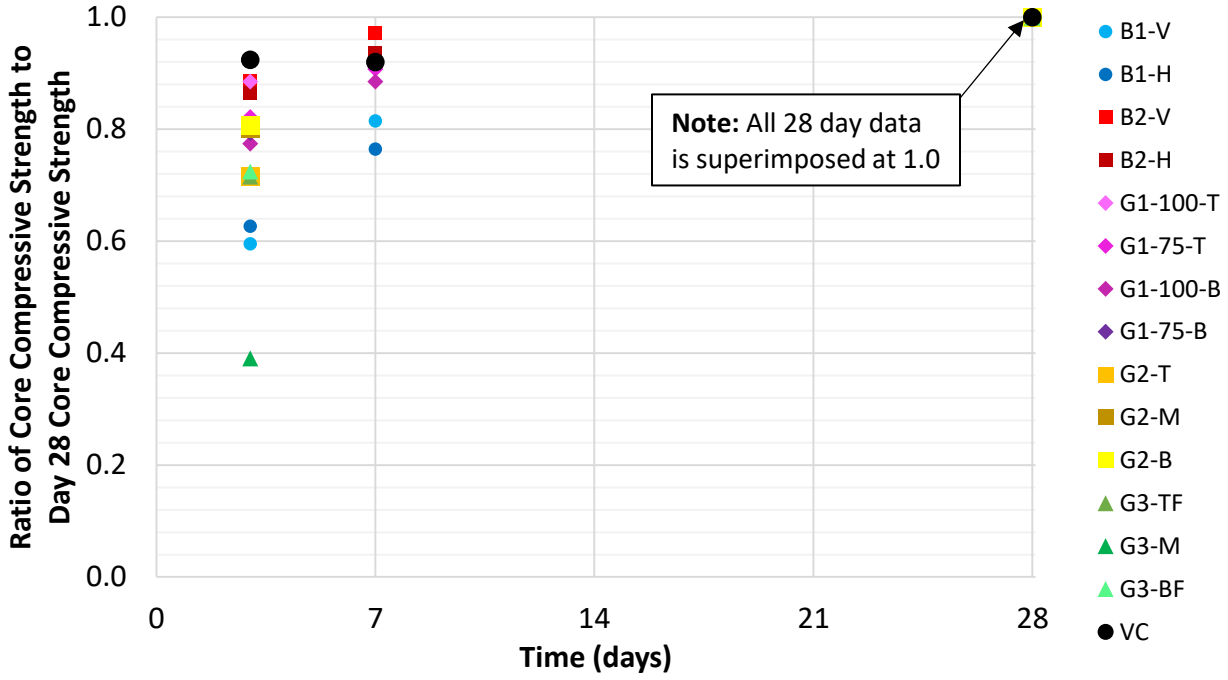

Figure 5.3 Compressive Strength of Cores on Day 3 and 7 Relative to Day 28 Strength

5.2 Compressive Strength of Cores versus Cylinders

The comparison of the average day 3 compressive strengths of cores and cylinders illustrates the difference between the lab structures and the precast structures. For the lab structures, the cores' strengths were approximately 120% of the cylinder strengths as shown in Figure 5.4, whereas the early strength of the precast plant structures was only approximately 87% of the cylinder strengths. The effect of wooden formwork and controlled ambient temperature in the lab versus the steel formwork and outdoor temperatures is believed to be responsible for this difference.

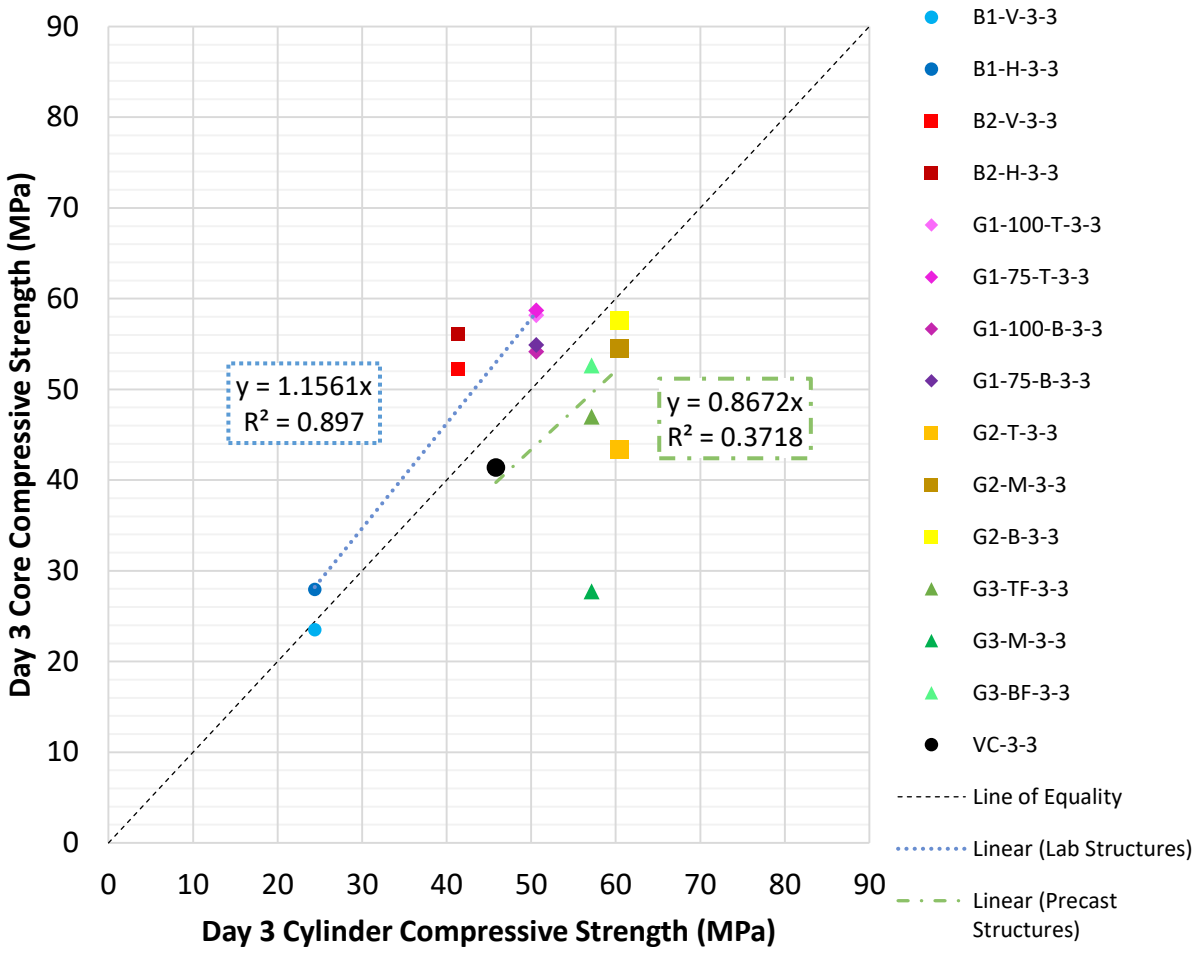

Figure 5.4 Average Day 3 Compressive Strength of Cores versus Cylinders

This separation between the lab structures and precast structures is not observed in the comparison of core and cylinder strengths at 28 days (Figure 5.5). With the exception of the B1 beams, the average compressive strength of the cores is lower than that of the cylinders. The trendline for the results from all the structures and that for only the high-strength concrete structures (B2, G1, G2, and G3) indicate the same result: that the average 28 day compressive strength of the cores is approximately 91% of the average 28 day cylinder compressive strength.

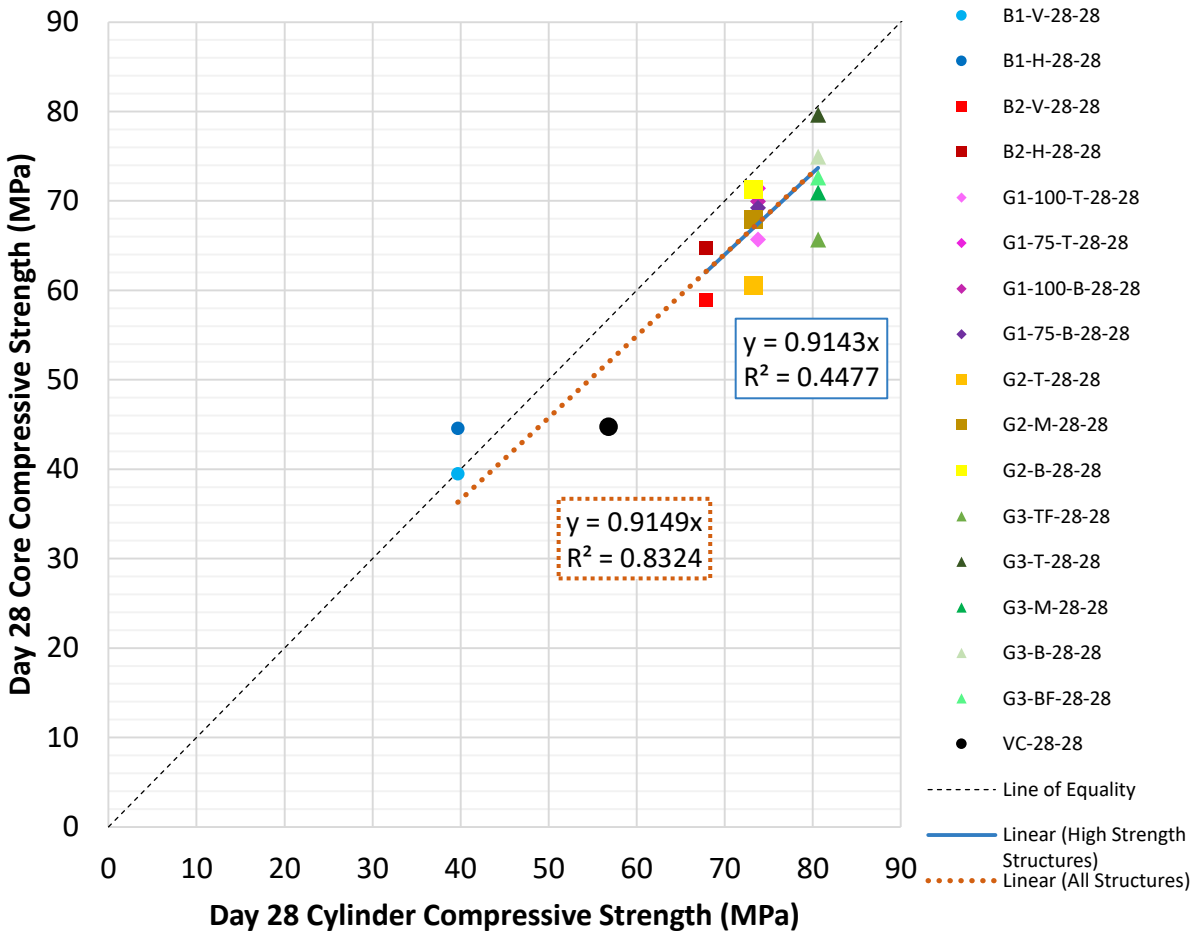

Figure 5.5 Average Day 28 Compressive Strength of Cores versus Cylinders

5.3 Electrical Resistivity

The day 3 and day 7 bulk resistivity relative to their day 28 bulk resistivity are shown in Figure 5.6. If the results from the VC and B2-H outlier cores (discussed in Section 4.4) are omitted from the general trend, the results indicate that the day 3 and day 7 resistivity are approximately 55% and 70% of their day 28 values. Unlike the early development of the compressive strength, the resistivity increases at a slower rate between day 7 and 28. Therefore, in order to assess the concrete for early age acceptance, the day 3 or day 7 resistivity should be evaluated on its projected day 28 resistivity.

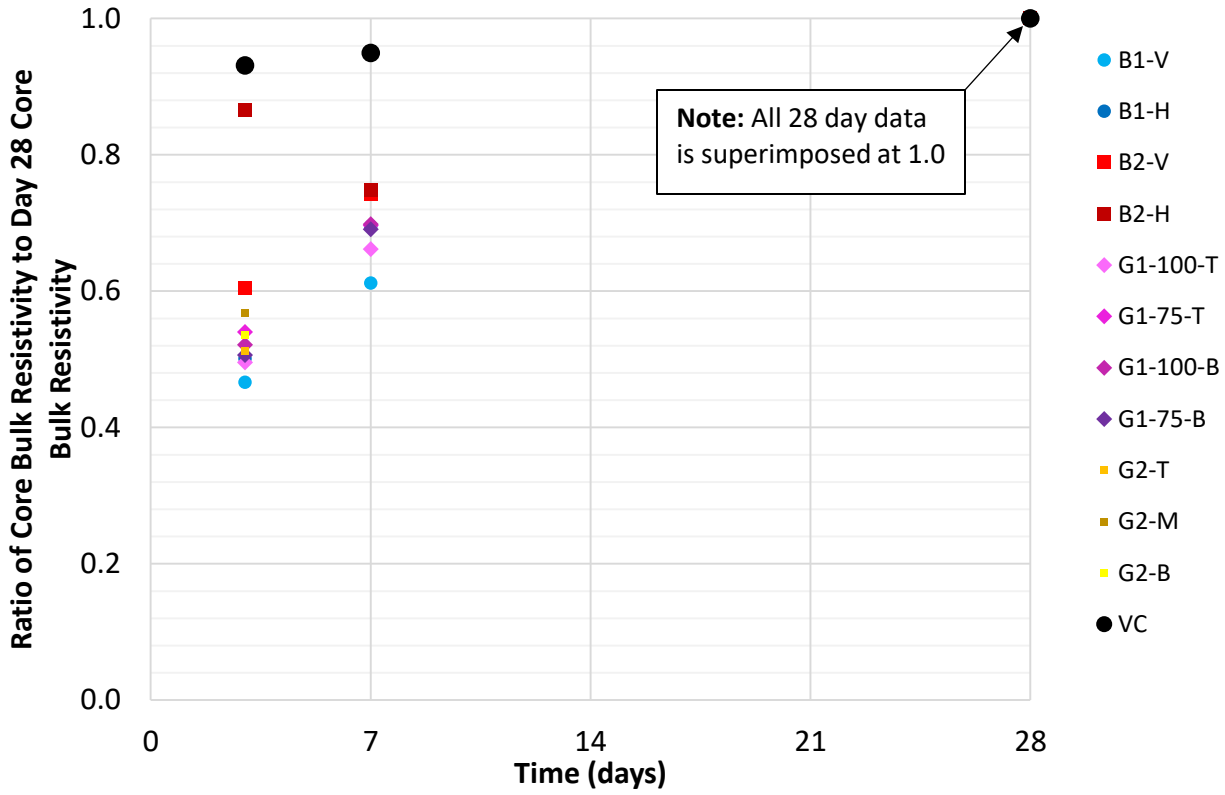

Figure 5.6 Bulk Resistivity on Day 3 and Day 7 Relative to Day 28

5.4 Vertical and Horizontal Cores

The locations of the vertical and horizontal cores were chosen to represent the possible coring that would be experienced during the construction of the bridge infrastructure. Cores can be extracted vertically from elements, such as pier caps or beams, before girders are placed on top, but if the top of the pier cap or beam is inaccessible, horizontal cores would likely be extracted from the mid height of the element. The results indicate that the average horizontal core strength was 1.1 times stronger than the average vertical core strength on days 3, 7, and 28 for both B1 and B2 beams (Figure 5.7). This was found to be caused by increased temperature during hydration and slightly better compaction in the middle of the beams compared to the top.

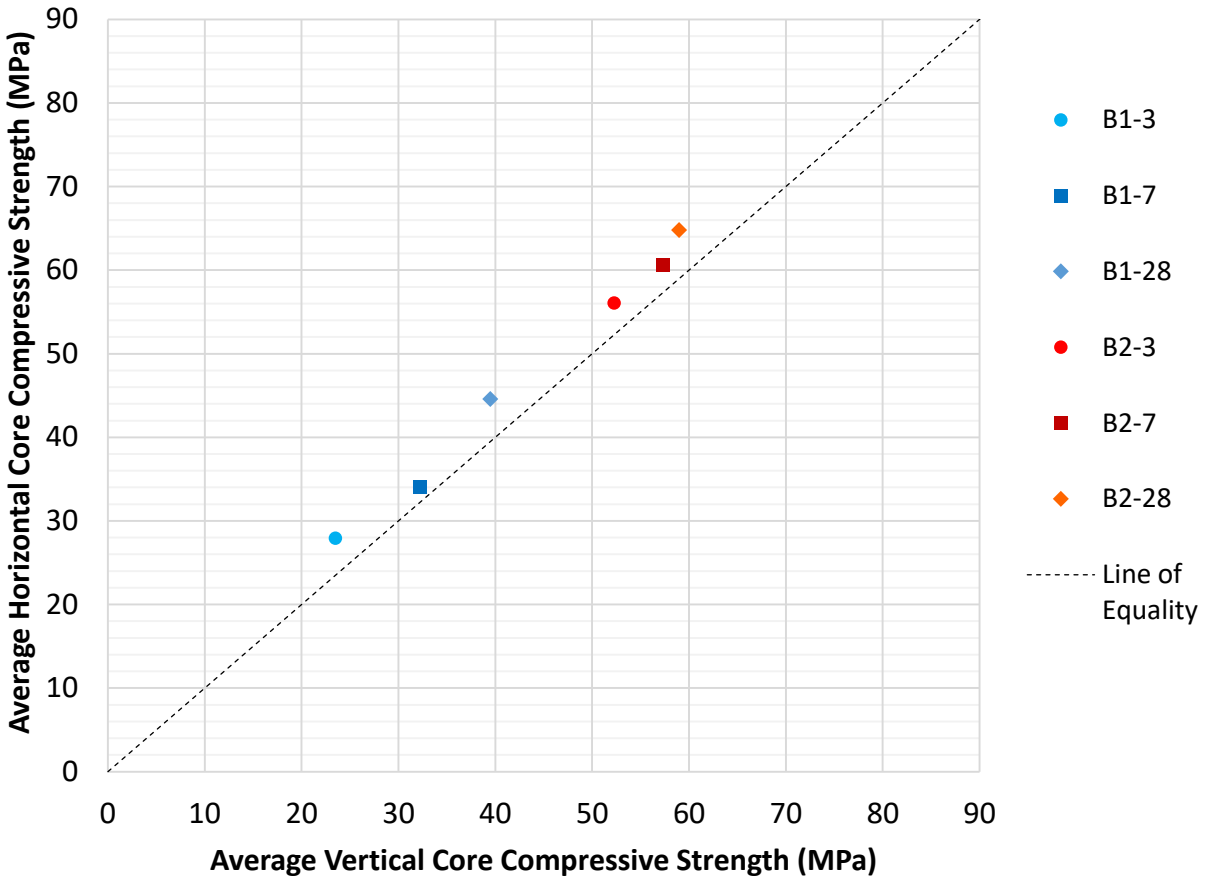

Figure 5.7 Average Horizontal Core Strength versus Average Vertical Core Strength

In the case of the bulk resistivity results, the B1 horizontal and vertical cores had approximately equal resistivity on days 3, 7, and 28, while the B2 horizontal cores, on average, were approximately 1.1 times more resistive than their vertical counterparts (Figure 5.8). The one outlier was the day 3 bulk resistivity of the horizontal (discussed previously in Section 4.4.2). The difference between the B1 and B2 concretes relating to vertical and horizontal cores is due to the greater hydration temperature seen in the B2 concrete which contained silica fume and is more sensitive to changes in the pore structure of the concrete caused by temperature.

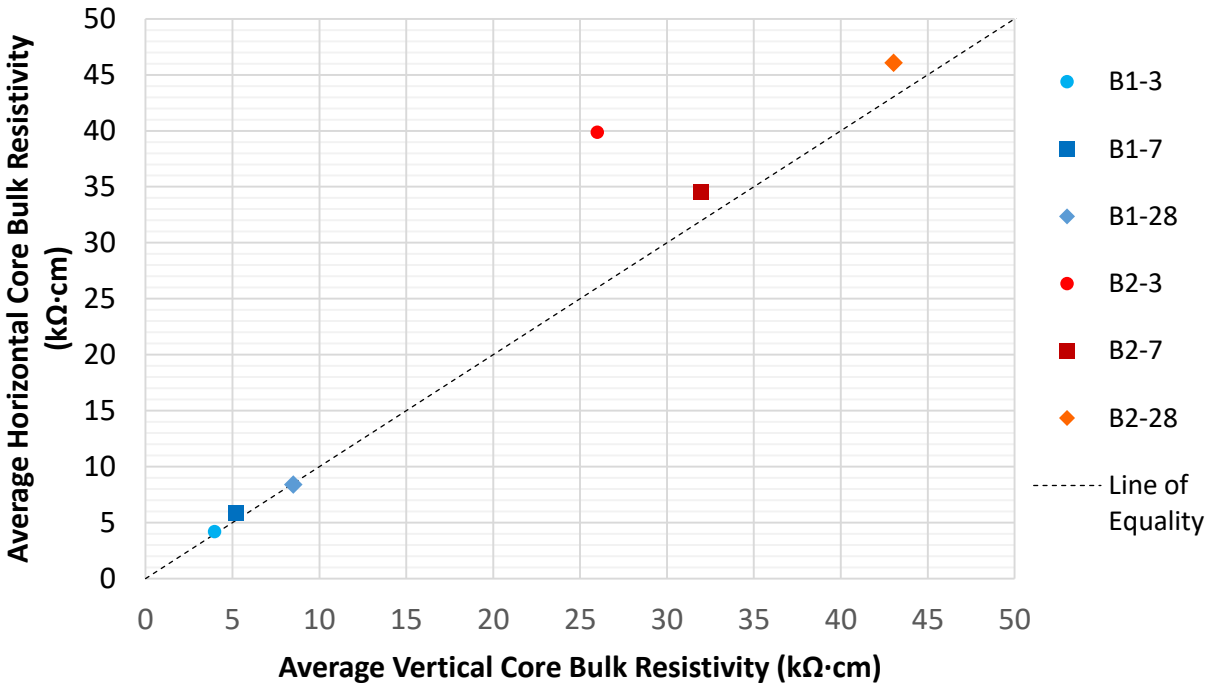

Figure 5.8 Average Horizontal Core Bulk Resistivity versus Average Vertical Core Bulk Resistivity

5.5 Variation in Performance of Cores with Height

The variation in compressive strength with height was investigated in the G1, G2, and G3 girders. The influence of height on the day 3 compressive strength varied between the 3 girders (Figure 5.9). The G1 top cores had higher day 3 strengths than the bottom cores due to slightly higher hydration temperature in top section of the web (Section 4.2.4). The G2 structure was primarily affected by poor consolidation of the top of the web resulting in lower compressive in the top cores (Section 4.2.5 and 4.6). The day 3 testing of the G3 girder did not include top and bottom cores from the web section in addition to the mid-height web cores recording exceptionally lower compressive strengths compared to the top and bottom cores from the flange sections. Due to the poor consolidation of the G2 structure and missing information from the G3 structure, the variation in compressive strength with height cannot be determined from the day 3 results.

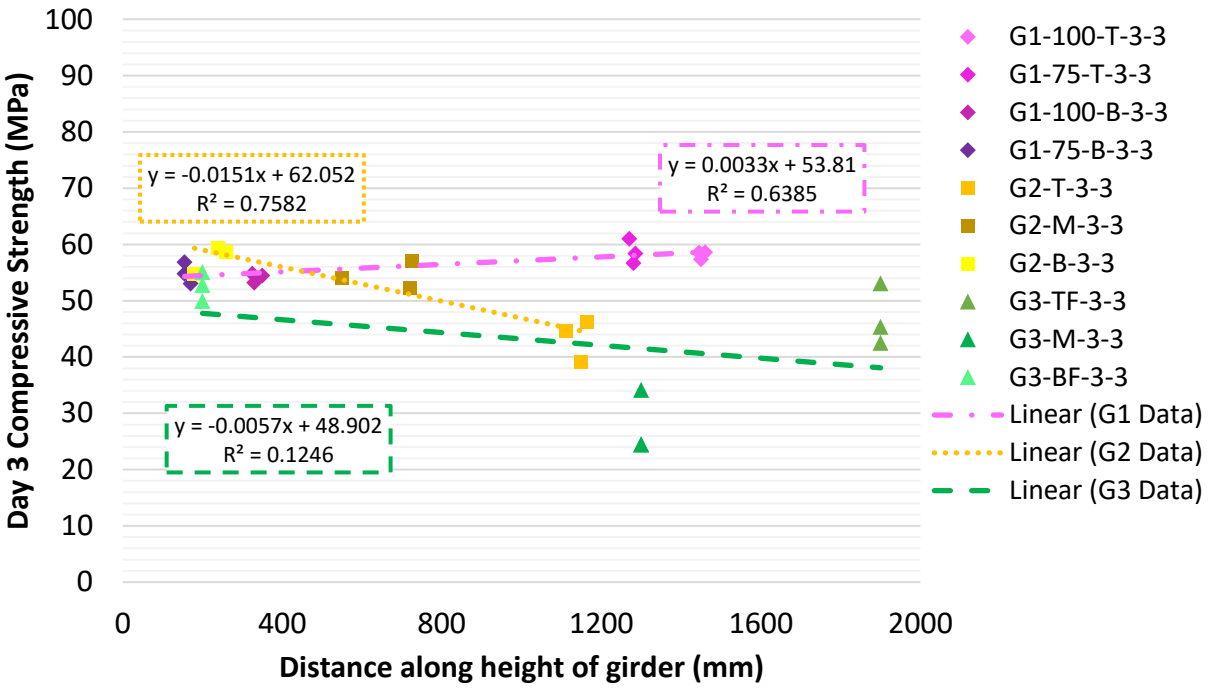

Figure 5.9 Variation in Day 3 Compressive Strength with Height

The 28 day compressive strength of the G1 and G3 girder cores remained fairly constant along the height of the web of the girders as shown in Figure 5.10. The only exception would be the cores from the top flange in the G3 girder which had lower strength associated with a decreased density, similar to the G2 cores (Section 4.6). Based on these findings, in particular the G1 and G3 girders, the variation in compressive strength on along the height is expected to be relatively small and, therefore, cores can be extracted from the top or bottom of the web on day 28 and similar compressive strengths would be expected.

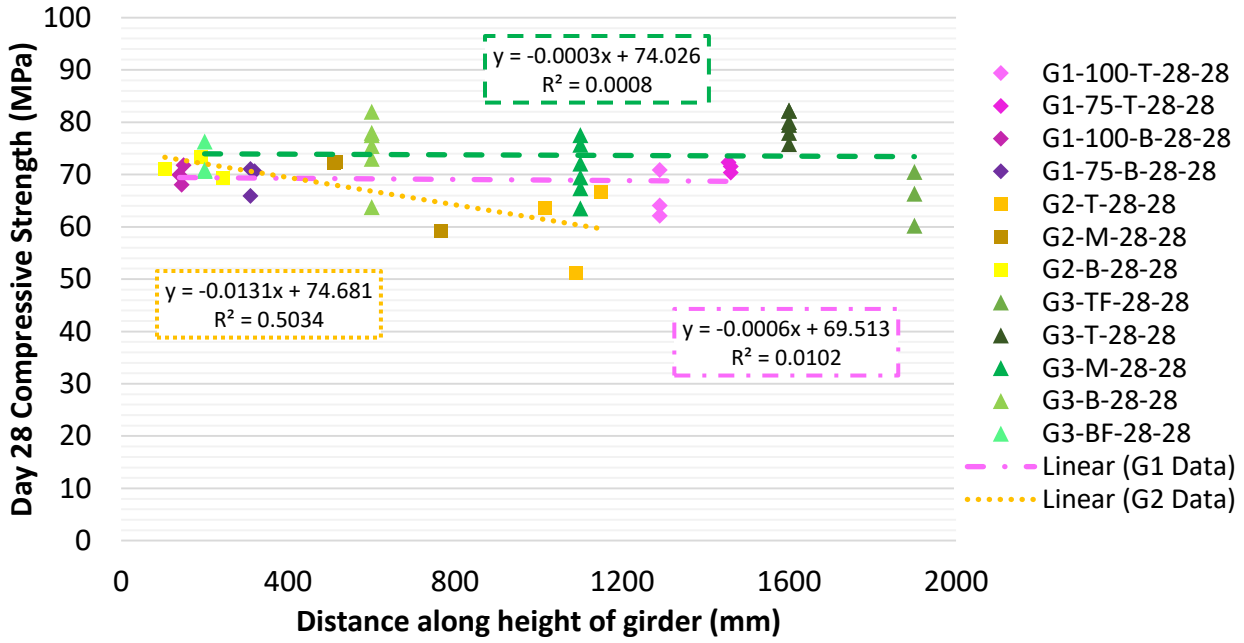

Figure 5.10 Variation in Day 28 Compressive Strength with Height

The bulk resistivity remained fairly constant along the height of the G1 and G2 girder webs on both day 3 and day 28 (Figure 5.11 and Figure 5.12). The bottom cores recorded slightly higher resistivity than the top cores due to slightly greater paste content in the top cores which lead to lower resistivity since the ions are carried through the pores in the paste.

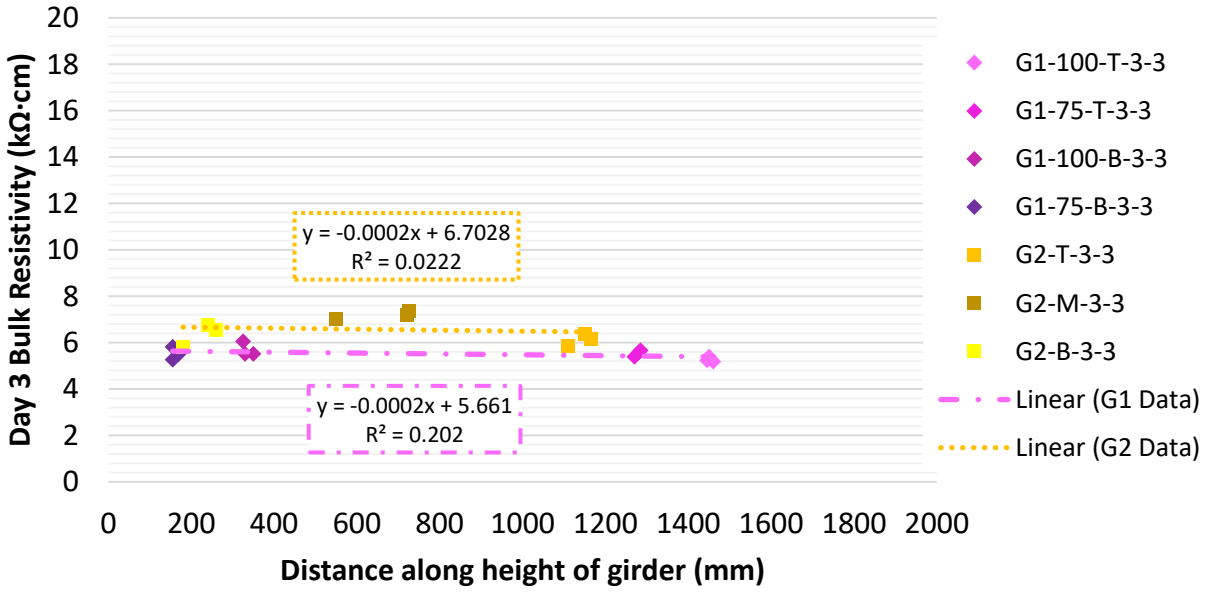

Figure 5.11 Variation in Day 3 Bulk Resistivity due to Height

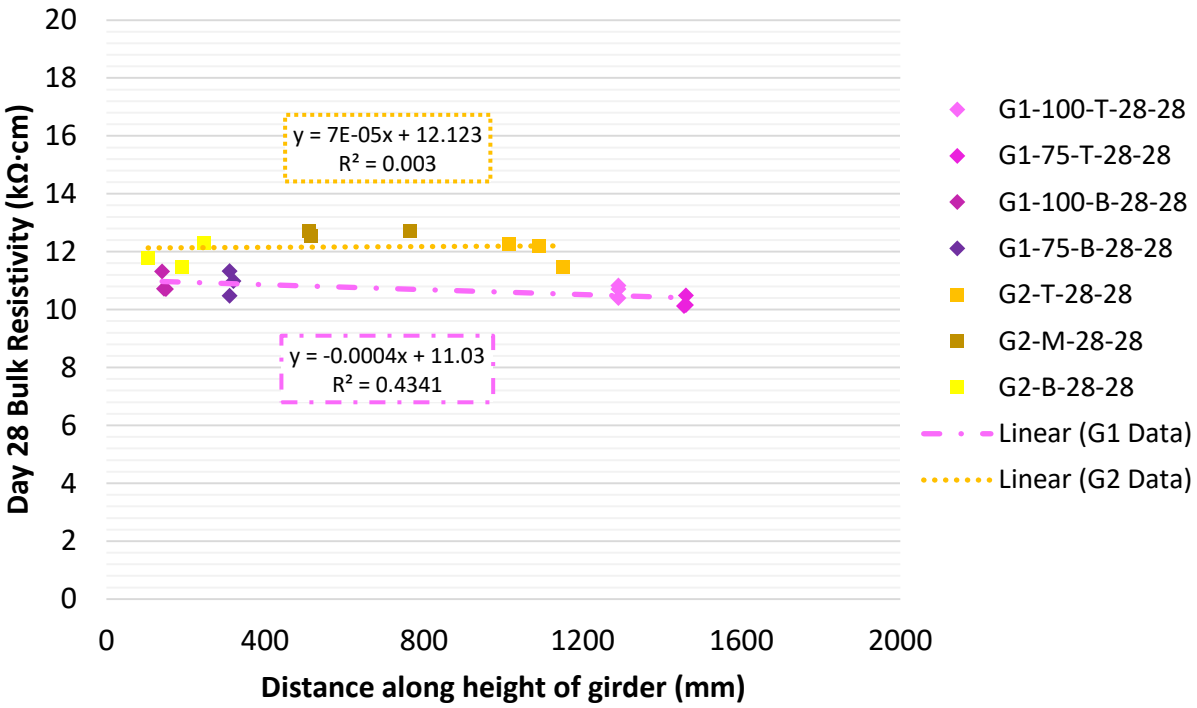

Figure 5.12 Variation in Day 28 Bulk Resistivity due to Height

In conclusion, the compressive strength and bulk resistivity on day 28 were found to be fairly constant along the height of the tested girders which indicates that it is possible to extract cores at any preferred location along the height of the girder web for acceptance on day 28.

5.6 Rapid Chloride Permeability and Electrical Resistivity

As it was previously discussed, an alternative to the RCP testing procedure is an electrical resistivity measurement of the concrete. Theoretically, an inverse relationship can be determined between the charge passed and the resistivity as indicated in Equation 2 (Layssi et al. 2015).

$$Q = I \cdot t = \frac{V}{R} \cdot t = \frac{V}{\frac{L}{A}\rho} \cdot t = \left(\frac{V \cdot A \cdot t}{L}\right) \cdot \frac{1}{\rho} \qquad (2)$$

Where Q is the charge passed from the RCP test, I is the current, t is the time, V is the potential difference, R is the resistance of the material, L and A are the length and cross-sectional area of the sample, and ρ is the resistivity. The expression (V·A·t / L) is a constant and, therefore, an inverse relationship between Q and ρ is found. Conductivity, σ, is the inverse of resistivity and, therefore, a linear relationship exists between the charged passed and the conductivity. The value of this constant is

determined by setting the potential as 60 Volts, time as 21600 seconds (6 hours for RCP test), area as the cross-sectional area of a 10 cm (100 mm) diameter sample, and length as 5 cm (50 mm) resulting in a value of 20358 V·s·cm (Equation 3).

$$Q = 20358 \cdot \sigma \tag{3}$$

where Q is in Coulombs and σ is in $(k\Omega \cdot cm)^{-1}$. It is noted here that the results of resistivity and RCP testing presented in Figure 5.13 are from cores which were extracted on days 3, 7, and 14, and maintained in a saturated state in calcium hydroxide until time of testing on day 28. The trend of the test results follows the theoretical line closely, however, the results from the VC structure tend to deviate further from the line than the other cores due to the poor curing of the VC structure. The day 3 extracted core is closest to the trendline, but the day 7 and day 14 cores which spent longer periods of time exposed to the elements, deviate further from the trend. The day 7 and day 14 VC outliers were removed and the resulting trend more accurately follows the theoretical correlation (Figure 5.14).

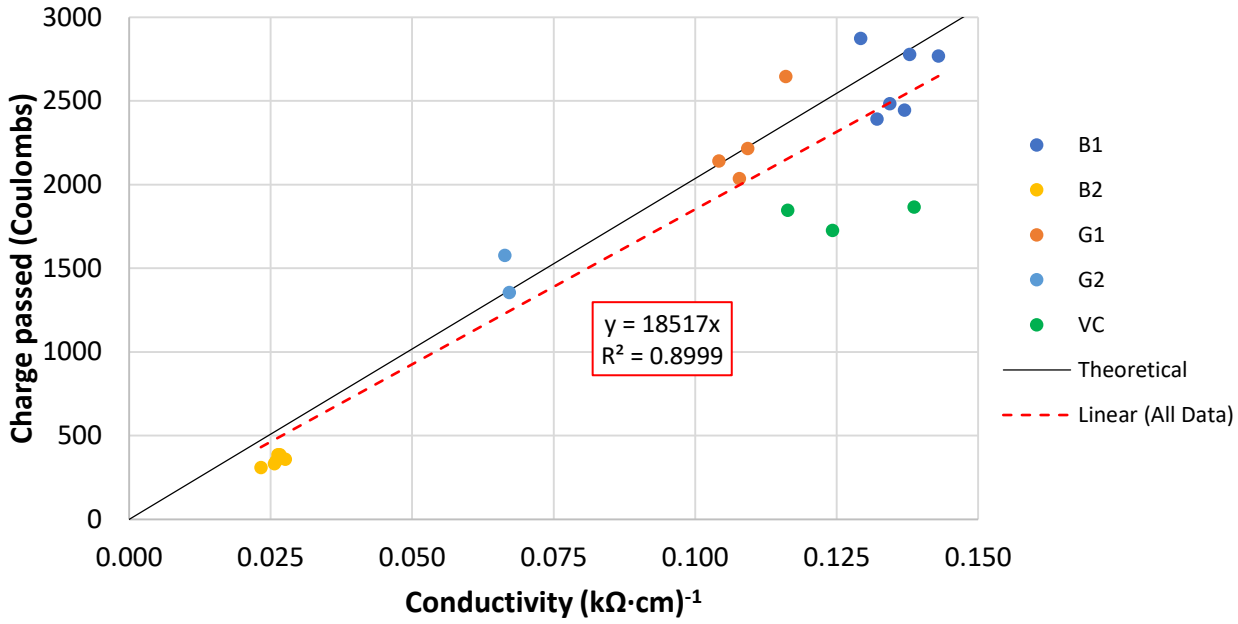

Figure 5.13 Rapid Chloride Permeability Test Results versus Bulk Conductivity

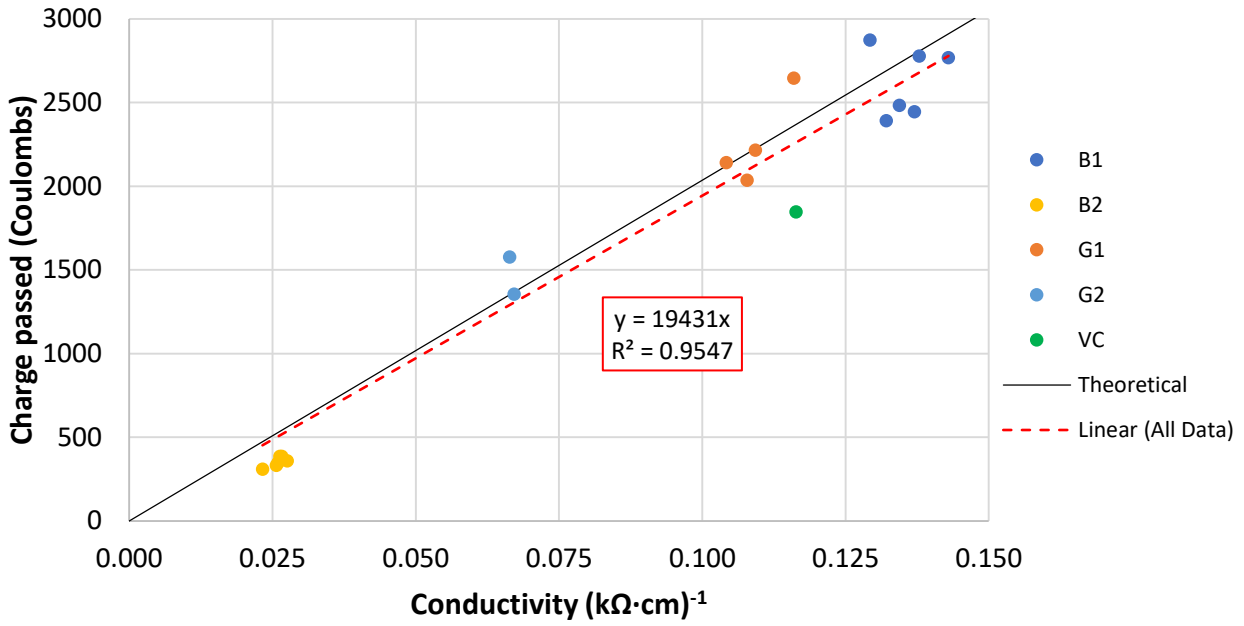

Figure 5.14 Rapid Chloride Permeability Test Results versus Bulk Conductivity with Outliers Removed

The resistivity measurement is quicker to perform than the RCP testing procedure. Using the trend between the RCP test results and bulk conductivity, bulk resistivity and conductivity values associated to the RCP test limits defined in OPSS 1350, OPSS 909, and SSP 999 can be established (Table 5.1). For concretes containing silica fume, the proposed associated limits would be a conductivity smaller than 0.05 kΩ·cm^{-1} or a resistivity greater than 20 kΩ·cm. For all other concretes, the proposed limits would be a conductivity smaller than 0.125 kΩ·cm^{-1} or a resistivity greater than 8 kΩ·cm.

Table 5.1 Predicted Conductivity and Resistivity Values for Associated Ontario Provincial RCP Acceptance Test Results

Concrete Type	RCP Test Result (Coulombs)	Conductivity (kΩ·cm)$^{-1}$	Resistivity (kΩ·cm)
Containing Silica Fume	1000	0.05	20
All Other Concretes	2500	0.125	8

6 Summary, Conclusions, and Recommendations

The research presented in this thesis introduced the performance of cores extracted from structures at early age for the purpose of early acceptance of concrete in highway infrastructure. It is evident from the limited amount of research available on early age concrete coring that extracting and testing cores at earlier ages than day 28 is not very common. The experimental component of this research included testing and evaluating cores extracted on days, 3, 7, and 28 from different structures constructed in the University of Waterloo laboratory and in three prefabrication plants. The cores were evaluated for compressive strength, rapid chloride permeability, electrical resistivity, density, and air void system to understand the changes in performance during the early stages of concrete hydration until day 28. The goal of the research was to assess the feasibility of coring at early ages in order to make informed decisions about the early acceptance of the concrete while understanding the expected day 28 performance.

6.1 Summary

- The cores extracted from the structures had day 3, day 7, and day 28 compressive strengths of approximately 90%, 110%, and 120%, respectively, of the 28 day specified design strength. This indicates that the strength of the structure exceeds the design strength by day 7 and is followed by little growth in strength between day 7 and day 28. Comparing the day 3 and day 7 compressive strengths of the cores to their 28 day strength, it was found that the day 3 and day 7 strengths were approximately 80% and 90% of the their 28 day strength, respectively. The one exception from these results are the B1 beams which had a 28 day design strength of 30 MPa and were cast using the smallest total cementitious content compared to the remaining concretes resulting in slower development of properties. The cores from the B1 beams were found to have day 3 and day 7 strengths of 60% and 80%, respectively, of their day 28 strength.
- The electrical resistivity behaviour was fairly similar among all of the concretes used in this research and was found to have day 3 and day 7 bulk resistivity results of approximately 55% and 70% of their 28 day resistivity, respectively. This indicates that the development of the concrete microstructure relating to the transfer of ions through the concrete is slower than the growth of the compressive strength of the concrete in the structure.
- The day 3 comparison of cores and cylinders indicated different performance between the lab structures and the precast structures. The lab structures, which were maintained in a more controlled environment during the curing period inside the University of Waterloo lab, had a

stronger influence from the hydration temperature resulting in core compressive strengths on average 120% of the cylinder compressive strengths on day 3. The precast structures, which required removal from formwork after approximately 24 hours and moving to another curing location, were found to have core compressive strengths that were on average 87% of the cylinder strengths. However, on day 28, the performance of the lab structures and precast structures was similar and the cores compressive strengths were found to be approximately 91% of the cylinder compressive strengths.

- A comparison was made between vertical and horizontal cores to represent the possible coring from various bridge elements. Cores can be extracted vertically from the top surface of exposed elements, such as pier caps or beams, before girders are placed on top but, if this is not possible, horizontal cores would likely be extracted from the mid height of the pier cap or beam. The average horizontal core strength was found to be 1.1 times stronger than the average vertical core strength on days 3, 7, and 28. Similarly, the horizontal cores from silica fume blended concrete had approximately 1.1 times higher bulk resistivity than the vertical cores, while the resistivity of horizontal and vertical cores from the lower strength blast furnace slag blended concrete was approximately the same on days 3, 7, and 28.
- Investigation of the variation in performance along the height of the web of large girders found that there was little difference in compressive strength and bulk resistivity on day 28 along the height of the web. The day 3 results did not have any conclusive trends due to missing information or construction defects from the prefabricated structures. Day 7 data were not collected from the field structures and, therefore, no conclusions can be drawn for coring location along the height at early age. The results of the lab constructed girder, which was constructed and maintained in a controlled environment, concluded that the performance at the top and bottom of the web was similar on days 3, 7, and 28.
- The rapid chloride permeability and bulk conductivity were found to have a linear correlation. The bulk conductivity is taken as the inverse of the bulk resistivity which is a quicker measurement to perform compared to the rapid chloride permeability testing procedure. Using the linear relationship between the rapid chloride permeability test results and bulk conductivity, values for bulk resistivity and conductivity associated to the current rapid chloride permeability test limits defined in OPSS 1350, OPSS 909, and SSP 999 are established. For concretes containing silica fume, the proposed day 28 limits would be a conductivity smaller than 0.05 $k\Omega \cdot cm^{-1}$ or a resistivity greater than 20 $k\Omega \cdot cm$. For all other concretes, the proposed

associated limits would be a conductivity smaller than 0.125 $k\Omega \cdot cm^{-1}$ or a resistivity greater than 8 kΩ·cm.

- The temperature during curing and the ambient temperature surrounding the structure during the hydration were found to have a profound effect on the performance of the concrete. This was evident in the difference between the lab structures and precast structures, particularly on day 3, where cores from lab structures, which were cast using wooden formwork and maintained in a controlled room temperature environment, tended to have compressive strengths higher than cylinder strengths. The effect of freezing temperature during the first 28 days was seen in the results of the valve chamber structure placed outside 2 days after casting and resulted in very little growth in compressive strength and bulk resistivity between day 3 and day 28.

6.2 Conclusions

- This research has shown that it is reasonable to extract and test cores as early as day 3 from high strength concretes and it is acceptable to extract and test cores as early as day 7 for all concretes. On day 7 testing, it is expected that on average the strength of the structure should exceed the design strength and that the bulk resistivity should be approximately 70% of its 28 day bulk resistivity.
- For the lower strength concrete, which exhibits slower growth in properties, coring prior to day 7 may not provide meaningful assessment of the performance of the concrete.
- It is concluded from the laboratory studies that cores extracted near the top or bottom of the web on days 3, 7, and 28 will have similar strengths and bulk resistivity. However, due to the uncertainty from the field structures, it is suggested that cores should be extracted near the top and bottom of the web of the girder to check adequacy of consolidation and variation in quality of the concrete relating to compressive strength, resistivity, rapid chloride permeability, density, paste content, and air void system.
- The temperature during hydration and the ambient temperature surrounding the structure during the curing period was found to have a profound effect on the development of concrete properties. This was evident in the difference between the lab structures and precast structures, particularly on day 3, where cores from lab structures, which were cast using wooden formwork and maintained in a controlled room temperature environment, tended to have compressive strengths larger than cylinder strengths on day 3. However, on day 28, the cylinders tended to have compressive strengths larger than the cores. The effect of freezing temperature during

curing was seen in the results of the valve chamber structure placed outside 2 days after casting which resulted in very little growth in concrete properties between day 3 and day 28.

- It is concluded that an extended exposure period in a controlled environment is required to ensure adequate hydration of the concrete in the structure.

6.3 Recommendations for Future Practice

Based on the conclusions described above, some recommendations are provided for practitioners who wish to consider using cores for early concrete acceptance.

Coring and testing for concrete acceptance is clearly acceptable as early as day 7. The research has shown that on average, the concrete in the structure has reached approximately 90% of its day 28 compressive strength and exceeded the specified design strength by day 7. Additionally, 7 days after casting can be coordinated well to occur on a weekday as a part of the construction sequence. Day 3 coring was found to reasonable for higher strength concretes, however, further testing is recommended to ensure its feasibility.

The influence of curing environment was found to have a profound impact on performance of the concrete. Exposing the concrete at early age to freezing temperatures prevents adequate development of concrete properties and it is recommended to cure the concrete as long as possible and maintain the structure above freezing temperature until the internal temperature of the structure has decreased to the ambient temperature.

Lastly, it is recommended to use the bulk resistivity measurement in place of the rapid chloride permeability test. The bulk resistivity test was found to correlate well with the results of the rapid chloride test for all the concretes tested in this research. The bulk resistivity measurement is a quicker measurement to perform and requires less work for sample preparation compared to the rapid chloride permeability test.

6.4 Recommendations for Future Research

Future research is recommended to address some of the areas that this thesis research was unable to cover. The investigation into the effect of coring location along the height of girder webs of the field structures should be repeated. Further testing at early age, particularly day 7 coring and testing of field structures, to assess the feasibility of taking cores at any location along the height at early age. For the concretes tested in this research, a linear relationship between rapid chloride permeability (RCP) testing and bulk conductivity was found to match the theoretical relationship. This relationship exists for cores

extracted at early age, conditioned in a saturated state, and then tested on day 28. In order to perform same-day coring and testing at early age, it will not be possible to conduct RCP testing since this requires sectioning and presaturating the samples and setting up the test cell. Therefore, it is recommended to test sections of the cores “as cored”, i.e. not fully saturated, for rapid chloride permeability and electrical resistivity at early age to determine (i) if the linear relationship still holds and (ii) the relationship between the early age test results and those of the early cored samples tested at 28 days.

Letter of Copyright Permission

American Concrete Institute

Always advancing

Adam Felinczak
University of Waterloo
200 University Avenue West
Waterloo, Ontario, N2L3G1
Canada

May 30, 2018

Subject: Use of ACI Copyrighted Material

Your request to:

__X__ Use information/figures/tables indicated below. Please credit American Concrete Institute, author(s) and publication.

__X__ Reprint the information described in the quantity indicated. Please add a note to the reprint similar to: *Authorized reprint from (publication) (issue/volume/year as appropriate.)*

_____ Payment of Right-to-Reprint fee of ($0) is required.

Permission is granted to reference and reprint *Figure 5 "Compressive strength of concrete dried in laboratory air after preliminary moist curing"* from *Journal of the American Concrete Institute "Factors Influencing Concrete Strength" February 1951, Vol. 47, No. 2*

Signed: Angela Matthews Date: 30 May 2018

Angela Matthews
Editor, Publishing Services
Angela.Matthews@Concrete.org

Gmail **Adam Felinczak <adamfelinczak@gmail.com>**

Permission Request: Properties of Concrete (Request ID: 27825)

PearsonedEMA, Permissions <permissions@pearson.com> Wed, Jun 6, 2018 at 3:51 AM
To: Adam Felinczak <adamfelinczak@gmail.com>

Dear Adam

I am pleased to be able to grant permission for your use of ***Figures 6.1 and 7.6 from Pages 272 and 325 of Properties of Concrete, 5th Edition by A. M. Neville, ISBN 9780273755807,*** to be reproduced in your ***Thesis at University of Waterloo.***

Permission is granted free of charge, subject to acknowledgement to author/title and ourselves as publishers.

Permission does not extend to material that has been acknowledged to another source.

Acknowledgement: Title, author, Pearson Education Limited and Copyright line as it appears in our publication (note where figure and diagrams are reproduced, this acknowledgement is to appear immediately below them.

This permission is for non-exclusive World wide electronic rights in the English language for one use only.

Regards

Michael Prince

Global Innovations & Services
Pearson UK

4th Floor, Auto Atlantic

Corner Hertzog Boulevard and Heerengracht

Cape Town, 8001

South Africa

E: permissions@pearson.com

Learn more at za.pearson.com

Pearson

[Quoted text hidden]

Gmail **Adam Felinczak <adamfelinczak@gmail.com>**

Civil Engineering for Practicing and Design Engineers

Jones, Jennifer (ELS-OXF) <J.Jones@elsevier.com> Wed, Jun 27, 2018 at 6:03 AM
To: "adamfelinczak@gmail.com" <adamfelinczak@gmail.com>

ELSEVIER

Dear Adam Felinczak

We hereby grant you permission to reproduce the material detailed below at no charge **in your thesis, in print and on UWSpace** and subject to the following conditions:

1. If any part of the material to be used (for example, figures) has appeared in our publication with credit or acknowledgement to another source, permission must also be sought from that source. If such permission is not obtained then that material may not be included in your publication/copies.

2. Suitable acknowledgment to the source must be made, either as a footnote or in a reference list at the end of your publication, as follows:

"This article was published in Publication title, Vol number, Author(s), Title of article, Page Nos, Copyright Elsevier (or appropriate Society name) (Year)."

3. Your thesis may be submitted to your institution in either print or electronic form.

4. Reproduction of this material is confined to the purpose for which permission is hereby given.

5. This permission is granted for non-exclusive world **English** rights only. For other languages please reapply separately for each one required. Permission excludes use in an electronic form other than as specified above. Should you have a specific electronic project in mind please reapply for permission.

6. This includes permission for the Library and Archives of Canada to supply single copies, on demand, of the complete thesis. Should your thesis be published commercially, please reapply for permission.

Yours sincerely

Jennifer Jones
Permissions Specialist

Elsevier Limited, a company registered in England and Wales with company number 1982084, whose registered office is The Boulevard, Langford Lane, Kidlington, Oxford, OX5 1GB, United Kingdom.

12 Jun 2018 7:10pm

Question	Answer
Title	Mr.
First name	Adam
Last name	Felinczak
Institute/company	University of Waterloo
Address	200 University Avenue West
Post/Zip Code	N2L3G1
City	Waterloo
State/Territory	Ontario
Country	Canada
Telephone	9059296583
Email	adamfelinczak@gmail.com
Please select the type of publication	Journal

Question	Answer
Journal - Title	Civil Engineering for Practicing and Design Engineers
Journal - ISSN	0277-3775
Journal - Volume	4
Journal - Issue	8
Journal - Year	1985
Journal - Pages from	607
Journal - Pages to	615
Journal - Author	B.A. Suprenant
Journal - Article Title	AN INTRODUCTION TO CONCRETE CORE TESTING
I would like to use (please select one of the following options)	Figure(s)
If using figures/tables or illustrations please specify the quantity	1
If using excerpts please provide a total word count	
Are you the author of the Elsevier material?	No
If not, is the Elsevier author involved with your project?	No
If yes, please provide details of how the Elsevier author is involved	
In what format will you use the material?	Print and Electronic
Will you be translating the material?	No
If yes, please specify the languages	

Question	Answer
Information about your proposed use	Reuse in a thesis/dissertation
Proposed use text	Posting in Institutional Repository
AdditionalComments/Information	The desired figure I would like to use from the article is Figure 2: Planes of Weakness Due to Bleeding in a Grade Beam

---

References

Aitcin, Pierre-Claude. 1999. “Does Concrete Shrink or Does It Swell?” *Concrete International* 77–80.

Ariöz, Ö., M. Tuncan, K. Ramyar, and A. Tuncan. 2006. “A Comparative Study on the Interpretation of Concrete Core Strength Results.” *Magazine of Concrete Research* 58(2):117–22. Retrieved (http://www.icevirtuallibrary.com/doi/abs/10.1680/macr.2006.58.2.117).

ASTM C1202-12. 2012. “Standard Test Method for Electrical Indication of Concrete’s Ability to Resist Chloride Ion Penetration.” *American Society for Testing and Materials* 1–8.

ASTM C457/C457M-12. 2012. “Standard Test Method for Microscopical Determination of Parameters of the Air-Void System in Hardened Concrete.” *American Society for Testing and Materials* 05:1–15.

Bartlett, F. Michael and James G. MacGregor. 1994. “Assessment of Concrete Strength in Existing Structures.” *NRC Canada* 1029–37. Retrieved (https://era.library.ualberta.ca/files/5425k983w/SER198.pdf).

Bartlett, F. Michael and James G. MacGregor. 1994. “Reliability-Based Assessment of Concrete Strength in Existing Structures.” 321.

Bartlett, F. Michael and James G. MacGregor. 2000. *Reinforced Concrete: Mechanics and Design*. 1st ed. Toronto: Prentice Hall Canada Inc.

Bentz, Dale P., Gaurav Sant, and Jason Weiss. 2008. “Early-Age Properties of Cement-Based Materials. I: Influence of Cement Fineness.” *Journal of Materials in Civil Engineering* 20(7):502–8.

Bloem, D. L. 1965. “Concrete Strength Measurement - Cores versus Cylinders.” *Proceedings, American Society for Testing and Materials* 65:668–96.

Carroll, Adam C., Aaron R. Grubbs, Anton K. Schindler, and Robert W. Barnes. 2016. “Effect of Core Geometry and Size on Concrete Compressive Strength.” (1):122.

Cheng, An-Shun, Tsong Yen, Yu-Wen Liu, and Yeong-Nain Sheen. 2008. “Relation between Porosity and Compressive Strength of Slag Concrete.” *Structures Congress 2008* 1–8. Retrieved (http://ascelibrary.org/doi/abs/10.1061/41016%28314%29310).

CSA A23.1 / CSA A23.2. 2015. *A23.1-14 Concrete Materials and Methods of Concrete Construction / A23.2-14 Test Methods and Standard Practices for Concrete*.

Diamond, S. 1996. “Delayed Ettringite Formation - Processes and Problems.” *Cement and Concrete Composites* 18(3):205–15.

Goto, Seishi and Della M. Roy. 1981. “The Effect of w/c Ratio and Curing Temperature on the Permeability of Hardened Cement Paste.” *Cement and Concrete Research* 11(4):575–79.

Hassan, K. E., J. G. Cabrera, and R. S. Maliehe. 2000. “The Effect of Mineral Admixtures on the Properties of High-Performance Concrete.” *Cement and Concrete Composites* 22(4):267–71.

Khatri, R. P., V. Sirivivatnanon, and W. Gross. 1995. “Effect of Different Supplementary Cementitious Materials on Mechanical Properties of High Performance Concrete.” *Cement and Concrete Research* 25(1):209–20.

Kosmatka, Steven H., Beatrix Kerkhoff, R. Douglas Hooton, and Richard J. McGrath. 2011. *Design and Control of Concrete Mixtures*. 8th ed. Ottawa: Cement Association of Canada.

Layssi, Hamed, Pouria Ghods, Aali R. Alizadeh, and Mustafa Salehi. 2015. “Electrical Resistivity of Concrete.” *Concrete International* (May):41–46.

LS-432. 2017. “Method of Test for Microscopical Determination of Air Void System Parameters in Hardened Concrete.” *Ministry of Transportation, Ontario Laboratory Testing Manual* (31).

LS-433. 2011. “Method of Test for Electrical Indication of Concrete ’ s Ability to Resist Chloride Ion Penetration.” (26).

Malhotra, V. M. 1977. “Contract Strength Requirements-Cores Versus In Situ Evaluation.” *ACI Journal Proceedings* 74(4):163–72.

Mehta, P. Kumar. 1986. *Concrete: Structure, Properties, and Materials*. Englewood Cliffs, New Jersey: Prentice Hall.

Neville, Adam. 2001. “Core Tests: Easy to Perform, Not Easy to Interpret.” *Concrete International* (November):59–68. Retrieved (http://www.csa.com/partners/viewrecord.php?requester=gs&collection=TRD&recid=20020724 2084CE).

Neville, Adam M. 2011. *Properties of Concrete*. 5th ed. Harlow: Pearson Education Limited.

OPSS.PROV 1350. 2016. “Material Specification for Concrete - Materials and Production.” 1–33.

OPSS.PROV 904. 2014. “Construction Specification for Concrete Structures.” 1–25.

OPSS.PROV 909. 2016. “Construction Specification for Prestressed Concrete - Precast Girder.” 1–32.

Portland Cement Association. 1998. “Control of Air Content in Concrete.” *Concrete Technology Today* 19(1):1–8.

Powers, T. C. 1958. “Structure and Physical Properties of Hardened Portland Cement Paste.” *Journal of the American Ceramic Society* 41(1):1–6. Retrieved (http://dx.doi.org/10.1111/j.1151-2916.1958.tb13494.x).

Price, Walter H. 1951. “Factors Influencing Concrete Strength.” *ACI Journal* 47(2):417–32. Retrieved (http://www.concrete.org/Publications/ACIMaterialsJournal/ACIJournalSearch.aspx?m=details&ID=12003).

Shideler, J. J. and W. H. Chamberlin. 1949. “Early Strength of Concrete as Affected by Steam Curing Temperatures.” *Journal of American Concrete Institute* 46(18):273–82.

SSP 999F31. 2016. “Construction Specification for Non-Prestressed Precast Concrete Bridge Elements.” 1–19.

Suprenant, Bruce. 1985. “An Introduction to Concrete Core Testing.” *Civil Engineering for Practicing and Design Engineers* 4(8):607–15.

Suprenant, Bruce. 1995. “Core Strength Variation of In-Place Concrete.” *National Ready Mxixed Concrete Association* 1–3.

Szypula, A. and J. S. Grossman. 1990. “Cylinder versus Core Strength.” *Concrete International: Design and Construction* 12(2):55–61.

Taylor, H. F. W., C. Famy, and K. L. Scrivener. 2001. “Delayed Ettringite Formation.” *Cement and Concrete Research* 31(5):683–93.

Yener, Muaffer and Wai-Fah Chen. 1984. “On In-Place Strength of Concrete and Pullout Tests.” *Cement, Concrete and Aggregates* 6(2):90–99.

Appendix A - Additional Compressive Strength Lab Results

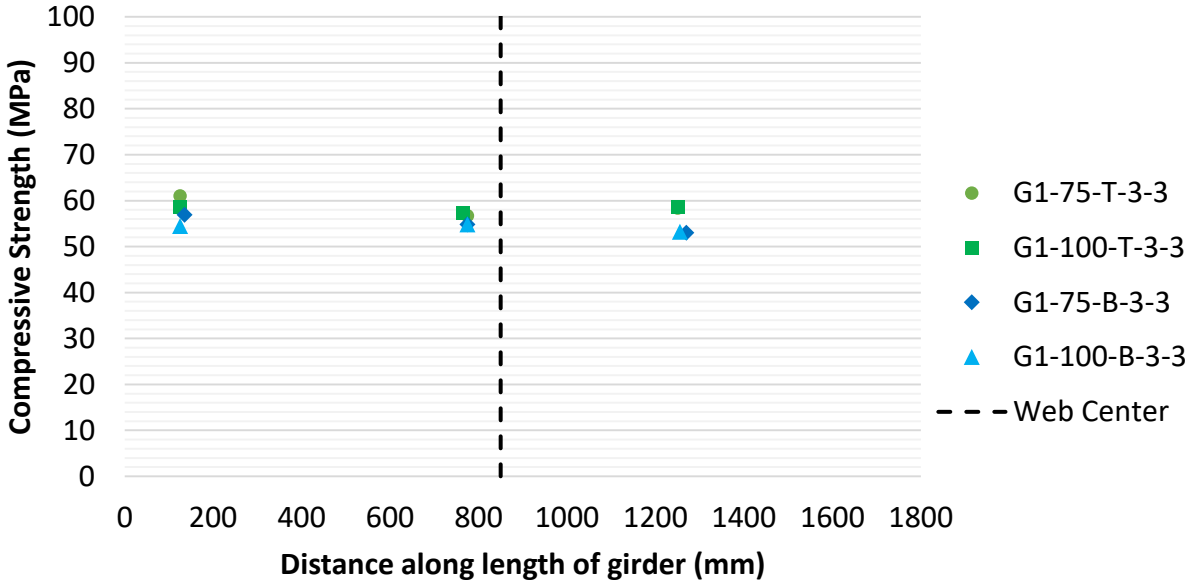

Figure A.1 Day 3 Compressive strength of individual cores versus length of G1 Girder Webs

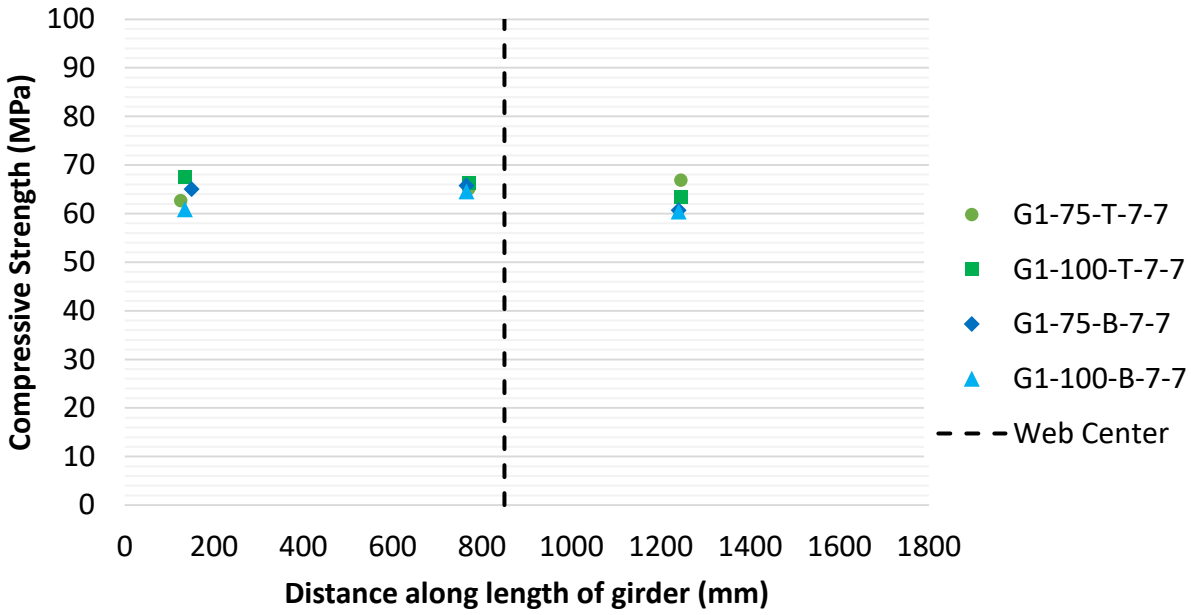

Figure A.2 Day 7 Compressive strength of individual cores versus length of G1 Girder Webs

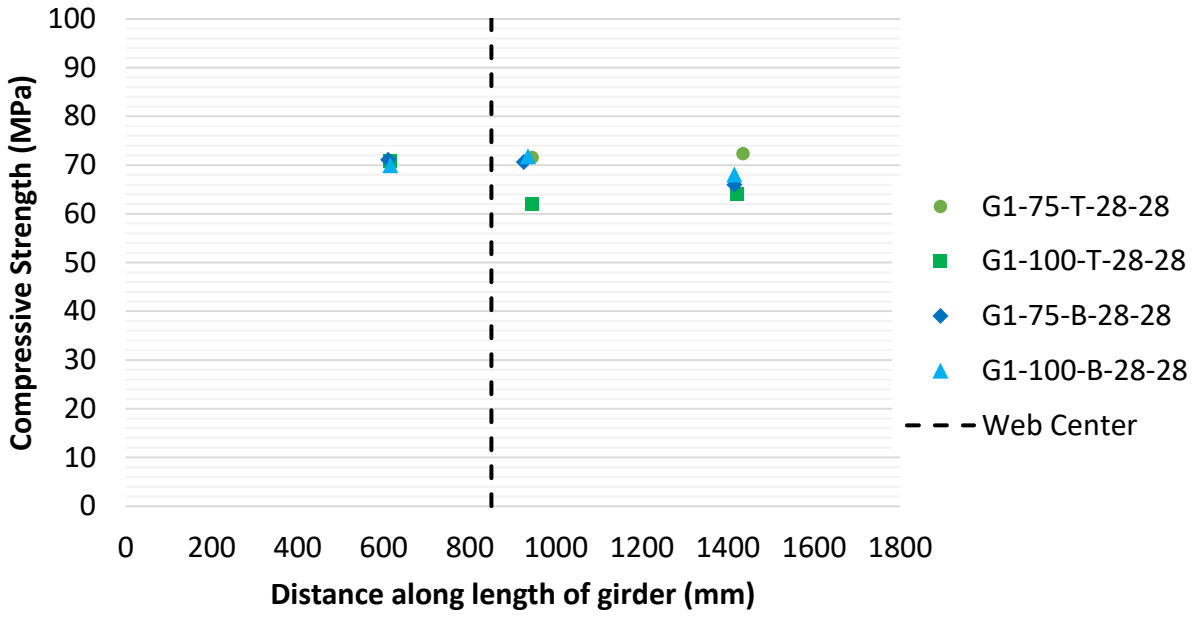

Figure A.3 Day 28 Compressive strength of individual cores versus length of G1 Girder Webs

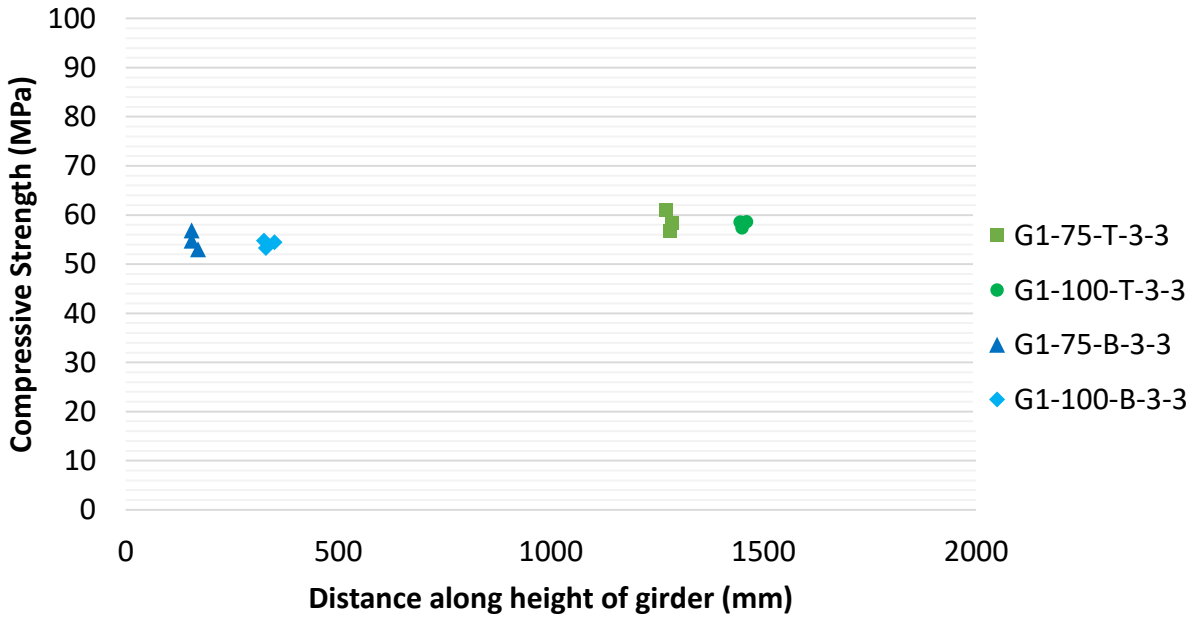

Figure A.4 Day 3 Compressive strength of individual cores versus height of G1 Girder Webs

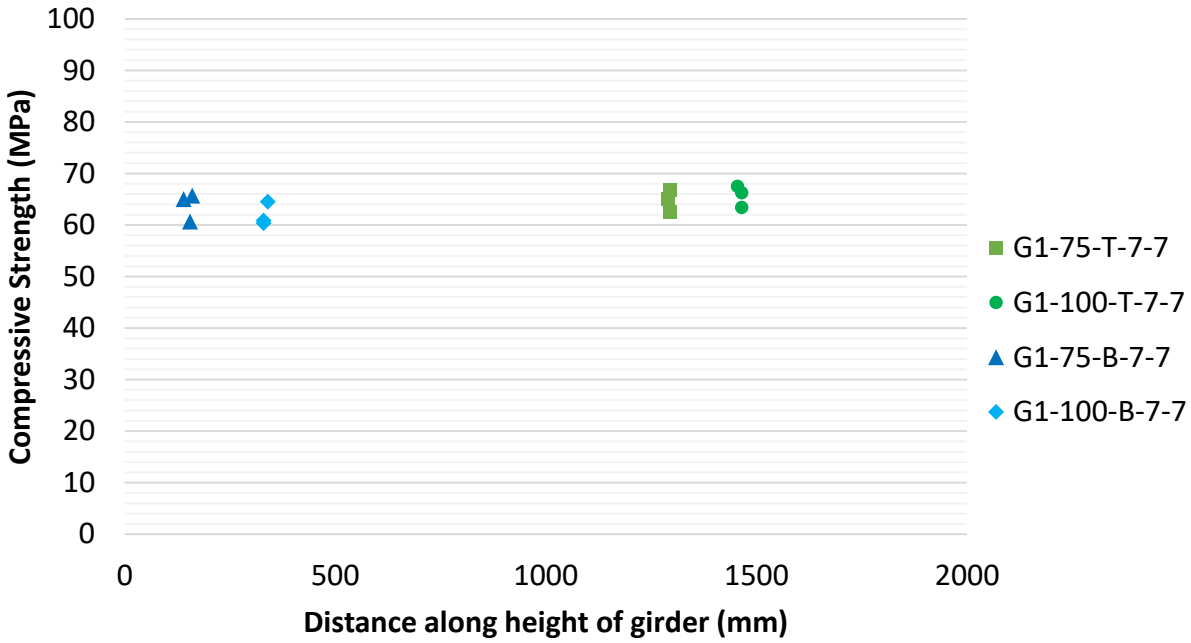

Figure A.5 Day 7 Compressive strength of indivudal cores versus height of G1 Girder Webs

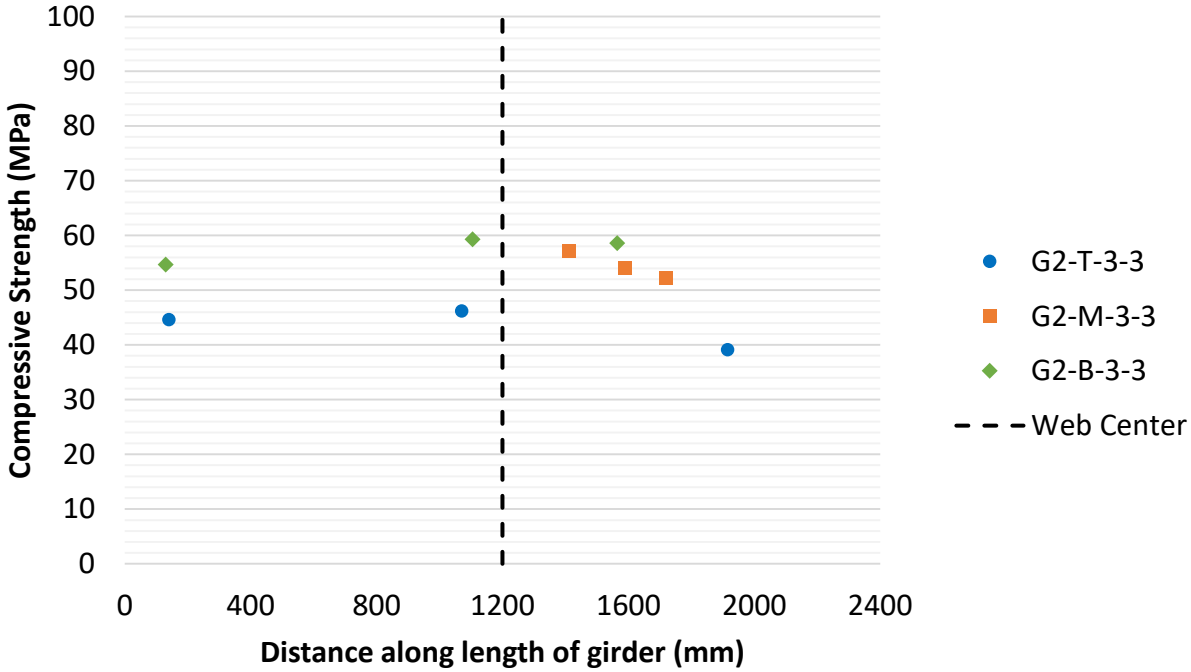

Figure A.6 Day 3 Compressive strength of individual cores versus length of G2 Girder Web

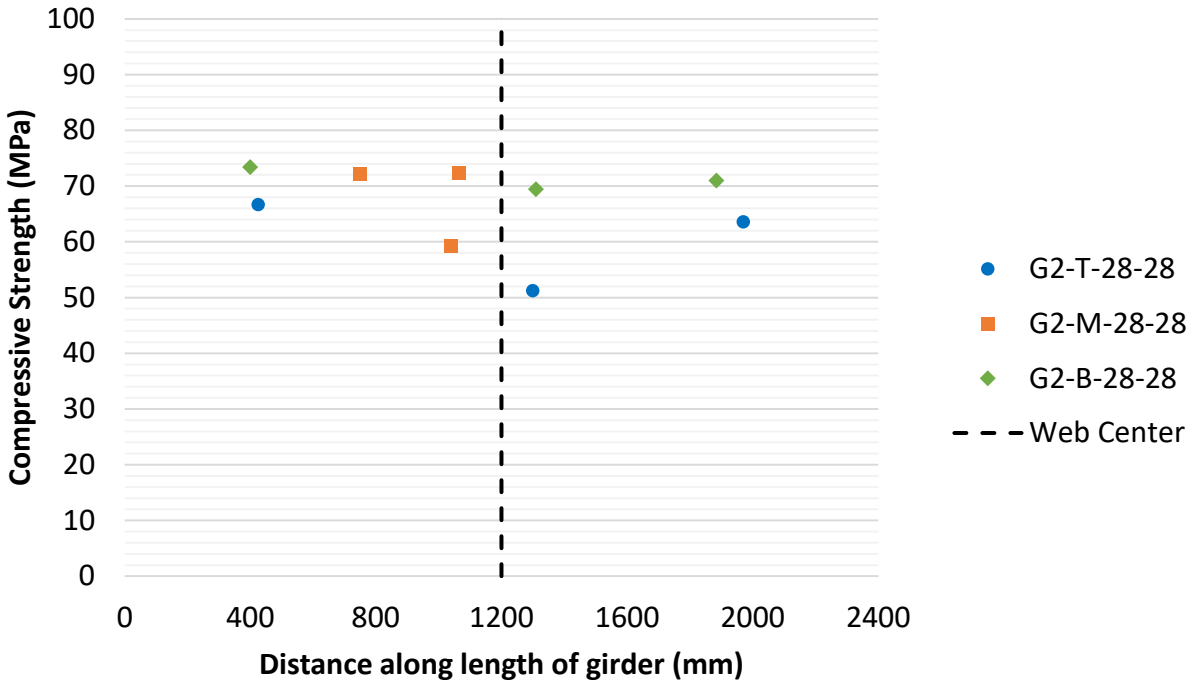

Figure A.7 Day 28 Compressive strength of individual cores versus length of G2 Girder Web

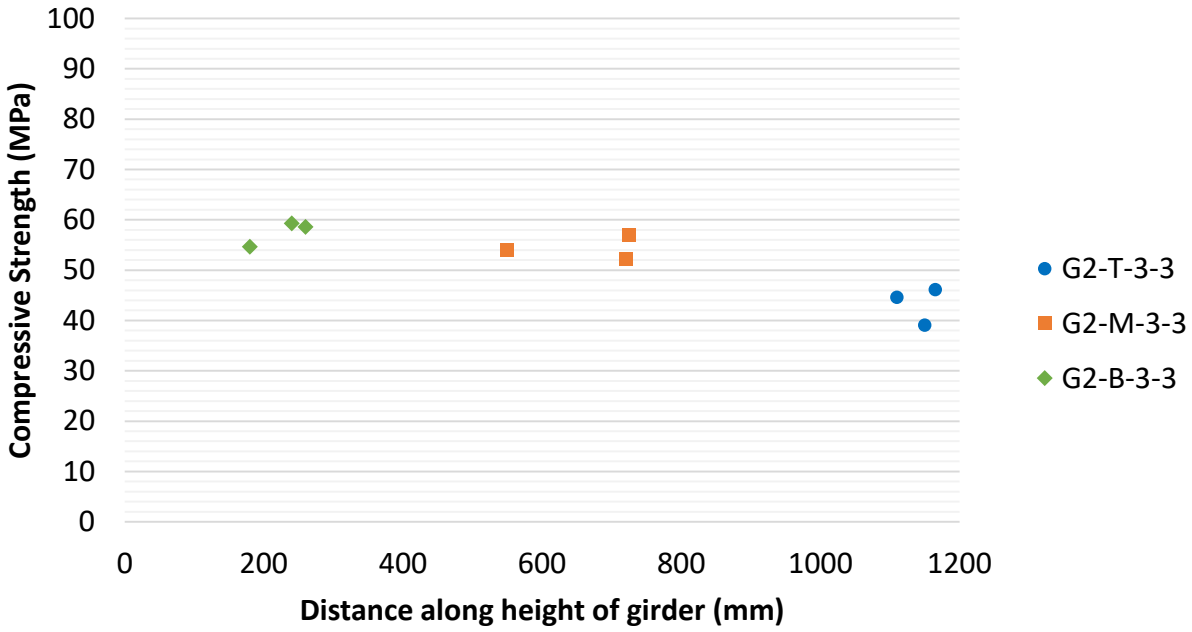

Figure A.8 Day 3 Compressive strength of individual cores versus height of G2 Girder Web

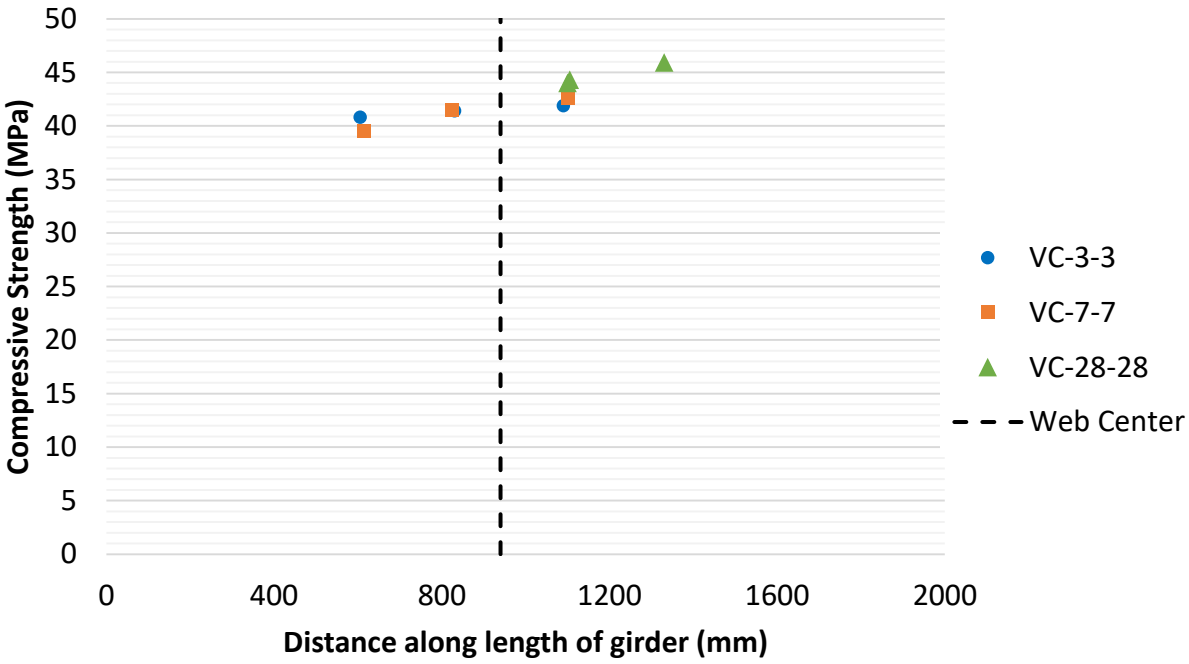

Figure A.9 Compressive strength of individual cores versus length of VC Chamber

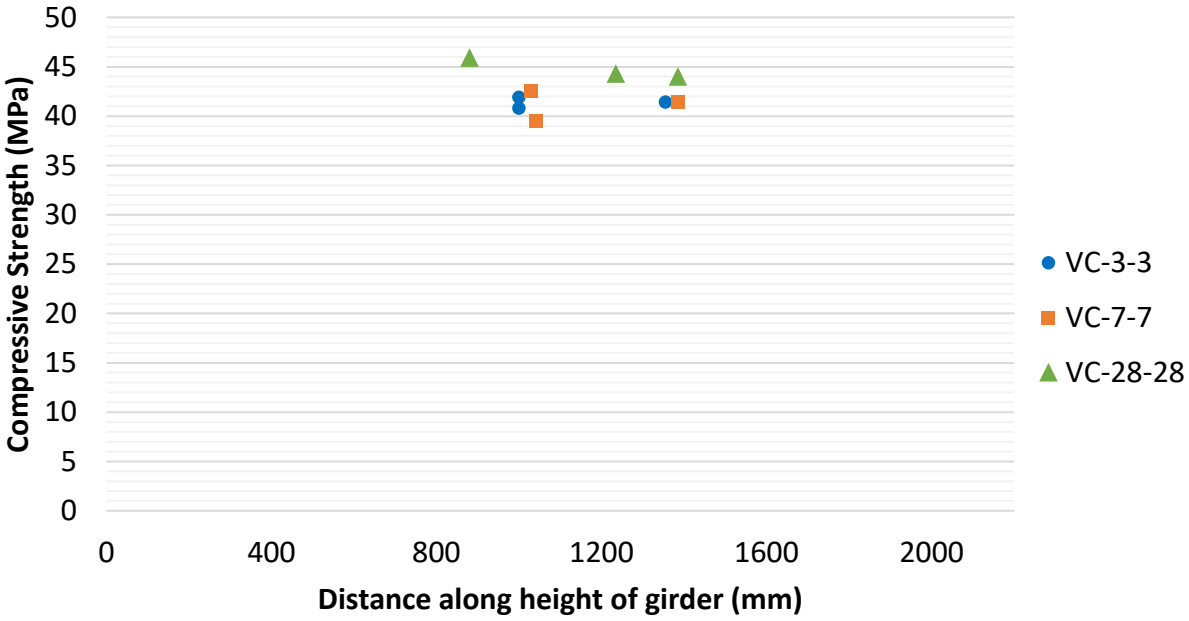

Figure A.10 Compressive strength of individual cores versus height of VC Chamber

Appendix B - Additional Electrical Resistivity Lab Results

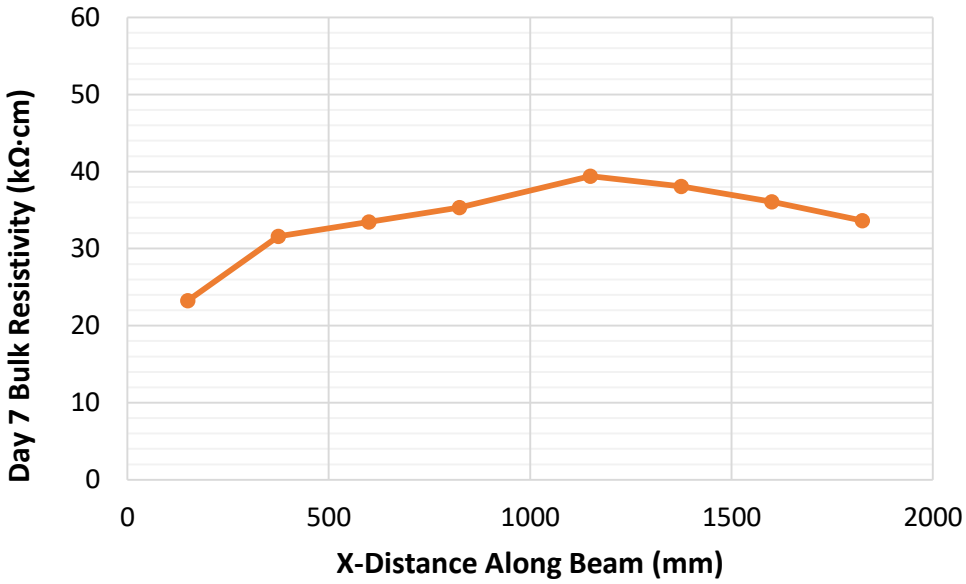

Figure B.1 Variation of B2 Cores Bulk Resistivity along Length of Beam on day 7

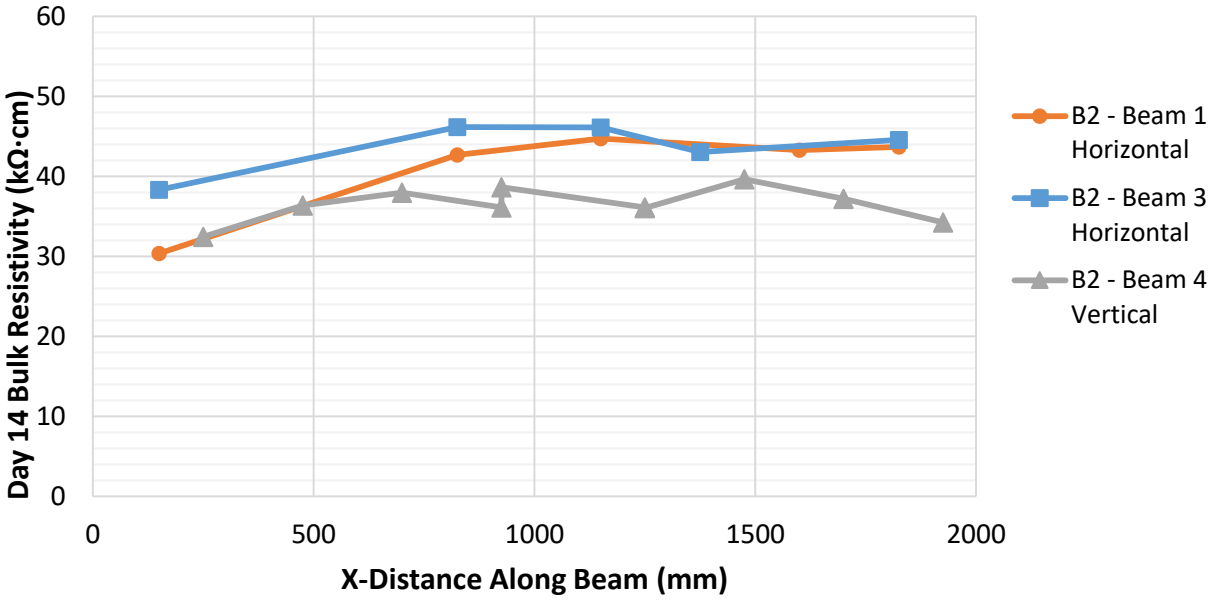

Figure B.2 Variation of B2 Cores Bulk Resistivity along Length of Beam on day 14

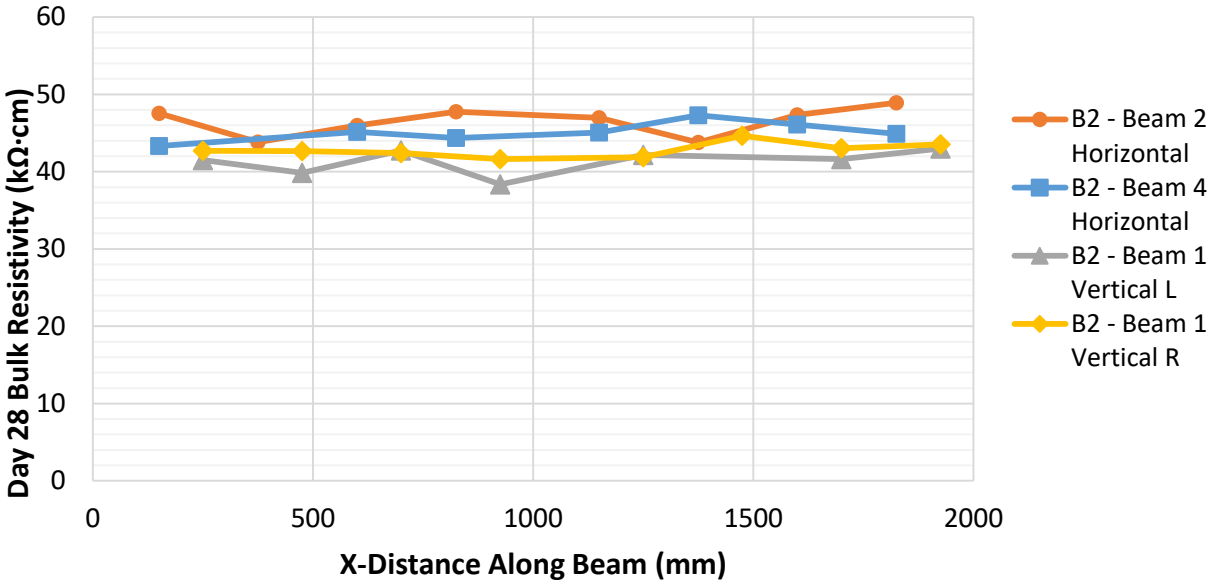

Figure B.3 Variation of B2 Cores Bulk Resistivity along Length of Beam on day 28

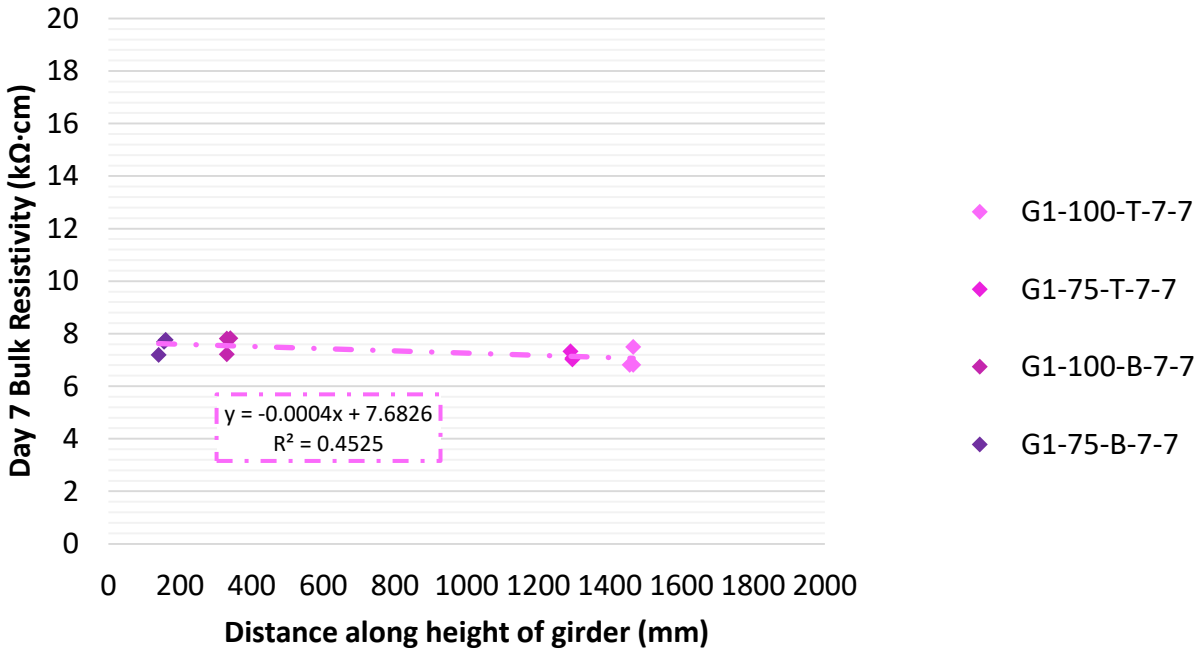

Figure B.4 Variation of G1 Cores Bulk Resistivity along Height of Girder on day 7